National Library of Canada

Acquisitions and Bibliographic Services Branch

395 Wellington Street
Ottawa, Ontario
K1A 0N4

Bibliothèque nationale du Canada

Direction des acquisitions et des services bibliographiques

395, rue Wellington
Ottawa (Ontario)
K1A 0N4

Your file Votre référence

Our file Notre référence

NOTICE

The quality of this microform is heavily dependent upon the quality of the original thesis submitted for microfilming. Every effort has been made to ensure the highest quality of reproduction possible.

If pages are missing, contact the university which granted the degree.

Some pages may have indistinct print especially if the original pages were typed with a poor typewriter ribbon or if the university sent us an inferior photocopy.

AVIS

La qualité de cette microforme dépend grandement de la qualité de la thèse soumise au microfilmage. Nous avons tout fait pour assurer une qualité supérieure de reproduction.

S'il manque des pages, veuillez communiquer avec l'université qui a conféré le grade.

La qualité d'impression de certaines pages peut laisser à désirer, surtout si les pages originales ont été dactylographiées à l'aide d'un ruban usé ou si l'université nous a fait parvenir une photocopie de qualité inférieure.

Canada

MOLLUSCAN MECHANOSENSORY NEURONS: STRUCTURE AND, FOLLOWING INJURY, THE PROCESS OF RECOVERY

Isabella Steffensen

Thesis submitted to the
School of Graduate Studies and Research
University of Ottawa
in partial fulfillment of the requirements for the
Ph.D. degree in the

Ottawa-Carleton Institute of Biology

ISBN 0-612-04883-7

UNIVERSITÉ D'OTTAWA
UNIVERSITY OF OTTAWA

This thesis is dedicated to my mother and father.

TABLE OF CONTENTS

ACKNOWLEDGEMENTS

I would like to thank my supervisor, Dr. Cathy Morris, for giving me the perfect amount of supervision, being available when I needed help, but otherwise giving me much needed space. Dr. Morris has taught me the finer art of writing, an invaluable skill for which I will be forever grateful. Finally, I would like to thank her for being generous with me on various occassions, and for allowing me to attend many international meetings.

I would like to thank my collaboraters, Dr. Naweed Syed, Dr. Andy Bulloch, and Dr. Ken Lukowiak from the University of Calgary, and Dr. Terry Walters and Mike Dulin from the University of Texas. These collaborations were fundamental to my doctoral studies, providing me with theoretical insight into the field.

I would like to acknowledge Dr. Dave Brown for access to his lab and equipment, and special thanks to Bea Valentine and Andrew Vaillant for their technical expertise. Thanks are also due to Dr. Bill Staines for teaching me immunohistochemistry and to Vijay Kapal for assistance with the *in situ* hybridization.

I would like to extend my appreciation to the members of my advisory committee, Dr. Dave Brown, Dr. Bill Staines and Dr. Bill Bates for their constructive criticisms and helpful suggestions when reviewing my work. I'm also indebted to my examining committee for their careful readings of this thesis.

My greatest debt is undoubtedly to my close friend and lab mate, Christine Murray, whose help and support on countless occassions in the last four years has made the sometimes trying experience of graduate work a hell of a lot easier. Many thanks also

to Dr. Michael Hermes, Dr. Cathy Jarvis, Dr. Tom Cunningham, Dr. Ralph Nissen, Dr. Margaret Sullivan, Dr. Charles Yang, Maureen Joyce, and the rest of the Neuroscience crew at the Loeb Institute, OCH.

I am very grateful to my parents for their everlasting support, both emotionally and financially. I would be remiss if I didn't thank my sister Sabina and my brother-in-law Paul for their encouragement, and my nieces Adriana and Clara for just being there. Thanks also to my soon-to-be husband, Mike, for his love and kindness.

Finally, I wish to acknowledge OGS (Ontario Graduate Scholarship Program) for their support.

PREFACE

This dissertation describes work which was carried out in Dr. C.E. Morris' lab, Department of Biology, University of Ottawa between May 1990 and September 1994. The work described is my own except for the biocytin study presented in Chapter 4, which was carried out in collaboration with Mike Dulin, who performed biocytin injections (Mike Dulin is a doctoral student with Dr. E.T. Walters, Department of Physiology and Cell Biology, University of Texas at Houston). Reference is made in the text to ultrastructural studies of *Aplysia* body wall tissue (Steffensen et al., 1994) that were performed by Michel Anctil (Département de Sciences Biologiques, Université de Montreal) while on sabbatical in Dr. C.E. Morris' lab. In addition, behavioural and electrophysiological studies which were performed by Mike Dulin are described in the Appendix, and referred to in the text. Work described in this thesis took a new direction when it became possible to specifically localize sensory neurons in the periphery, using an antibody to sensorin-A which was provided by R. Hawkins and E.R. Kandel (Center for Neurobiology and Behaviour, Columbia University). While visiting the University of Calgary (molluscan neuroscience group - A.G.M. Bulloch, K. Lukowiak and N.I. Syed), to learn molluscan cell culture techniques, work that is described in Chapter 5 was initiated.

ABBREVIATIONS

Adig-AP:	anti-digoxigenin alkaline phosphatase conjugate
AP:	action potential
APGWamide:	ala-pro-gly-trp-NH_2
ASW:	*Aplysia* seawater
BSA:	bovine serum albumin
CNS:	central nervous system
DTAF:	dichlorotriazinylaminofluorescein
FMRFamide:	Phe-Met-Arg-Phe-NH_2
HRP:	horseradish peroxidase
MSNs:	mechanosensory neurons
PBS:	phosphate buffered saline
PB:	phosphate buffer
RT:	room temperature
SCP_B:	small cardioactive $peptide_B$
SEM:	scanning electron microscopy
SW:	artificial seawater
TEA:	tetraethylammonium
TEM:	transmission electron microscopy

LIST OF FIGURES

ABSTRACT

Examination of *Aplysia californica's* defensive withdrawal reflexes has been particularly powerful in understanding learning-related phenomena. The tail withdrawal reflex is mediated in large part by identified tail mechanosensory neurons in the pleural ganglia. Although learning-induced changes at the synapses between the identified tail mechanosensory neurons (MSNs) and their follower motor neurons have been extensively studied, the peripheral sensory endings have not been characterized.

Using a combination of immunohistochemistry (with an antibody to a neuronal-specific tubulin) and electron microscopy, putative mechanosensory structures in the tail region were identified. These neural structures penetrated the epithelium and terminated as endings consisting of mixed cilia and microvilli.

Brunet et al. (1991, Science 252:856) have identified a peptide, sensorin-A, that is specific for the *Aplysia* MSNs. To determine if the cilia/microvilli endings were the sensory endings of the MSNs, immunostaining for sensorin-A was performed in the tail region. Sensorin-A immunofluorescence did not colocalize with the ciliated/microvillar sensory structures, but did reveal the endings of the MSNs. Confocal microscopy of the sensorin-A fibers revealed that they terminated as coiled structures deep in the body wall. The general morphology of these endings most resembled that of vertebrate muscle spindles. Although the ciliated endings were determined not to be associated with the sensorin-A MSNs, it is possible that they are the unidentified low-threshold mechanoreceptors for which there is physiological evidence.

Electrophysiological experiments (Brunet et al., ibid) suggest that sensorin-A acts

as a neurotransmitter centrally. In the periphery sensorin-A immunofluorescence was localized predominantly to varicosities in the MSNs. Immunogold electron microscopy revealed that at the ultrastructural level, sensorin-A was localized mainly to dense granules, and dense-core vesicles, a distribution consistent with a neuroactive peptide. Sensorin-A's presence peripherally raises the possibility of a parallel with substance-P, a neuroactive peptide released at primary afferent terminals of vertebrate nociceptors.

The mechanoafferents that innervate the tail are carried from the ganglia to the tail region in nerve p9. To determine if the tail MSNs have the ability to regenerate, bilateral crushes of nerve p9 were performed. Regeneration was monitored morphologically using immunostaining for sensorin-A, and behaviourally by examining the tail withdrawal reflex. Functional recovery, indicated by a return of the tail withdrawal reflex, was observed between 10 and 15 days, and growth of sensory fibers (as observed by sensorin-A immunostaining) down p9 paralleled the time course for behavioural recovery.

Recently, the pond snail *Lymnaea stagnalis* has emerged as a model system for studying rhythm generation. Nothing is however known about the mechanosensory inputs that affect behaviours such as respiration, locomotion and feeding. Sensorin-A immunostaining on the *Lymnaea* CNS, and *in situ* hybridization with a probe to the sensorin-A gene of *Aplysia*, revealed putative mechanosensory neurons. These putative sensory cells did not colocalize with previously identified motor neurons, interneurons or neurosecretory cells. As would be expected for a mechanoafferent, sensorin-A positive fibers were found in nerve tracts innervating the body wall.

CHAPTER 1

INTRODUCTION

1.1 Invertebrate models of mechanosensory systems

Mechanoreceptors allow living organisms to respond to their mechanical environments by detecting mechanical deformation and transducing it into an electrical response. The mechanism of transduction, however, is not well known. The following reviews several invertebrate mechanosensory systems which have been extensively studied. In addition, the chosen examples demonstrate a wide range of techniques that have been used to examine this system, including ultrastructural studies, genetic analysis, and pharmacological and physiological studies. Although detailed descriptions of mechanoreceptors are also available in arthropods, they will not be reviewed here (for review of arthropod mechanoreceptors see French, 1992).

Touch sensitivity in the nematode *Caenorhabditis elegans*

The simple soil nematode, *C. elegans*, has become a model system to study neuronal development. Each of the 302 neurons within the animal's nervous system have been ultrastructurally and physiologically identified (White et al., 1986). Over the past decade, many nervous system mutants of *C. elegans* has been isolated through extensive genetic analysis (e.g. Herman, 1987; Desai et al., 1988; Chalfie and Au,

1989).

In *C. elegans*, touch sensitivity is mediated by a set of six touch receptor neurons, the microtubule cells (Chalfie and Sulston, 1981). When a fine hair is drawn across the animal's head it moves backwards. When it is drawn across the tail, the animal moves forward. Ablation of the three anterior touch cells with a laser microbeam eliminates the head response, while ablating the two posterior touch cells eliminates the tail response (Chalfie and Sulston, 1981). One of the touch cells, which is located midway along the body, has all the characteristics of a microtubule cell but does not mediate a touch response in wild-type animals (Chalfie and Sulston, 1981). However, in mutants in which this cell is located more anteriorly, the cell mediates a detectable anterior touch response (Chalfie et al., 1983).

Like most neurons in *C. elegans*, the touch cells have a simple structure. Each cell has a long receptor process that extends anteriorly from the cell body, runs longitudinally, and lies next to the cuticle. This process contains unusually large microtubules that are found only in the touch receptor neurons, giving the cells their name (Chalfie and Thomson, 1982). Near the end of the receptor process is a radial branch (synaptic branch) on which most of the synapses to other neurons are made. The anterior microtubule cells (but not the posterior cells) are joined by gap junctions at the ends of their synaptic branches. In electron micrographs, the touch receptor cells can be identified not only by their unusual microtubules, but also by an associated extracellular material called the mantle which anchors the receptor process to the cuticle (Chalfie and Sulston, 1981).

The microtubules in touch receptor neurons have more protofilaments (15 instead of 11) than the microtubules found in other *C. elegans* neurons (Chalfie and Thomson, 1982). These larger microtubules respond differently to anti-mitotic drugs, fixation protocols, temperature, and mutation (Chalfie and Thomson, 1982). The arrangement of the 15-protofilament microtubules within the cell is more orderly than that of the 11-protofilament microtubules (Chalfie et al., 1986). Unlike the smaller microtubules, the larger ones form bundles in which each microtubule maintains its relative position. These ordered microtubules do not span the entire touch receptor process; the receptor process is 400-500 μm long whereas the microtubules are 10-20 μm long. Such short microtubules could slide relative to each other and thus permit stable microtubule organization in the face of changes in cell length (i.e. during sinusoidal bending of the animal). The anti-mitotic drugs colchicine and podophyllotoxin selectively act on the microtubules of the touch receptor neurons (microtubules in other neurons are normal in the presence of these drugs; Chalfie and Thomson, 1982). For example, animals grown in 1 mM colchicine show the same growth rate as untreated animals, but their touch receptor processes completely lack microtubules (Chalfie and Thomson, 1982). Such animals are touch insensitive but otherwise normal. Since these large microtubules have the ability to associate and form bundles, they may function in providing a rigid cytoskeleton against which the cell might be deformed by touch stimuli.

The finding that the 15-protofilament microtubules are found only in the touch receptor neurons and primarily within the receptor process of the cell, suggests that

these microtubules may function in sensory transduction. The most striking evidence for a specialized role for the larger microtubules comes from studies of animals carrying mutations in the gene mec-7 (mechanosensory abnormal; Chalfie and Sulston, 1981). Mec-7 mutants exhibit normal touch cell processes, but they are devoid of the 15-protofilament microtubules and instead contain a smaller number of 11-protofilament microtubules. Despite normal nerve outgrowth these mutants are insensitive to touch, implicating the 15-protofilament microtubule bundle in sensory reception or transduction. The sequence of the cloned mec-7 gene reveals that it encodes a ß-tubulin (Savage et al., 1989). It is likely that this ß-tubulin is selectively required in the *C. elegans* touch cells since mutations in mec-7 do not detectably affect other cells. In addition to the larger microtubules, it appears that the mantle, an area of extracellular material that lies along the peripheral edge of the process, is also required for sensory transduction since mutants which lack this structure (i.e. mec-1) are also insensitive to touch (Chalfie and Sulston, 1981).

Also interesting, is the detection of a gene, mec-4, which is needed for mechanosensation, but does not affect the morphology of the touch receptor neurons (i.e. the touch receptor neurons in mec-4 mutants are insensitive to touch, but are morphologically normal; Driscoll and Chalfie, 1991). However, three dominant mec-4 mutations (mec-4(d)) cause fully-formed touch receptor neurons to degenerate (Driscoll and Chalfie, 1991). Degenerating touch receptor neurons typically swell to several times their normal diameter before they disappear, presumably by lysis. The vacuolar appearance observed in degenerating cells suggests that the mec-4(d) gene product may

disrupt membrane integrity or cause osmotic imbalance in the touch receptor neurons. Mec-4 has extensive sequence homology with deg-1 (degeneration), another gene whose dominant mutations induce neurodegeneration of other non-mechanosensory neurons in *C. elegans* (Chalfie and Wolinsky, 1990). Together with deg-1, mec-4 defines a new gene family (degenerin; Driscoll and Chalfie, 1991). The sequence of mec-4 and deg-1 cDNA, which in their aberrant form disrupt osmotic balance, suggests that the genes may encode transmembrane proteins similar in general structure to membrane receptors (Chalfie and Wolinsky, 1990; Driscoll and Chalfie, 1991). Recently, a related mammalian gene, rat alpha-rENaC, has been shown to induce an amiloride-sensitive Na^+ current when expressed in *Xenopus* oocytes, providing evidence that degenerin genes encode ion channel proteins (Canessa et al., 1993). Deduced amino acid sequences of the degenerins include two predicted membrane spanning domains (Chalfie et al., 1993). A recent study by Hong and Driscoll (1994), shows that conserved amino acids within the second putative membrane spanning domain are critical for mec-4 activity; in the mec-4(d) dominant mutation, specific substitutions in this region block or delay the onset of degeneration, suggesting that the mutations may be affecting the channel's permeation.

Mechanosensory neurons in the leech, *Hirudo medicinalis*

Mechanical stimulation of the leech, *H. medicinalis*, produces a variety of behavioural responses, depending on the intensity and location of the stimulus. For instance, touching the head end produces whole-body contraction, whereas the same

stimulus applied to the tail end elicits swimming (Kristan et al., 1982). More intense mechanical stimuli produce complex responses, usually starting with violent writhing movements.

The central nervous system (CNS) of the leech consists of 21 segmental ganglia which are bilaterally symmetrical and contain ~300-400 neurons each (Nicholls and Baylor, 1968). Within each ganglion a number of neurons with constant morphological and physiological properties can be identified on the basis of size and position. The identifiable neurons include the mechanosensory neurons (MSNs) which respond to light touch (T cells), pressure (P cells) and noxious stimuli (N cells) such as squeezing, pinching, or pinpricks (Nicholls and Baylor, 1968). On either side of each ganglion are three T cells, two P cells and two N cells.

The electrical properties of these MSNs have been determined by mechanically stimulating the peripheral skin and recording from these cells centrally (Nicholls and Baylor, 1968). T, P and N cells respond to mechanical stimulation of the skin with overshooting action potentials (APs). The sensory discharge elicited by peripheral stimulation adapts rapidly in T cells and slowly in both the P and N cells. All three modalities have a frequency of discharge that is graded with the strength of stimulation. It appears that these cutaneous MSNs are primary sensory neurons since 20 mM Mg^{2+} for up to 12 hrs does not block the electrical response of these neurons to peripheral skin stimulation (Nicholls and Baylor, 1968). The receptive fields of the T, P, and N cells are well defined and have been mapped physiologically (Nicholls and Baylor, 1968). Each of the MSNs innervates a discrete oval shaped territory that divides the

lateral body wall of each segment into thirds for the T cells and into halves for the P and N cells. Although there is overlap between receptive fields of adjacent segments, receptive fields are not found on the contralateral skin and the dorsal and ventral midlines constitute sharp boundaries.

By injecting horseradish peroxidase (HRP) into the cell bodies of individual T (Blackshaw, 1981) or N (Blackshaw et al., 1982b) cells it has been possible to study the morphology of their receptive terminals. In successful injections the processes of these cells can be traced from their origin in the segmental ganglia to their terminals in the skin. Major axon branches of the T cells can be seen in the nerve root going out to the body wall where they dip between the different muscle layers (i.e. longitudinal, oblique and circular). When axons reach the layer of the skin, extensive branching occurs and fine branches turn towards the surface going between epithelial cells. T cell terminals appear as simple nerve endings (with no specialized structures such as cilia), between the profiles of the epithelial cells and terminate a few microns from the surface. These terminals are frequently beaded with varicosities; in electron micrographs, the varicosities are seen to contain mitochondria and a cluster of vesicles (Blackshaw, 1981). It is possible that the T cells are not primary sensory neurons and that instead, the epithelial cells transduce mechanical stimuli and in turn excite the T cell terminals by synaptic transmission. However, apart from having close contact, no specializations of the opposing membranes (i.e. gap junctions) are seen which might suggest that the epithelial cells are electrically coupled to the sensory terminals (Blackshaw, 1981).

Unlike the T cells whose processes divide repeatedly and become progressively finer closer to the skin, N cell axons give rise with an abrupt decrease in diameter to much finer calibre branches (~1 μm), which run within the network of peripheral nerves at deep levels of the body wall (Blackshaw et al., 1982b). Some branches have been traced to superficial levels where they run at the base of the layer of epithelial cells in the skin. It is considerably more difficult with N cells than with T cells to visualize the fine branches and trace them to their terminals. N cell axons appear to end deep to the epithelial cell layer and have never been seen to terminate between the epithelial cells at the surface like the T cell terminals. Specialized endings of the N cells have not been seen in their receptive fields in the body wall (Blackshaw et al., 1982b).

In addition to the central MSNs (i.e. the T, P and N cells), peripheral stretch-receptors lie within the body wall (Blackshaw and Thompson, 1988; Blackshaw, 1993). Unlike the central MSNs, the stretch-receptor neurons do not generate overshooting APs, but instead produce decrementally graded conducting signals (Blackshaw and Thompson, 1988). These neurons respond to stretch of body wall muscle with maintained hyperpolarizing potentials and to release of stretch with depolarization (Blackshaw and Thompson, 1988). Injection of HRP or lucifer yellow into their cell bodies has revealed a distinctive morphology (Blackshaw and Thompson, 1988). The peripheral stretch-receptors have two expanded, disc-shaped dendrites arranged in series, separated by the cell body and a 300 μm process. These disc-shaped terminals are 70 μm across at their widest point but only a few microns deep, and are associated

with bands of body wall muscle. The stretch-receptors are innervated by fine branches of the N cells which cross the surface of the fan-shaped dendrites 10-20 times, forming a coiled terminal (Blackshaw et al., 1982b). Electrophysiological studies have shown that the stretch-receptor neurons are post-synaptic to the N cells (Blaskshaw et al., 1984).

Crustacean stretch receptors

a) The crayfish abdominal muscle receptor organ

In the abdominal muscle receptor organ of the crayfish, stretch-receptor cell bodies are large and lie peripherally, making them accessible to intracellular recordings and therefore a good model to study mechanotransduction (Brown et al., 1978). The abdominal stretch-receptors occur in pairs, each pair being composed of a phasic receptor which adapts rapidly to a maintained stretch, and a tonic receptor which is slowly adapting. From the stretch receptor cell body arise large (about 10 μm near the origin) primary dendrites which are surrounded by many layers of sheath cells and connective tissue (Tao-cheng et al., 1981). Numerous microtubules fill most of the central portion of the dendrites, and other organelles such as mitochondria are usually located in narrow peripheral zones. Primary dendrites ramify into smaller dendrites called dendritic branches. Portions of the dendritic branches (dendritic forks) give rise to very small (0.1-0.2 μm) cylindrical shaped terminals called dendritic tips (Tao-cheng et al., 1981). Dendritic tips are clearly distinguishable from other parts of the dendrites. These terminals are devoid of mitochondria and sheath cells and are

embedded directly inside a large mass of connective tissue that is located in the middle of the stretch receptor muscle. The only organelles occasionally found in the dendritic tips are microtubules and vesicles. Stretch stimuli produce marked structural changes in the dendritic tips (following stretch, swollen regions alternate with narrow, unswollen regions), suggesting that the dendritic tips are the primary site of the production of the receptor potential (Tao-cheng et al., 1981). A study which examined the spatial organization of the cytoskeleton of the crayfish stretch receptor (Tskhovrebova et al., 1991), has shown that the cytoskeleton has a helical structure in which all the microtubules are arranged in parallel helices. Following muscle elongation, a decrease in the amplitude, and spatial desynchronization of the microtubule helices was observed. Tskhovrebova et al., (1991) suggest that the neuronal cytoskeleton behaves like a spring or a bundle of interconnected springs that elongate during the stretch of the receptor muscle. Thus, *in vivo* the cytoskeleton in the dendritic region of the stretch receptor may undergo a reversible change during the stretch of receptor muscle.

Mechanical distortion of the dendritic terminals causes a depolarizing receptor potential that normally leads the neuron to fire an AP (Brown et al., 1978). The generator potential produced in the dendritic terminals spreads electrotonically for several hundred microns to the axonal site of spike initiation, a segment of the axon with a lower threshold than the surrounding axonal membrane (Ringham, 1971). The generator potential is produced by the movement of cations through a large non-selective cation channel whose open probability increased with stretch (Edwards et al.,

1981). This channel is permeable to both Na^+ and K^+, and somewhat permeable to Ca^{2+}, as well as Mg^{2+}, Sr^{2+} and Ba^{2+} (Edwards et al., 1981). However, under physiological conditions Na^+ is the main carrier of the current through the transducer channels. Single-channel recordings from the cell body and primary afferents (dendritic tips are not accessible to patch electrodes) have revealed the presence of a stretch-activated cation channel which fulfils the criteria for the mechanotransduction channel (Erxleben, 1989). Besides its sensitivity to stretch, this channel has the low cation selectivity previously established for the receptor current in voltage-clamp experiments (Brown et al., 1978). Stretch-activated channels have recently been directly linked to the receptor current in an experiment demonstrating that gadolinium, a known blocker of stretch-activated ion channels, blocks the receptor response (Swerup et al., 1991).

The receptor potential of the crayfish stretch-receptor consists of an initial peak (dynamic phase) which decreases rapidly to a more or less constant static phase (Ottoson and Swerup, 1985). There is considerable evidence that the early adaptation of the generator potential is caused by an outward K^+ current activated by depolarization (Ottoson and Swerup, 1985). Intracellular injection of the potassium channel blocker, TEA, almost abolishes the early adaptation, providing additional support for this hypothesis (Ottoson and Swerup, 1985). Recently, Ca^{2+} influx through stretch-activated channels has been shown to generate the outward K^+ current through activation of Ca^{2+}-dependent K^+ channels (Erxleben, 1993).

A tissue culture model to study mechanotransduction has been established using

the abdominal crayfish stretch-receptors (Golas and Pasztor, 1991). In culture, both tonic and phasic neurons regenerate axonal and dendritic processes. Mechanical stimulation of the dendritic ends results in characteristic firing patterns as seen *in vivo*.

b) The lobster oval organ

The lobster oval organ is a proprioreceptor which lies within the ventilatory appendage and monitors the continuous beating of the gill bailer (Pasztor, 1979). The oval organ consists of an oval mass of dendritic endings which arise from three large afferent fibers, X, Y and Z. The dendritic mass is supported by a conical array of connective tissue strands which span the region of maximum flexion near the base of the gill bailer. The cell bodies of the three sensory neurons lie centrally in the subesophageal ganglion, adjacent to the motor neurons innervating the ventilatory muscles. Unlike the more familiar crayfish abdominal muscle receptor organ, the oval organ lacks a receptor muscle or any efferent innervation (Pasztor, 1979).

Each of the three sensory fibers responds to mechanical stimulation in a characteristic way (Pasztor and Bush, 1982; 1983a). Each response comprises, in differing proportions, overshooting APs and an underlying graded response. Fibre X has the fewest spikes (1-6) and the largest graded potential, whereas fibre Z attains the highest firing frequencies but shows the smallest graded potential. Fibre Y has intermediate properties. Both the amplitude of the graded potential and the number of spikes are directly related to the strength of stimulation. Although most sensory neurons convey temporally coded impulses, several examples of graded nonspiking

transmission have been found. The oval organ is a unique example of afferent fibers that use both APs and graded depolarizations to transmit a signal over a distance of 1 cm or more into the CNS. Although the graded response declines as it travels from the dendrites to the cell body, the response would still be large enough to cause transmitter release and bring about postsynaptic events in the CNS (Pasztor and Bush, 1982; 1983a).

When the isolated oval organ is stimulated repetitively, the response of the three afferents habituates (Pasztor and Bush, 1983b). Both components of the response are affected, but the decline in spiking is more pronounced than that of the graded potential. When sinusoidal stretch stimuli are used, imitating the normal beating pattern of the gill bailer, spiking disappears and the afferent fibers respond solely in the non-impulsive mode. This suggests that under normal conditions feedback information from the oval organ would be provided by small oscillations in membrane potential; any perturbations in the regular cycle of stretch and relaxation would disrupt habituation and restore spiking, therefore providing an enhanced release of transmitter.

Peripheral modulation of the sensory response of the lobster oval organ has been described *in vitro* (Pasztor and Bush, 1987; 1989). Two neuroamines, serotonin and octopamine, depress receptor potentials and impulse discharges of the Y and Z fibres, whereas the pentapeptide proctolin enhances these responses. X fibers were unaffected by all three neuroactive substances. The two amines serotonin and octopamine have been detected in lobster hemolymph at concentrations of 10-50 nM. These values are higher than the concentrations which have been shown to be effective *in vitro* (i.e. 10-

100 pM). Thus, it is certainly possible that the available circulating levels of these hormones modulate these proprioreceptors *in vivo*. Although assays of the hemolymph failed to show significant concentrations of free proctolin, proctolin immunoreactivity of the peripheral dendrites suggested that the mechanoreceptive terminal could be serving a dual role as both transducer and neurosecretory release site. To quantify the content of proctolin in the peripheral sensory organ, and to determine if it is released in response to stretch, high-performance liquid chromatography coupled with a sensitive bioassay was utilized (Pasztor et al., 1988). Repetitive stretch stimuli at physiological amplitudes resulted in a significant increase in the release of proctolin from the oval organ *in vitro*. Approximately 12% of the total proctolin stored in the oval organ was released during a 5 min stimulation period. These results, coupled with the previous studies that demonstrated the excitatory effects of proctolin on the afferent fibers (Pasztor and Bush, 1987; 1989), suggest that endogenous proctolin may function to self-modulate the sensory transduction mechanism of these sensory terminals.

1.2 Mechanosensory neurons in *Aplysia californica*

The marine mollusc *Aplysia californica* has a relatively simple nervous system, and a correspondingly simple behavioural repertoire (Kandel, 1979). With its large and identifiable neurons, the *Aplysia* has proved to be a useful model for the study of cellular mechanisms that underlie short- and long-term memory. For example, mechanisms for short-term sensitization of the defensive withdrawal reflex of the tail and of the siphon and gill have been extensively studied (Walters et al., 1983b; Scholz

and Byrne, 1987). The tail withdrawal refex, which is elicited by delivery of a tactile stimulation to the tail (Walters et al., 1983a), has features similar to those of the siphon-gill withdrawal reflex, which is produced by stimulating the siphon (Byrne et al., 1974).

MSNs which innervate the gill, siphon and mantle are found in four clusters (rLE, LE, RE, RF) in the abdominal ganglion (Byrne et al., 1974; Byrne, 1980; Dubuc and Castellucci, 1991). The posterior part of the animal is innervated by a cluster of MSNs on the ventrocaudal surface of each pleural ganglion (Walters et al., 1983a; Zhang et al., 1993). Sensory neurons within these clusters project out the three pedal nerves p7, p8 and p9, although some also project out the cerebral-pleural connectives to innervate the head (Zhang et al., 1993). Two clusters, J and K, have their receptive fields in the head and neck region and are located in each hemiganglion of the cerebral ganglion (Rosen et al., 1979). The MSNs in these clusters have similar morphological and electrophysiological properties (Byrne et al., 1974; Rosen et al., 1979; Byrne, 1980; Walters et al., 1983a; Dubuc and Castellucci, 1991). Each cluster contains 20-100 small cells (~50 μm) which are orange in colour and have a uniform appearance. These cells are silent unless stimulated and show no electrical coupling. Responses are graded with the intensity of mechanical stimulation and adapt slowly with a maintained stimulus. Since they respond with maximal activation to noxious stimulation (Walters et al., 1983a; Clatworthy and Walters, 1993), it is appropriate to refer to them as nociceptive MSNs (Walters, 1991, 1992). The organization of the excitatory receptive fields of each population is similar in the extent of overlap and variation in size of the

individual fields. In addition, the pleural clusters and the cerebral J and K clusters each show some somatotopic organization. When peripheral and central synaptic transmission is blocked with $MgCl_2$, the sensory response persists suggesting that these MSNs are primary sensory neurons (Byrne et al., 1974; Rosen et al., 1979; Byrne, 1980; Walters et al., 1983a; Dubuc and Castellucci, 1991).

Using differential screening of *Aplysia* cDNA libraries, Brunet et al. (1991) have isolated a messenger RNA that is specific for the *Aplysia* MSNs, and is expressed in every mechanoreceptor cluster in the *Aplysia* CNS (demonstrated by in situ hybridization). This messenger RNA encodes a peptide, sensorin-A, that appears to function as an inhibitory cotransmitter. Using the inferred amino acid sequence, Brunet et al. (1991) generated an antibody against sensorin-A. Immunoreactivity to sensorin-A was observed in all the MSNs, and in every sensory cluster, agreeing with results from the in situ hybridization.

Mechanisms of nociceptive plasticity in *Aplysia* mechanosensory neurons

Recent investigations have shown that noxious stimulation of the tail causes sensitization of the tail MSNs which involves central and peripheral alterations (Billy and Walters, 1989a; Woolf and Walters, 1991). The mechanosensory cell bodies display various plastic changes (i.e. decrease in AP threshold, facilitation of synaptic transmission to follower motor neurons, increase in number of APs to a set stimulation) which enhance the sensory signals in the CNS (Walters et al., 1983b; Walters, 1987a,b). Recently, Clatworthy and Walters (1993) have demonstrated that in addition

to an enhancement in AP discharge, plastic changes in the soma generate an afterdischarge that amplifies the sensory signal.

Peripheral sensitization of the tail MSNs following noxious stimulation involves a reduction in the mechanosensory threshold, an increase in receptive field size and a sensitization of these fields (afferent activity recorded from peripheral nerve; Billy and Walters, 1989a). The increased peripheral excitability suggests that field alterations involve sprouting of peripheral mechanosensory processes (Billy and Walters, 1989a). The effects of noxious stimulation are greatest in sensory neurons directly activated by a noxious stimulus (site-specific sensitization), presumably to heighten the animal's responsiveness to stimuli at the site of noxious stimulation (Walters, 1987a,b).

Although noxious stimulation of the tail produces sensitization of the tail MSNs, it has been shown to produce inhibition as well as sensitization of the siphon-gill withdrawal reflex (Mackey et al., 1987). This inhibition may serve to transiently reduce potentially interfering withdrawal responses during escape locomotion (Mackey et al., 1987; Walters, 1991). Similar enhancement and inhibition of sensory signals can be produced by the endogenous neuromodulators serotonin, small cardioactive peptide$_B$ (SCP_B), Phe-Met-Arg-Phe-NH_2 (FMRFamide), acetylcholine, and dopamine in the tail (Siegelbaum et al., 1982; Ichinose et al., 1989), siphon (Abrams et al., 1984; Dubuc and Castellucci, 1991) and head (Rosen et al., 1989) MSNs. Serotonin and SCP_B have an excitatory effect by decreasing the AP threshold and increasing its duration, whereas dopamine, FMRFamide, and acetylcholine have opposite effects and inhibit the MSNs. When these neuromodulators are injected into the tail region, peripheral modulation of

the tail MSNs is observed which functionally parallels the central neuromodulatory effects (Billy and Walters, 1989b). Serotonin and SCP_B reduce the mechanosensory threshold while FMRFamide, dopamine and acetylcholine elevate it. These findings suggest that the endogenous neuromodulators may normally regulate central and peripheral regions of the MSNs, and support the hypothesis that noxious stimulation modulates the signalling strength of the entire cell.

Nociceptive plasticity of the *Aplysia* MSNs is mediated in part by neuromodulators, however, since noxious stimuli can damage peripheral axons, additional signals for plasticity may be generated at the site of axonal injury. Walters et al. (1991) have demonstrated that axonal injury induces long-term (2-23 days) sensitization of the *Aplysia* MSNs. Following axon crush, sensory neurons show decreases in AP threshold, accomodation, and afterhyperpolarization, and increases in AP duration, afterdischarge, and synaptic transmission, all of which act to increase the signalling effectiveness of the sensory neuron. Recently, MSNs of the J and K clusters of *Aplysia* have been shown to exhibit virtually identical alterations following crush of the nerves that contain their axons (Clatworthy and Walters, 1994). Clatworthy and Walters (1994) also show that long-term plasticity fails to occur when nerves that do not contain axons of the tested sensory neurons are crushed. This axonal specificity, and the long latency of soma plasticity, argues against a role for neuromodulator release from interneurons in producing the injury induced plasticity. Clatworthy and Walters (1994) suggest that the inducing signal could be 1) intracellular signals released directly by axonal injury, or 2) extracellular signals released locally by other

axons or injured support cells, or by immunocytes attracted to the injured site.

1.3 Mechanical nociceptors in vertebrates

Animal tissues are innervated by nociceptors that respond with increasing discharge frequency to stimuli that have the potential to cause tissue damage. In vertebrates, the MSNs that respond to intense or noxious mechanical stimuli are called mechanical nociceptors (review: Dubner and Bennet, 1983). These nociceptors are primary sensory neurons that have their cell bodies (dorsal root ganglion neurons) in sensory ganglia, a central process that makes synaptic connections with interneurons (dorsal horn neurons) in the CNS, and an afferent process that terminates as a free nerve ending in peripheral tissues. Both myelinated and unmyelinated nociceptive terminals have been identified, however, much less is known about unmyelinated nociceptors.

The receptor structure associated with myelinated nociceptive afferents has been examined in the cat (Kruger et al., 1981). Mechanical nociceptors in the skin of the cat possess receptive fields consisting of a number of punctate areas from which maximal firing can be elicited by intense mechanical stimuli. Kruger et al., (1981) examined these skin areas with light and electron microscopy and found thin myelinated axons that extended to the papillary layer, where they became unmyelinated. Unmyelinated axons, that were surrounded by thin Schwann cell processes, were found to penetrate the epidermal basal lamina, and terminate in the basal epidermal layer. At the epidermal penetration site, the axons contained both

small clear vesicles, and large dense core vesicles and, at this level, the surrounding Schwann cell cytoplasm exhibited numerous pinocytotic vesicles. Kruger et al. (1981) suggest that the axon-Schwann cell complex at the zone of penetration may constitute the receptive apparatus for myelinated mechanical nociceptors.

The most extensively studied neuropeptide in nociceptors is substance P. This peptide has been shown to be present in nociceptors (Cameron et al., 1988; Pleinderleith et al., 1990), and to be released from peripheral terminals when they are activated by noxious stimuli or by antidromic activation of the peripheral nerve (Moskowitz et al., 1984; White and Helm, 1985). Direct application of substance P to peripheral tissues produces a number of effects including stimulating release of histamine from local mast cells (Johnson and Erdos, 1973), inducing vasodilation (Lembeck and Holzer, 1979), and acting as a chemoattractant for white blood cells (Helme and Andrews, 1985).

1.4 Regeneration following nerve injury: vertebrate preparations

Upon injury, axons in the CNS of mammals form a few abortive sprouts, but otherwise fail to regenerate long processes (review: Skene, 1989). The failure of axons in the mammalian CNS to regenerate is due, at least in part, to the unfavourable properties of the glial environment surrounding the lesioned axons. Oligodendrocytes and myelin carry proteins on their surface that inhibit axonal growth (Caroni and Schwabb, 1988), and reactive astrocytes form a glial scar that also impedes axonal elongation (Bovolenta et al., 1991). Regeneration of lesioned axons is possible in the

peripheral nervous system (Bishop, 1982; McMahon and Kette-White, 1991) where nerves are surrounded by Schwann cells instead of oligodendrocytes and astrocytes.

The inability of neurons to regenerate in the CNS of mammals contrasts to the capacity of neurons in the CNS of several lower vertebrates, such as the lamprey and the goldfish, which readily regrow their axons following injury (McClellan, 1992; Stuermer et al., 1992). After optic nerve transection in the goldfish, the retinal ganglion cells re-extend their axons and reinnervate their target, the optic tectum, in the appropriate retinotopic order (Hope et al., 1976; Stuermer, 1988a,b). The regenerating axons form appropriate synaptic connections and restore vision (review: Gaze, 1970; Northmore, 1987). In the lamprey, there is recovery of locomotor function within 3-6 weeks after complete transection of the spinal cord (Selzer, 1977), with axons of both the brainstem and spinal neurons growing across the lesion and making new synaptic connections (reviews: Cohen et al., 1988; McClellan , 1990).

1.5 Regeneration following nerve injury: invertebrate preparations

Although some vertebrates have the ability to recover from injury to their CNS, invertebrate preparations offer certain advantages for the study of neuronal regeneration. Their nervous systems are relatively simple, with large, identifiable neurons that are easily accessible for morphological and electrophysiological investigations. In addition, several behaviours have been completely or partially analysed at the cellular level. This makes it is possible to correlate behavioural recovery with physiological and morphological changes in neurons that subserve

specific behaviours. This brief review of regeneration in the invertebrate nervous system is divided into three sections: behavioural recovery following injury, morphological evidence for regeneration, and finally, re-establishment of functional connections.

Behavioural recovery after neural injury in invertebrates

One seemingly simple assay for regeneration is to observe any loss of function associated with injury to the animal's CNS, and then use recovery of this function as an indicator for underlying neuronal regeneration.

In a study by Chase and Kamil (1983), regeneration in the tentacles of the land snail *Achatina fulica* was examined after complete removal of one of the tentacles. This study used the ability of the snail to orient itself appropriately towards an odor stimulus to determine when the tentacle was again functional. Following injury, the tentacle regenerated along with underlying sensory organs and connections to the CNS. It was found that within 4 weeks of injury, the regenerated tentacle was able to detect odors as effectively as the control side, and this sensory information was used by the CNS to appropriately orient the snail towards the odor.

Recovery of locomotion following pedal ganglion excision has been studied in the snail, *Melampus bidentatus* (Snyder and Moffet, 1990). In these studies, animals began locomoting with the denervated side of the foot between 4-8 weeks after ganglion excision. This behavioural recovery was mediated not only by axons that projected from intact central ganglia into the denervated foot, but also by newly formed

neurons and supportive cells which created a ganglion bud that bridged the gap between the CNS and the periphery.

In another experiment on the snail *Melampus*, Moffet (1992) determined that a reinervated penial complex could function in mating. The snails were not self-fertile, so their ability to transfer sperm, evaluated by production of fertile eggs, was the test of successful regeneration. Following nerve transections, snails produced fertile eggs within the two week time-span expected for axonal regeneration to the target organ.

The recovery of escape locomotion in *Aplysia* following a CNS lesion was investigated by Fredman (1988). This study looked at regeneration of central synaptic connections after bilateral crush of the pleural-cerebral connectives. This lesion disrupted the connections between command neurons responsible for initiating escape locomotion. Normal locomotion was not impaired as the sensory and motor connections mediating these responses were not damaged. Following nerve crush, the escape locomotion did recover, and full behavioural recovery of the escape response was observed as early as 15 days post-lesion.

In another study, Scott and Kirk (1992) examined recovery of feeding behaviour after crush of central connectives. They found that bilateral crush of the cerebral-buccal connectives in *Aplysia* abolished consummatory feeding behaviour (i.e. the biting response). Behavioural recovery was observed within 9 days post-lesion, and the biting response gradually increased in magnitude between days 9 and 19.

Morphological evidence for regeneration

Most of the evidence for regeneration in the invertebrate nervous system has been obtained using morphological techniques. In the snail *Achatina fulica*, axonal regeneration following crush of the cerebral-buccal connective was examined using nickel-lysine backfills (Croll and Baker, 1990). Based on observations of the staining pattern at various times after nerve crush, they concluded that axonal sprouting is rapid and restores most projections seen in control animals within the first few weeks. The extensive sprouting that occurred after injury resulted in growth of extra neurites. However, these fibers were transient and disappeared with time, leading to restoration of nearly normal morphology.

Several studies on the pond snail *Helisoma trivolis* have indicated that the morphology of regenerating neurites depends on the proximity of the axotomy to the cell body (Bulloch and Kater, 1982; Allison and Benjamin, 1985; Kruk and Bulloch, 1992). When the axotomy site is far from the soma, a number of neurites emerge from the proximal axon stump, grow within the nerve and reinervate target organs (e.g. Murphy and Kater, 1978). However, when the axotomy site is close to the soma, many new neurites sprout from other regions of the neuron and often project in inappropriate directions (Bulloch and Kater, 1982; Allison and Benjamin, 1985). In a recent study, Kruk and Bulloch (1992) observed that in the case of the identified buccal motor neuron B4 in *Helisoma*, axonal regeneration usually failed if axotomy was so close to the cell body that no axon stump remained. Since regeneration was observed following distal axotomy (which left an axon stump attached to the cell body) they hypothesized

that a damaged axonal stump may be a condition for the initiation of regeneration.

In the leech, Bannatyne et al. (1989) used HRP to study new growth in MSNs elicited by cutting or crushing peripheral nerves. They observed sprouting of new processes, either centrally within the ganglion or at the site of lesion in the peripheral nerve. Different modalities of MSNs responded differently to lesions of their axons. Cutting or crushing the axons of the N cells elicited sprouting centrally and peripherally, whereas cutting or crushing T cells elicited sprouting at the site of the lesion only. Both modalities regenerated more successfully following axon crush than after axotomy.

In a similar study in the leech, Peinado et al. (1987) used anterograde labelling with HRP to follow the pathway taken by peripheral sensory neurons as they regenerate towards the CNS following peripheral nerve crush. Of all HRP-labelled axons that had grown beyond the crush site, 88% were found in the normal sensory tract in the nerve, indicating that they travel in a well-defined path after injury. Since the distal stumps of these sensory neurons do not degenerate following axotomy, Peinado et al. (1987) suggest a guidance mechanism for growing axons that involves surface markers that are retained on the distal axon stumps.

Regenerating axons of sensory neurons in the leech usually reconnect with their normal targets by growing the entire distance from the site of lesion to the target. However, in a small number of cases rapid restoration of the normal arborization occurs when the regenerating axon connects with the severed distal segment (Frank et al., 1975; Deriemer et al., 1983; Camhi and Macagno, 1991). Severed axons have been

shown to rejoin either by direct fusion (Deriemer et al., 1983) or by forming an electrical synapse that restores the severed connection (Frank et al., 1975; Camhi and Macagno, 1991). Camhi and Macagno (1991) compared regeneration patterns of identified leech neurons following crush of the whole nerve, or photoablation of a small segment of the identified neuron. Crushed neurons regenerated by extensive sprouting of the proximal segment, whereas after photoablation 70% reconnected by forming an electrical synapse. The results demonstrated that, if the axon is severed in a way that preserves the structural integrity of the surrounding tissue, axonal regeneration can take a dramatically different form than it does following a standard crush procedure.

One of the most dramatic cases of regeneration following injury to the nervous system was reported by Moffet and Austin (1982). They showed that following excision of the cerebral ganglion, the snail *Melampus* can regenerate an entire cerebral ganglion that is similar to a control ganglion. However, creation of a whole ganglion required 11-12 months - a significant portion of the animal's 3-4 year life span.

Re-establishment of functional connections

Invertebrate studies that have attempted to link regeneration with re-establishment of functional connections in the nervous system are limited. In *Helisoma*, a pair of identified neurons (buccal motor neurons 4R and 4L) rapidly regenerate after axotomy, and functionally reinnervate their former target organs, the salivary glands (Murphy and Kater, 1980). Functional reinnervation occurred in 40% of the preparations at 6 days, and in 100% of the preparations at 11 days post-lesion.

Functional regeneration of an identified serotonergic neuron (C1) has also been described in *Helisoma* (Murphy et al., 1985a). Following axotomy, neuron C1 in the cerebral ganglion rapidly regenerates (7-8 days) to recover its regulation of feeding motor output from neurons in the buccal ganglia.

In the *Aplysia*, the feeding muscles are innervated by motoneurons located in the buccal ganglia (Cohen et al., 1978). The identified buccal motor neuron B15 projects a single axon out nerve 4 and innervates and produces contractions in the intrinsic buccal muscles 14 and 15 (Cohen et al., 1978). Following crush of nerve 4, Ross et al. (1994) found that B15 rapidly regenerated its neuromuscular synaptic connections with profuse growth of fine processes from the proximal stump of the severed axon. The first evidence for neuromuscular reinervation by B15 was observed 3 weeks after nerve crush, and its synaptic input strengthened until it reached control amplitudes at about 8 weeks post-lesion.

In the leech, touch sensory neurons in each ganglion (see above: Mechanosensory neurons in the leech, *Hirudo medicinalis*), make electrical synapses with other T cells and certain other neurons (S and C cells) in the neuropils of their own and of adjacent ganglia (Baylor and Nichols, 1969; Muller and Scott, 1981). Following axotomy, the T cells have been shown to regenerate electrical connections with other T cells (Baylor and Nichols, 1971), as well as with S and C cells (Macagno et al., 1985). However, regenerated connections are generally weaker than control connections, especially during the first 6 weeks after injury (Macagno et al., 1985).

Re-establishment of sensory connections by mechanosensory neurons has also

been examined in the leech (Van Essen and Jansen, 1977). After lesions of peripheral nerves, sensory axons which reinnervated the skin always regained sensitivity to their original stimulus modality (touch, pressure, or noxious stimuli). Sensory neurons regained functional receptive fields between 15 and 29 days, however, the ability of sensory neurons to re-establish receptive fields in the appropriate location was dependent on the type of nerve lesion. Following nerve crush, the majority of cells (26 of 33) had receptive fields in the correct location. In contrast, after nerve cut, just over half the cells (15 of 27) had receptive fields in the appropriate region.

In another study in the leech, Blackshaw et al. (1982a) found that mechanosensory neurons expanded their receptive fields after other sensory neurons in the ganglion were ablated by pronase injection. When 3 out of 4 N cells in a hemiganglion were killed, the remaining N cell expanded to cover the denervated area of skin. Similarly if all the T cells in a hemiganglion were deleted, T cells from the unoperated half of the ganglion expanded across the midline, to innervate the denervated skin on the contralateral side. The intact receptive fields required ~4 weeks to expand sufficiently to cover the denervated areas. This effect was specific for the type of neuron; following deletion of a sensory neuron with a specific modality (i.e. touch pressure or nociceptive) the sensory neurons of the other two modalities were unaffected.

1.6 Homology in the nervous sytem of gastropod molluscs

Studies on diverse species of gastropod molluscs have led to the identification

of many specific neurons, based upon their morphological and physiological properties, and on the roles they play in behavioural responses. Information from a sufficient number of different preparations has made it possible to obtain evidence for neural homologies across species. For example, it has been suggested that a cluster of neurosecretory neurons in the parietal ganglion of *Achatina fulica* are homologous to the R3-R13 group of cells (also known as the rostral white cells) in the abdominal (parieto-visceral elsewhere) ganglion of *Aplysia* (Chase and Goodman, 1977). The proposed homology was based on a similarity of morphological and electrophysiological features, together with analogous locations in the respective ganglia.

One group of homologous cells that has been extensively studied consists of the giant cerebral cells of the pulmonate molluscs (Kandel and Tauc, 1966; Seddon et al., 1968; Cottrell and Macon, 1974; Granzow and Kater, 1977; Goldschmeding et al., 1981). These neurons, termed metacerebral cells, have been found in every species of pulmonate mollusc that has been studied. The metacerebral cells are considered to be homologous since they share a number of properties; for example, they all contain serotonin, and send axons out the cerebral-buccal connectives (review: Granzow and Rowell, 1981). The cerebral ganglion of *Aplysia* (Weiss and Kupfermann, 1976), as well as of other opisthobranch molluscs (Weinrich et al., 1973; Barber, 1983), has also been shown to contain giant serotonergic neurons that are homologous to the metacerebral cells of the pulmonate molluscs.

The buccal ganglia of numerous gastropod molluscs contain a pair of large

SCP_B-immunoreactive neurons that appear to be homologous (Murphy et al., 1985b; Lloyd and Willows, 1988; Lloyd et al., 1988a,b; Masinovsky et al., 1988; Watson and Willows, 1992). Watson and Willows (1992) examined seven different nudibranch molluscs, and in all cases found that the SCP_B neurons project out the gastroesophageal nerve and innervate the esophagus. In addition, stimulation of the SCP_B neurons enhanced expression of an apparent rhythmic feeding motor program, either by potentiating existing activity, or by eliciting it in quiescent preparations. These results, combined with previous contributions from other gastropods, suggest that the SCP_B-containing buccal neurons comprise a highly conserved neuronal system responsible for regulating central and peripheral aspects of gut regulation.

1.7 Research objectives

The mechanism of transduction of a mechanical stimulus into an electrical response is not well known. Initially, I had hoped to use the identified MSNs of *Aplysia* as an *in vitro* (cell culture) preparation to study the biophysics and cell biology of a physiological mechanotransducer. Using the *Aplysia* there were good prospects of developing an *in vitro* model to study mechanosensitivity. The basis for this optimism is that these neurons not only rearborize in culture, but also remember "who they are" *in vitro*, synapsing with the appropriate target motor neuron when given a choice (Glanzman et al., 1989). Since *in vivo* peripheral injury is a far more likely event than central injury, the likelihood that there has been selective pressure for correct peripheral regeneration of function is even higher than for central regeneration

of function.

Identified MSNs of *Aplysia* make monosynaptic connections with motor neurons in the CNS. These synaptic connections, and the synaptic changes associated with learning and memory, have been extensively studied at the sensory-motor synapse. However, the peripheral mechanosensitive terminals of these otherwise extensively studied neurons have not been characterized. Before we could attempt to regenerate a functional model of the mechanosensory endings *in vitro*, information was required about their structure *in vivo*. To obtain information about peripheral nerve endings, an antibody to a neuronal specific ß-tubulin was used on peripheral tissue. When a peptide specific to the *Aplysia* MSNs was discovered (sensorin-A, Brunet et al., 1991), I used an antibody to sensorin-A to directly examine the mechanosensory nerve endings in the periphery. To see if the mechanosensory machinery could regenerate, I asked if functional recovery occurs after the mechanosensory axons are severed *in vivo*. Finally, to see if the sensorin-A antibody could be used as a marker for MSNs in molluscs, sensorin-A immunostaining was performed on the CNS of the pond snail *Lymnaea stagnalis*.

CHAPTER 2

NEURAL STRUCTURES IN THE RECEPTIVE FIELD OF IDENTIFIED TAIL MECHANOSENSORY NEURONS OF *APLYSIA*

2.1 Introduction

Though *Aplysia californica* and related gastropod molluscs have simple nervous systems and correspondingly simple behavioural repertoires (Kandel, 1979), they have provided us with a detailed cellular understanding of important learning-related phenomena (Crow and Alkon, 1980; Walters and Byrne, 1983). Examination of *Aplysia*'s defensive withdrawal reflexes have been particularly powerful. Mechanical stimulation of the tail elicits a tail withdrawal reflex (Walters et al., 1983a; Walters, 1987a) comparable to the classical gill withdrawal response elicited by siphon stimulation (Byrne et al., 1974).

MSNs that innervate the tail of *Aplysia* have been identified. The cell bodies of these neurons are part of a cluster of about 200 homogeneous medium-sized cells on the ventrocaudal surface of each pleural ganglion (Walters et al., 1983a; Zhang et al., 1993). These MSNs make monosynaptic connections to tail motor neurons in the ipsilateral pedal ganglion, thereby strongly contributing to the short-latency tail withdrawal reflex. Although there is extensive electrophysiological evidence that these are primary sensory neurons (Walters et al., 1983a), the peripheral mechanosensitive

structures of these afferents have never been characterized. Recent electrophysiological evidence (Billy and Walters, 1989a; Woolf and Walters, 1991) indicates that noxious stimuli produce long term receptive field alterations that seem to involve sprouting of the peripheral mechanosensory processes. Clearly, there is a need to establish the morphology of these processes.

2.2 Materials and methods

Animals and dissection

Aplysia californica (100-200g, Marinus, Long Beach, CA) were maintained in aerated artificial seawater (SW; Forty Fathoms, Marine Enterprises, Baltimore, MD) at 15°C. Before dissection, animals were anaesthetized by injection of ~50% of their body weight with isotonic $MgCl_2$. *Aplysia* tissue from the tail region and from the posterior tentacles (rhinophores) was excised and cut into ~1 cm^3 pieces for immunohistochemistry and light microscopy, and into ~2-3 mm^3 pieces for scanning electron microscopy.

Immunohistochemistry

Tissue pieces were fixed in 4% paraformaldehyde in *Aplysia* seawater (ASW) for 4-6 h at room temperature (RT). ASW has the following composition (mM): NaCl, 460; KCl, 10; $MgCl_2$, 55; $CaCl_2$, 11; HEPES, 10; pH, 7.4 (adjusted with NaOH).

Following fixation, tissue was rinsed three times (5 min each) in phosphate buffered saline (PBS; pH 7.4), and then cryoprotected overnight in 15% sucrose in PBS. Samples were frozen in liquid isopentane at -40 to -60°C. 10 µm frozen cryostat sections were cut, collected on gelatin coated glass slides and kept at -20°C. Sections were rehydrated in PBS and then incubated in 10% normal goat serum in PBS with 0.3% Triton X-100 for 1 hr at RT. After triple-rinsing in PBS, sections were incubated with a monoclonal antibody against class III ß-tubulin (TuJ1; gift of Anthony Frankfurter; Lee et al., 1990b), at 1:100 in PBS with 0.3% Triton X-100, overnight at 4°C. After this primary antibody incubation, sections were triple-rinsed in PBS and incubated in a goat anti-mouse secondary antibody conjugated to the stable fluorophore dichlorotriazinylaminofluorescein (DTAF; Jackson Immunoresearch, West Grove, PA), at a dilution of 1:20 in PBS with 0.3% Triton X-100, for 1 hr at RT. Fluorescein was used instead of rhodamine since *Aplysia* tissue is autofluorescent in the wavelengths used for rhodamine. Following three PBS rinses, cells were mounted in 40 mM n-propyl gallate (a reagent used to reduce photobleaching; Giloh and Sedat, 1982; Sigma, St. Louis, MO) in 2:1 glycerol in PBS and viewed on a Carl Zeiss Universal microscope equipped with epifluorescence optics. Micrographs were taken on Ilford XP1-400 film.

Light microscopy

For Giemsa (BDH, Toronto, Canada) staining, 10 µm frozen sections were rinsed in 0.1M phosphate buffer pH 7.4 (PB) and then incubated in Giemsa solution

at 60°C for 7-10 min. Giemsa solution was diluted 1:10 in PB. After incubation in Giemsa, sections were rinsed in PB, dehydrated in 100% ethanol (three 15 min rinses), rinsed twice in xylene (5 min each) and mounted in Aquamount (BDH).

Scanning electron microscopy

Tissue pieces were fixed in 2% glutaraldehyde in ASW for 4-6 hrs at RT, then rinsed in ASW. For removal of surface mucous, tissue was incubated overnight in 16% glycerol at 4°C (Zaitseva and Bocharova, 1981). Tissue was rinsed in 20% ethanol for 15 min, then briefly in distilled water and postfixed in 1% OsO_4 in 0.1M sodium cacodylate buffer for 1 hr at RT. Samples were partially dehydrated in ethanols (15 min in both 25% and 50% ethanol, then into 70% ethanol), quick frozen in cooled liquid nitrogen at -210°C and freeze-dried in a vacuum (pressure 10^{-5} torr) to -70°C. Samples were coated with aluminum, placed on an Oxford cryostage (-180°C) and examined with a JSM-6400 scanning electron microscope.

2.3 Results

Immunofluorescent staining of *Aplysia* neurons with anti-ßIII

Class III ß-tubulin is a tubulin isotype expressed at the onset of neuronal differentiation; in higher vertebrates, class III ß-tubulin is neuronal-specific with the exception of a testis isoform (Lee et al., 1990a). We therefore wondered if

immunofluorescent staining of *Aplysia* tissue with the class III ß-tubulin antibody TuJ1 would stain neuronal tubulin and allow us to trace tracts to the periphery to look for mechanosensory processes. Figure 2.1 shows longitudinal (2.1 A,B) and cross-sectional (2.1 C,D) images of deep nerve tracts in the tail region of the *Aplysia*; it is clear that the axonal tracts, but not the surrounding tissue (muscle, connective tissue) are intensely immunoreactive with TuJ1. The scattered staining surrounding the nerve trunks can presumably be attributed to neurites and bundles branching off the main trunks. A control section containing both the dorsal and ventral tail incubated with the secondary antibody alone showed no immunofluorescence (Fig. 2.1 E,F).

The next step was to follow tracts in the periphery and localize putative sensory processes of pleural ganglion MSNs. As shown by Walters et al. (1983a) the receptive fields for the MSNs of the pleural ganglia occur in the dorsal and ventral tail. Given its locomotory and profuse mucous-secreting activities, the body wall of the ventral tail should be more heterogeneous in its innervation than the essentially mechanosensory dorsal tail. We therefore concentrated on the pattern of innervation of the dorsal tail. In the dorsal tail nerve bundles generally did not branch into finer processes until they reached the level of the subepidermis (Fig. 2.2 A-D). Had MSNs terminated as free endings in the connective tissue, a pattern of fluorescence ramifying below the epidermis should have been evident. Instead, the finest branches off the main trunks protruded through the epidermis at right angles and emerged at the external surface of the body. It was often possible to focus through a section, following individual processes from a major trunk to the surface. In no case did we observe fine processes

connected to fluorescent profiles that resembled cell bodies. The heavy innervation expected in the ventral tail is seen in Figures 2.2 E,F; part of this fluorescent staining is due to the same transepidermal pattern seen in the dorsal tail. As is strikingly evident in Figure 2.2 F, tubulin in the locomotory cilia of the ventral surface also stained with the TuJ1, suggesting that TuJ1 binds to more than one tubulin isotype in *Aplysia.*

Comparison of mechanosensory and chemosensory epidermal regions

TuJ1 staining can not discriminate among the different types of neuronal processes expected in the body wall (peripheral processes of MSNs, peripheral chemosensory processes, motor neuron terminals), but in the dorsal tail, we have been able to conclude, on two grounds, that sensory processes predominate. First, the dorsal tail lacks the major locomotory functions of the ventral tail (foot) and second, motor terminals should innervate subsurface targets (ie. muscle cells, gland cells, ciliated epithelial cells; Audesirk 1978; Syed and Winlow 1989) and so would not be expected to penetrate to the exterior. Thus, nerve processes that penetrate the epidermis are probably sensory in nature, but they could be chemosensory rather than mechanosensory. Comparison with TuJ1 immunostaining of the chemosensory groove of the *Aplysia* rhinophore (a structure described at the TEM level; Emery and Audesirk, 1978), however, suggests that the processes we observed in the dorsal tail are not chemosensory. Figures 2.3 A,B are a section from the rhinophore showing both inner chemosensory groove and mechanosensory exterior. Whereas the inner groove of the

rhinophore is highly chemosensitive, its exterior is unresponsive to chemical stimulation (Jahan-Parwar, 1969; Preston and Lee, 1973); rather, it exhibits mechanosensitivity (Preston and Lee, 1973). TuJ1 immunostaining of the chemosensory region of the rhinophore revealed a strikingly different pattern from that in the mechanosensory region of the rhinophore and from the dorsal tail. Consistent with the TEM study (Emery and Audesirk, 1978) the inner groove (Fig. 2.3 C,D) had a high density of epidermis-penetrating processes and local neuronal cell bodies organized as ganglia beneath the sensory epidermis. At higher magnification, (Fig. 2.3 E,F) it was evident that cell bodies had modified dendrites terminating distally as sensory cilia and axons converging proximally to form large tracts. These sensory cilia were also immunoreactive with TuJ1. Since TuJ1 reacted with ciliary tubulin, it is not surprising that the ciliated endings of the chemosensory neurons were readily evident. A comparison of the chemosensory rhinophore and the mechanosensory dorsal tail at the same magnification (compare Figs. 2.2 B, 2.2 D with 2.3 F) demonstrates that neuronal profiles typical of the chemosensory epidermis are absent from the dorsal tail. Electrophysiological evidence (Walters et al., 1983a) suggests that the somata of mechanosensory neurons are central (that is, in the pleural ganglia) and indeed, we saw no evidence of peripheral neuronal cell bodies in the dorsal tail. Also, if long ciliated endings similar to those in the chemosensory groove were present in the dorsal tail, they would have been detected at this magnification. By comparison, neural endings in the epidermis of the dorsal tail appeared to extend at most a few microns beyond the epidermal surface.

To further examine whether neurons that penetrate the epidermis of mechanosensory regions are associated with peripheral cell bodies, we stained for neuronal cell bodies using Giemsa. Giemsa stains the Nissl substance of neuronal somata; in *Aplysia*, it evidently also stains epidermal cells to varying degrees, but the colour is unlike that for neurons (it is brown instead of purple). The purple staining characteristic of neurons was seen for the known (Emery and Audesirk, 1978) neuronal cell bodies underlying the chemosensory epidermis of the rhinophore (Fig. 2.4 A, although colour not shown) but was absent from 3 mechanosensory epidermises: outer rhinophore (Fig. 2.4 B), dorsal tail (Fig. 2.4 C) and siphon (Fig 2.4 D).

Scanning electron microscopy

If our interpretation of the immunofluorescent images of mechanosensory epidermal surfaces is correct, that is, if mechanosensory processes penetrate the epidermis, then they may extend beyond the surface far enough to be observed as specialized structures in scanning electron micrographs. TEM studies (see Steffensen et al., 1994) have shown that the epidermal cells of the dorsal tail usually bear microvilli, and those of the ventral tail usually bear cilia. Ciliated epidermal cells of the type common to the ventral surface are rarely encountered in the dorsal epidermis. The subepidermis of the ventral tail has been shown to contain far more gland cells (necessary for ciliary locomotion) than the subepidermis of the dorsal tail.

Scanning electron microscopy (SEM) of the mechanosensitive surface of the dorsal tail revealed tufts of either short cilia or microvilli. These tufts extended beyond

the microvillar brush border by as much as 5 μm (Fig. 2.5 A-C) and were uniformly distributed at a density of approximately one per 350 μm^2. Similar structures were also seen on the surface of the siphon, but at a higher density (approximately one per 200 μm^2; Fig. 2.5 D,E). If the width of an epithelial cell is approximately 5 μm then we could expect a sensory receptor for every 14 cells in the dorsal tail and one for every 8 cells in the siphon. SEM of the chemosensory surface in the rhinophore showed tufts of long (at least 15 μm beyond the adjacent microvilli) interweaving cilia spreading across the surface (Fig. 2.5 F,G). On the basis of TEM images of this tissue (Emery and Audesirk, 1978), these are the ciliated chemoreceptors. As expected, the ventral surface of the tail (Fig. 2.5 H) was covered with the cilia of ciliated epidermal cells. Sensory structures were not readily identifiable amid the dense network of cilia.

TEM of the dorsal tail (see Steffensen et al., 1994) has revealed neural structures that could correspond to the structures that were observed with SEM. These structures consisted of fine neurites that wedged their way up between epidermal cells and could sometimes be seen to reach the surface. Their distal end, which was composed of cilia and long microvilli, formed a tuft that reached beyond the outer surface of the microvillar brush border.

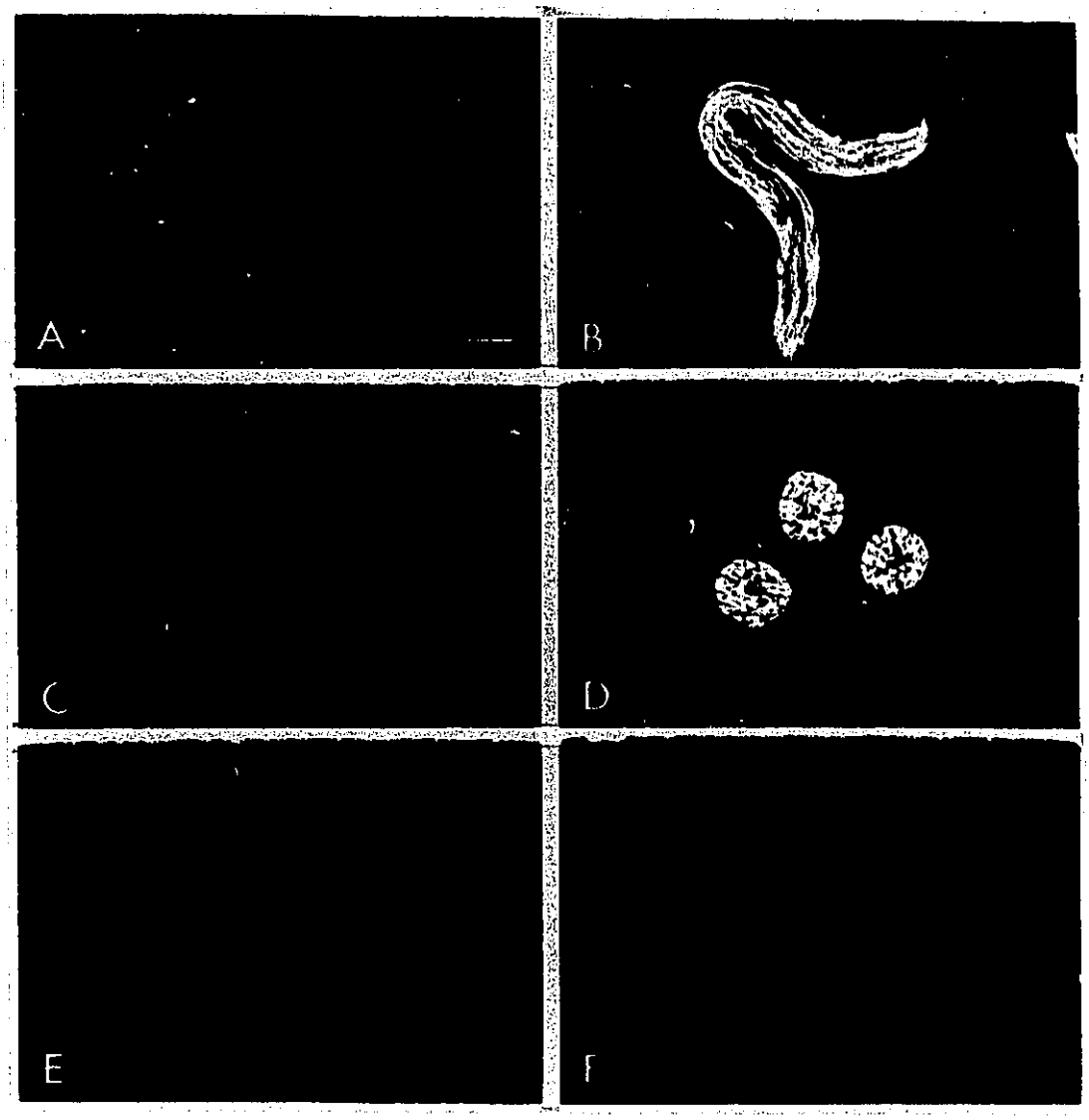

Figure 2.1. Immunofluorescence with TuJ1 as a neuronal marker in *Aplysia*. Phase contrast (**A**) and fluorescence (**B**) micrographs of a longitudinal section through a deep nerve tract in the tail region. **C**, phase contrast and **D**, fluorescence micrographs of a cross section of three deep nerve tracts from the same region. A control section containing both dorsal and ventral tail labelled with the DTAF-conjugated secondary antibody alone does not show any immunofluorescence (**F**). Corresponding phase contrast micrograph (the tissue on the left is the dorsal tail and that on the right is the ventral tail region from two serial sections) is shown in **E**. Bar: A-D, 25 μm; E,F, 50 μm.

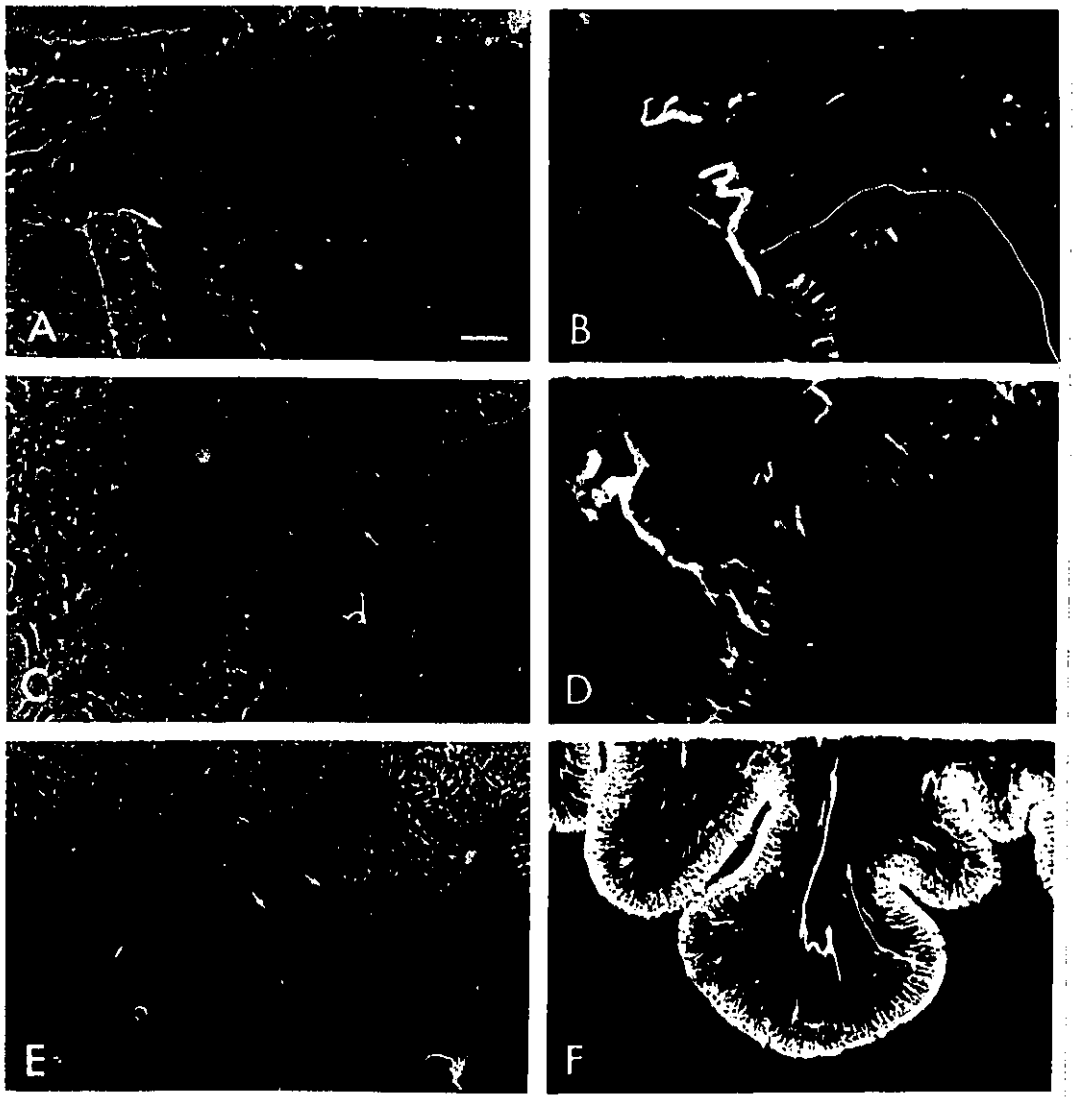

Figure 2.2. Comparison of TuJ1 staining in the dorsal and ventral tail of *Aplysia*. **A** and **C**, phase contrast micrographs of the dorsal tail. The corresponding fluorescence micrographs (**B** and **D**) reveal peripheral nerve tracts (eg. arrow in **B**) and finer processes penetrating the epidermis. Most of the out-of-focus fluorescence in the epidermis represents similar processes in focal planes other than that chosen for the micrograph. **E** and **F** are the phase contrast and corresponding fluorescence micrographs of the ciliated ventral tail. The ciliated epidermis of the ventral tail is highly innervated. Arrows indicate fragments of nerve tracts. Note that the cilia on the ventral tail stains intensely with TuJ1. Bar: A-D, 25 μm; E,F, 50 μm.

Figure 2.3. Establishing the TuJ1 staining pattern of a chemosensory epidermis in *Aplysia.* TuJ1 staining of the posterior tentacle (rhinophore): **A**, phase contrast micrograph of the rhinophore showing the chemosensory surface (arrow) and the mechanosensory exterior. Corresponding fluorescence micrograph (**B**) shows that the chemosensory (arrow) and mechanosensory epidermises have different staining patterns. The exposure used for **B** represents a compromise between overexposure of the chemosensory surface and underexposure of the mechanosensory surface. Phase contrast (**C**) and fluorescence (**D**) micrographs through the chemosensory groove (same section as **A** and **B** but optimal exposure). A higher magnification of this area (**F**) shows neuronal cell bodies in small ganglia beneath the sensory epidermis (curved arrow). These cell bodies terminate distally as sensory cilia in the groove, and proximally their axons join to form large tracts (straight arrow; this arrow is also in the lower magification micrographs **A-D**). **E**, corresponding phase contrast micrograph. Bar: A-D, 100 μm; E,F, 25 μm.

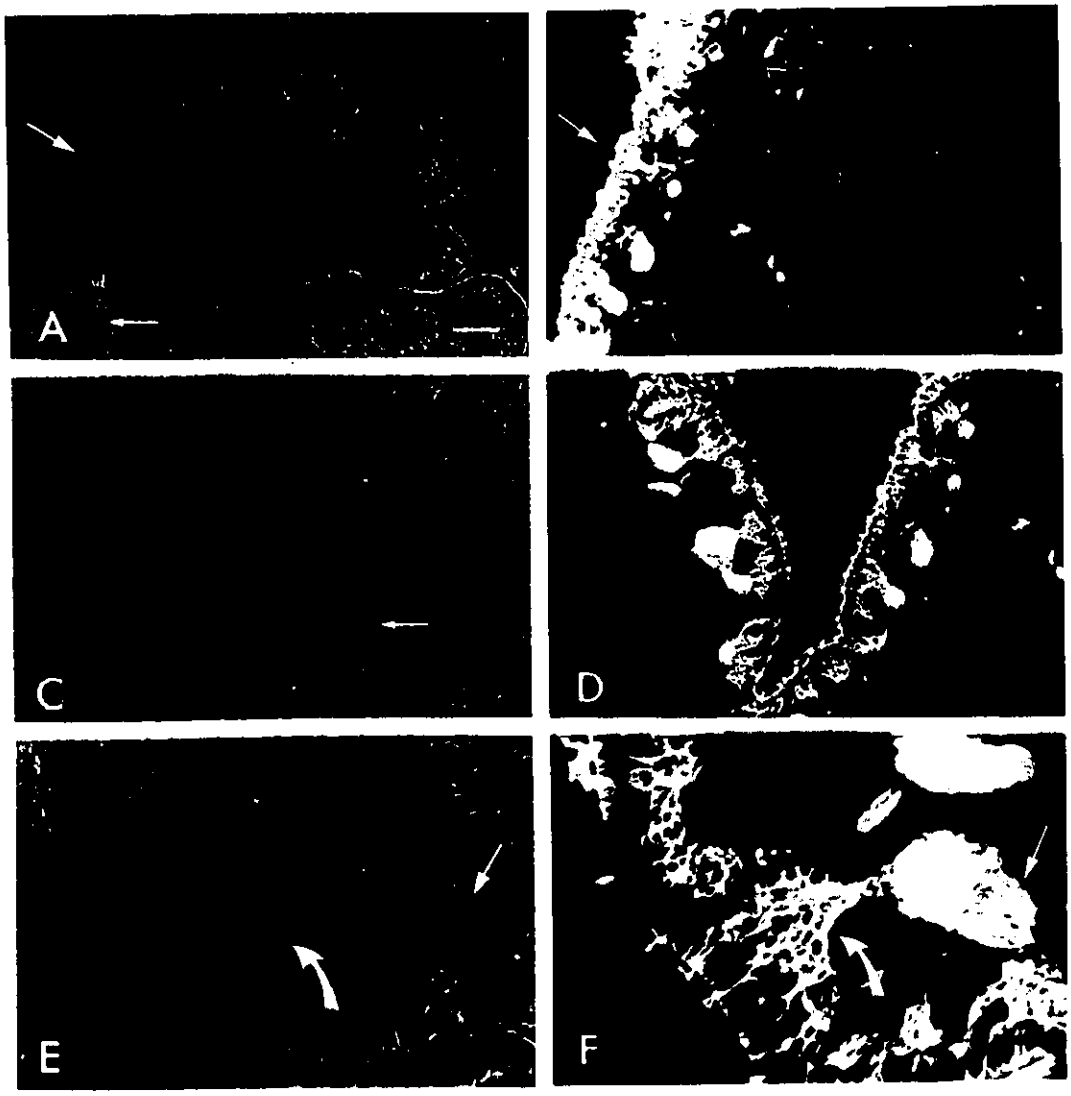
A
C
D
E
F

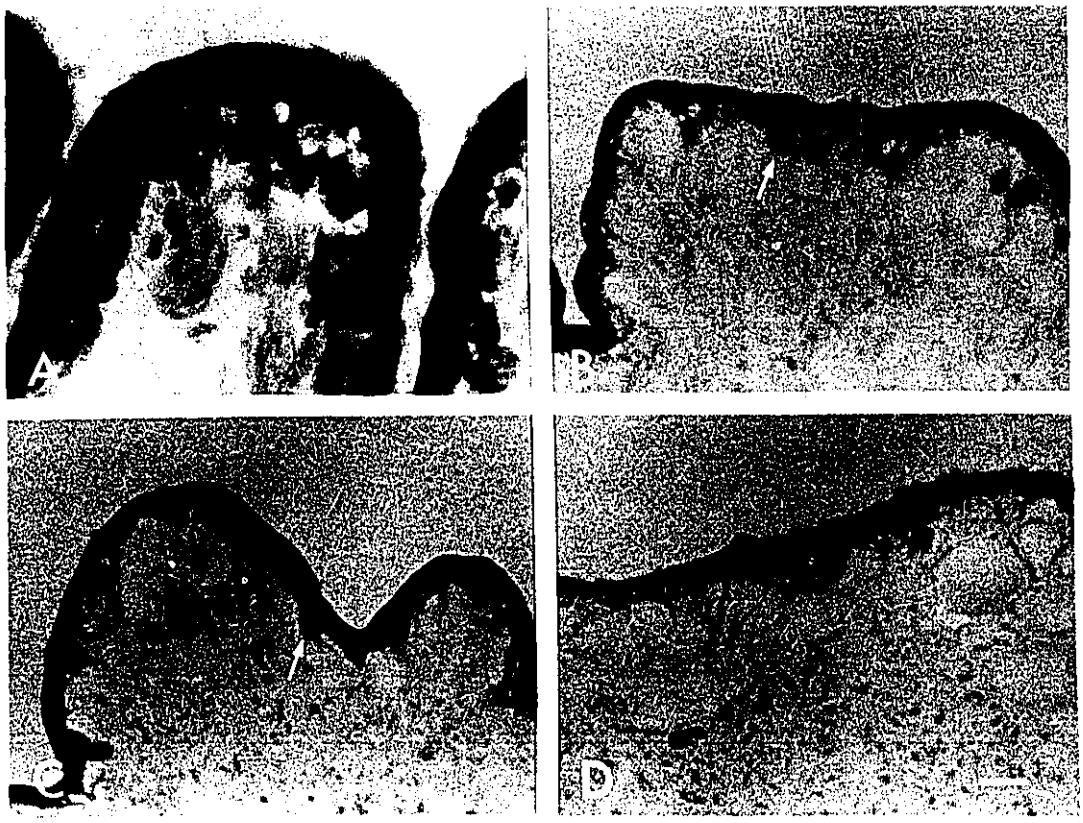

Figure 2.4. Confirmation of peripheral neuronal somata beneath the chemosensory but not mechanosensory epidermis. Bright field micrographs of sections from chemosensory and mechanosensory regions that have been stained for neuronal cell bodies using Giemsa. Cell bodies (arrow) are clustered beneath the chemosensory epidermis in the rhinophore (**A**). However, similar cell bodies are not seen beneath the mechanosensory epidermis of the tentacle (**B**), dorsal tail (**C**) or siphon (**D**). Note that although the mucous cells do not stain with Giemsa they are also detected with light microscopy (arrows in **B** and **C**). Bar: 50 μm.

Figure 2.5. Scanning electron microscopy of mechanosensory and chemosensory regions. **A** and **B**, the dorsal mechanosensory surface of the tail shows the presence of uniformly distributed tufts of either cilia or microvilli. **C**, high magnification of a putative sensory structure. The mechanosensitive surface of the siphon (**D**) posseses structures similar to those of the mechanosensory tail but at a higher density. **E**, a higher magnification of this area. The surface of the chemosensory groove in the rhinophore (**F**) shows an abundance of ciliated structures, the chemoreceptors, spread over the surface. **G**, a solitary chemoreceptor bearing numerous long interweaving cilia. The ventral surface of the tail (**H**) is covered with ciliated epidermal cells. Bars: 5 μm.

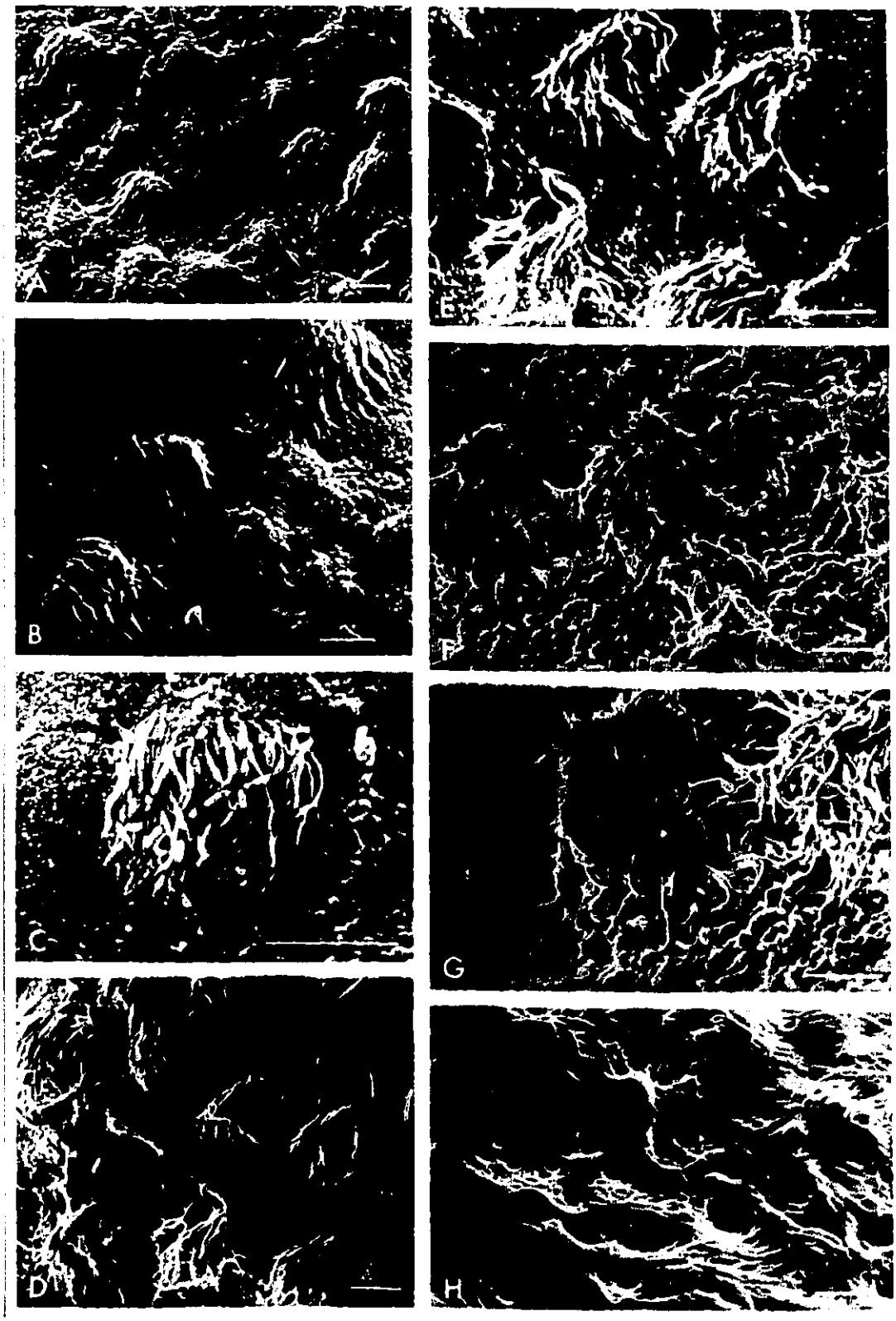
A
B
C
D
E
F
G
H

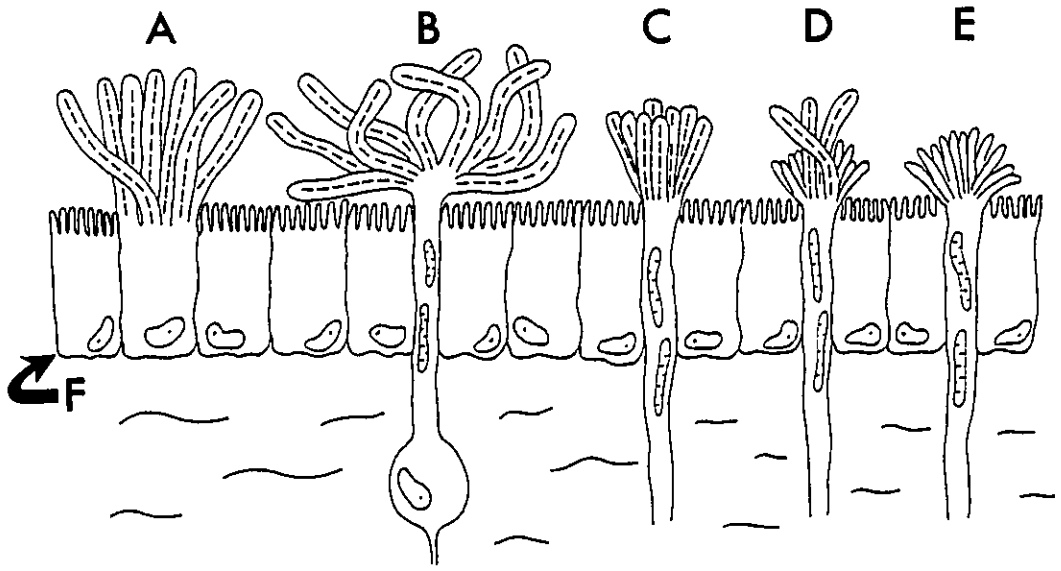

Figure 2.6. Schematic diagram of previously described epidermal sensory structures of gastropod molluscs. **A**, a ciliated epithelial cell. **B**, a chemosensory structure with numerous (20-40), long (15 μm) interwoven cilia. **C**, a sensory process with cilia that are apparently stiff and can be long (9-12 μm), short (2-6 μm) or both. In **D**, flexible cilia (5-12 μm) arise from the central portion of the dendrite with the remaining area occupied by rather long microvilli. **E**, afferents with only microvilli (1-6 μm) at their surface. **F**, a microvillied epithelial cell. Dashed lines represent cilia. (Zylstra, 1972; Wright, 1974; Emery and Audesirk, 1978; Philips, 1979; Zaitseva and Bocharova, 1981).

2.4 Discussion

Although HRP has been used effectively to trace central processes of *Aplysia* MSNs (Nazif et al., 1991), HRP and other traditional injection markers (ie. lucifer yellow) are unsuitable for the more distant peripheral processes. The approach we have used here - immunofluorescent staining with TuJ1 as a neuronal marker- does not distinguish efferents from afferents. Nonetheless, by comparative observations on functionally different epidermal regions, and by using a process of elimination, we reasoned that the immunofluorescent processes that penetrate to the epidermal surface of the dorsal tail may be mechanosensory.

SEM of the dorsal tail (and further comparisons with other regions), and TEM of the dorsal tail (see Steffensen et al., 1994) are consistent with the idea that the epidermis-penetrating processes are a type of ciliated free nerve ending (eg. Wright, 1974). The TEM images of ciliated neural processes (Steffensen et al., 1994) would lead one to expect that in SEM ciliated structures would be seen extending beyond the uniform brush border surface. Such structures were indeed seen. Apart from the carpet of microvillar tips of the brush border, tufts of short cilia and/or long microvilli (one can not distinguish between these two at SEM level) were the major feature of the dorsal tail. These tufts were uniform in appearance and were distributed in the roughly uniform manner one would have expected from the immunofluorescent images. It is most unlikely that these represent locomotory cilia - they are too short -and in any case, both TuJ1 staining and TEM (Steffensen et al., 1994) indicate that locomotory cilia are extremely rare in the dorsal tail. On the siphon, a tissue considered to be

extremely mechanosensitive (Byrne et al., 1978), similar structures were seen at an even higher density.

Epidermis-penetrating neural processes have been described in a variety of gastropods, and though it has often been suggested that certain of them are mechanosensory (eg. Theler et al., 1987), this has been conjecture. Figure 2.6 summarizes the morphology of epidermal sensory processes that have been described in gastropod molluscs. Although afferents with long interweaving cilia (Fig. 2.6 B) have been shown to be chemosensory, the sensory modality of the other structures (Fig. 2.6 C-E) is unknown. Of these "models" the dorsal tail processes most closely resemble type d with its mix of cilia and microvilli (determined by TEM, see Steffensen et al., 1994); the dorsal tail structures differ however, in that the cilia and microvilli appear to be the same length. In squid, a receptor organ that may serve a proprioceptive function (Preuss and Budelmann, 1991) contains clusters of ciliated primary sensory neurons whose structures would be categorized as type c. Mechanosensory processes with ciliated endings have also been described in *C. elegans* (Perkins et al., 1986).

The evidence presented here falls short of proving that the afferent processes of the pleural ganglion MSNs are a type of ciliated and/or microvillar structure. The possibility remains that the epidermal processes are associated not with pleural ganglion MSNs but with undetected cell bodies such as those embedded in peripheral nerve tracts (Bailey et al. 1979) or even with yet-to-be identified central MSNs. Another possibility - that the sensory processes ramify below the epidermal cells or form

dilations like the stretch receptor processes in the body wall of the leech (Blackshaw and Thompson, 1988) - seems unlikely. We saw no evidence of these configurations either with TEM or with TuJ1 staining.

Future studies using SEM, TEM and TuJ1 staining coupled with behavioural testing of the tail withdrawal reflex, before and after crushing the nerve trunk carrying the mechanoafferents (p9), would help determine whether the ciliated processes are the mechanotransducers. Antibodies to the recently described MSN-specific peptide, sensorin-A (Brunet et al., 1991), will undoubtedly prove valuable. If it is confirmed that these techniques reveal the mechanosensitive processes, antibody staining plus electron microscopy could be used to seek the morphological correlate of the increased peripheral excitability exhibited by these MSNs following noxious stimulation (Billy and Walters, 1989a).

CHAPTER 3

SPINDLE-LIKE MECHANORECEPTORS IN *APLYSIA* REVEALED BY SENSORIN-A IMMUNOFLUORESCENCE AND CONFOCAL MICROSCOPY

3.1 Introduction

Using differential screening of *Aplysia* cDNA libraries, Brunet et al. (1991) have isolated a peptide, sensorin-A, that is specific for the *Aplysia* MSNs. To determine if the cilia/microvilli endings that were described in Chapter 2 are indeed the sensory endings of the identified tail MSNs, immunostaining with an antibody against sensorin-A was performed in the periphery. Sensorin-A immunofluorescence in the tail region did not colocalize with the ciliated sensory structures. However, it did reveal the terminals of the "sensorin-A" tail MSNs.

3.2 Materials and Methods

Animals and dissection

Aplysia californica (100-200g, Marinus, Long Beach, CA) were maintained in artificial SW at 15°C. Prior to dissection, animals were anaesthetized by injection of ~50% of their body weight with isotonic $MgCl_2$. For immunohistochemistry and

confocal microscopy, body wall tissue was dissected from the posterior tail region and cut into ~1 cm^2 pieces. For immunogold electron microscopy, the pleural ganglia were desheathed, and sensory clusters were dissected from the ganglia.

Immunohistochemistry

Aplysia tissue was fixed in 4% paraformaldehyde in ASW. Following fixation, tissue was rinsed three times in PBS (10 min each) and then immersed overnight (at 4°C) in PBS with 15% sucrose to cryoprotect the tissue. Samples were frozen in liquid isopentane at -40 to -60°C, and 10 µm frozen cryostat sections (transverse sections of the tail) were cut and collected on gelatin coated glass slides. Frozen sections were incubated for 4-6 hrs in a blocking solution consisting of 10% normal goat serum (Jackson), 1% bovine serum albumin (BSA, Sigma) and 0.4% Triton X-100 in PBS. After a single quick rinse in washing buffer (0.1% Triton X-100 in PBS), sections were incubated overnight at 4°C with a rabbit polyclonal antiserum raised against sensorin-A (Brunet et al., 1991; gift from E. Kandel and R. Hawkins) at 1:400 in PBS with 0.4% Triton X-100. Following the primary antibody incubation, sections were rinsed four times in washing buffer (10 min each) and then incubated overnight at 4°C with a DTAF conjugated goat anti-rabbit secondary antibody (Jackson) at 1:100 in PBS with 0.4% Triton X-100. After three rinses in washing buffer (10 min each), sections were mounted in a 3:1 solution of glycerol in PBS with 1% n-propyl gallate. Sections were viewed with a Zeiss Universal microscope equipped with epifluorescence optics, and with a Leica Confocal microscope and imaging system. Photomicrographs were taken

on Kodak Echtachrome-400 film.

Immunoelectron microscopy

Aplysia nervous tissue was fixed for 1 hr in 4% paraformaldehyde in ASW at RT and then rinsed three times (10 min each) in PBS. Paraformaldehyde was used instead of glutaraldehyde, since sensorin-A immunoreactivity was absent in glutaraldehyde (0.01%) fixed tissue. Following fixation, tissue was dehydrated in a graded ethanol series, two times for 15 min each in 30%, and 1 hr each in 50, 70 and 90%. Tissue was infiltrated by incubating (two times for 45 min each) in a 1:1 90% ethanol-LR White mixture at -20°C and then in 100% LR White for 12 hrs at -20°C. Tissue was embedded in LR White in gelatin capsules and polymerized with UV light (sensorin-A immunoreactivity was destroyed when heat was used to polymerise capsules) for 12 hrs at 4°C. Ultrathin sections (silver to gold interference colours) were collected on to nickel grids. Sections were incubated for 1 hr in a blocking solution (1% normal goat serum and 1% BSA in PBS with 0.05% Tween), rinsed briefly in PBS and then incubated for 1 hr in anti-sensorin-A (1:400 in PBS with 1% BSA and 0.05% Tween). Following primary antibody incubation tissue was rinsed in PBS, incubated for 1 hr in a 10nm gold-conjugated goat anti-rabbit secondary antibody (1:100 in PBS with 1% BSA and 0.05% Tween; Sigma) and then rinsed in PBS. Sections were stained for 1 min in Reynold's lead citrate, rinsed in distilled water, stained for 5 min in 1% uranyl acetate in 50% methanol and rinsed in 50% methanol. Sections were examined on a Philips 300 electron microscope.

3.3 Results

Sensorin-A immunofluorescence and confocal microscopy

To determine if sensorin-A was present in peripheral mechanoafferents in the tail region, sensorin-A immunostaining was performed on frozen sections of the posterior tail. In the tail region, immunofluorescence revealed a subset of fibers in peripheral nerve tracts that were sensorin-A immunopositive (Fig. 3.1). All nerve tracts (nerve tracts could be identified by phase-contrast microscopy) were observed to contain sensorin-A fibers, and the proportion of fibers that were sensorin-A positive was similar in all tracts.

To follow MSNs in the periphery and to examine the structure of sensory terminals, sensorin-A fibers were traced in the tail region. In the body wall, nerve tract segments decreased in size as they advanced towards the epidermal layer (see Fig. 3.4). In the muscular layer of the body wall, nerve tracts branched to the point where single sensorin-A fibers (eg. Fig. 3.3 B) were observed among the muscle tissue. Sensorin-A fibers did not penetrate to the epidermal layer, where the sensory endings described in Chapter 2 are located (see Fig. 3.4). Focusing through the tissue sections revealed single sensorin-A fibers which appeared to form coiled structures (Fig. 3.2). Upon repeatedly switching between phase-contrast microscopy, which reveals muscle fibers, and conventional fluorescence microscopy, it appeared that the sensorin-A fibers coiled around muscle fibers.

Although this intricate structure could be inferred from the collective image seen

while focusing, it could not be depicted in a single image; with conventional fluorescence microscopy at high magnifications, out-of-focus fluorescence causes blurring of the image. Thus, to further examine these structures, confocal microscopy of sensorin-A fibers was performed. Confocal microscopy revealed that the coiled structures were 2-3 μm wide, ~60 μm long and had a clearly helical structure with a pitch of ~1 turn per 4 μm, with varicosities present along the coil (Fig. 3.3 B,C). Scanning through a coiled structure within a section revealed that the sensory fiber terminated at the end of a coil, suggesting that the coils constitute true nerve endings (see Fig 3.4).

Confocal microscopy revealed that sensorin-A fibers in nerve tracts, and single sensorin-A fibers, are also beaded with varicosities (Fig. 3.3 A,B). In all cases, the most intense staining was associated with varicosities (Fig. 3.3).

Immunoelectron microscopy

Electrophysiological experiments (Brunet et al., 1991) have suggested that sensorin-A acts as an inhibitory neurotransmitter centrally. To determine if sensorin-A is localized to dense granules or dense-core vesicles, as would be expected for a neuroactive peptide, immunogold staining for TEM was performed. The sensorin-A antigen was found to be sensitive to several processing steps found in standard immunogold protocols for electron microscopy. The optimal protocol for immunogold labelling of sensorin-A involved using paraformaldehyde as a fixative, using the acrylic resin LR White as an embedding media, and, using UV light to polymerize capsules.

In addition, post-fixation with osmium tetroxide could not be performed; osmium tetroxide reacts strongly with lipids, and since it is electron dense it tends to mask gold particles. Although sensorin-A immunoreactivity was maintained under these conditions, the morphological preservation was not optimal. To facilitate localization of the peptide, immunogold staining was performed on isolated MSNs. Gold particles were localized mainly to dense granules and dense-core vesicles (Fig. 3.6) in the extranuclear region of the cell body (Fig. 3.5). Some of the "dense-granules" may actually be dense-core vesicles, since membranes were difficult to observe. Gold particles were also observed free in the extranuclear cytoplasm (Fig. 3.6). No gold particles were observed in a control experiment (Fig. 3.7)

Figure 3.1. Immunostaining for sensorin-A in the tail region reveals sensory fibers in peripheral nerve tracts from the p9 nerve. Phase contrast **(A)** of a section taken from deep in the tail region. The fluorescent micrograph of the same region **(B)** reveals a subset of nerve fibers that are immunopositive for sensorin-A in the three large nerve tracts that are present in this section. Fibers can be seen longitudinally (long arrow) and in cross-section (short arrow). Bars: 25 μm.

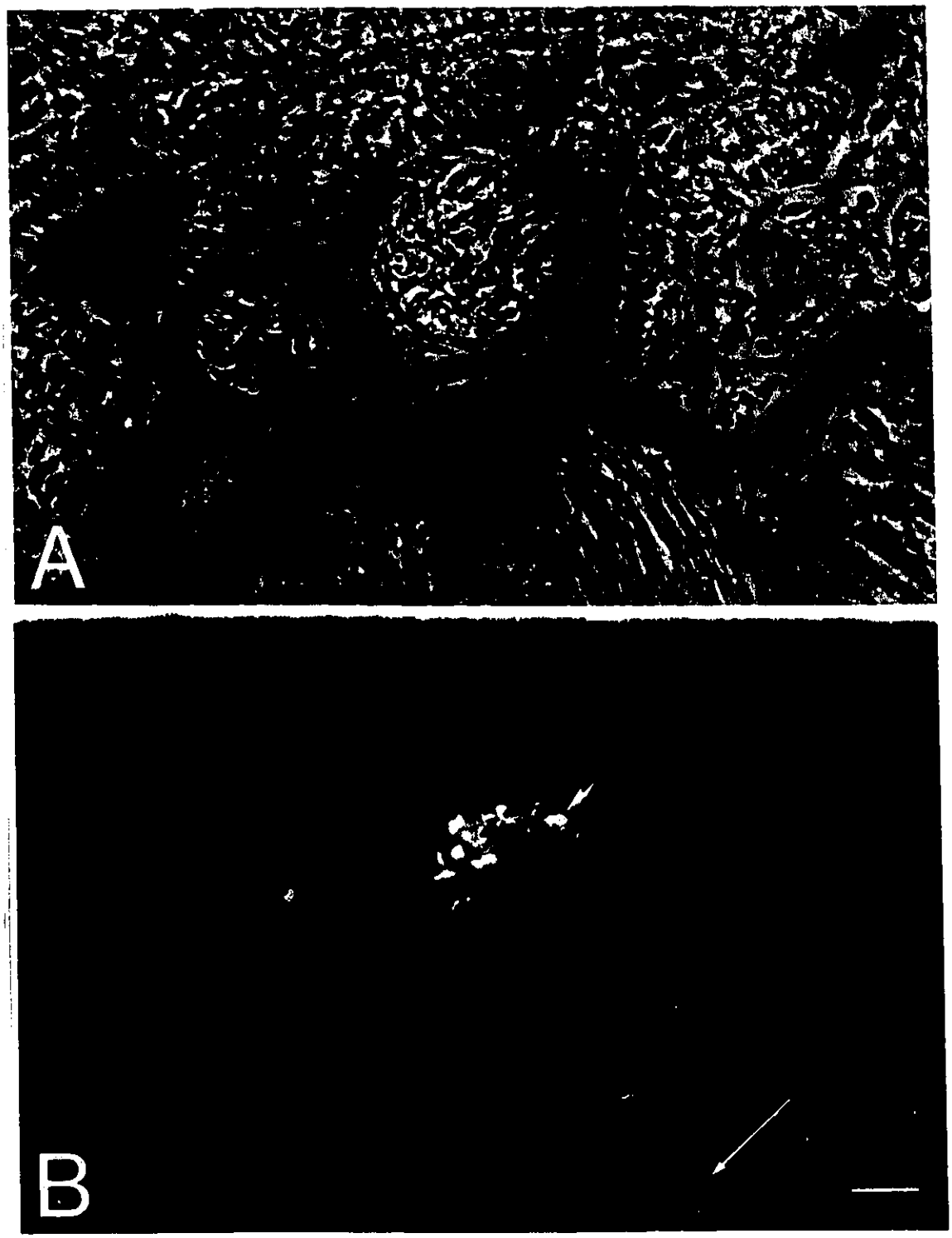
A
B

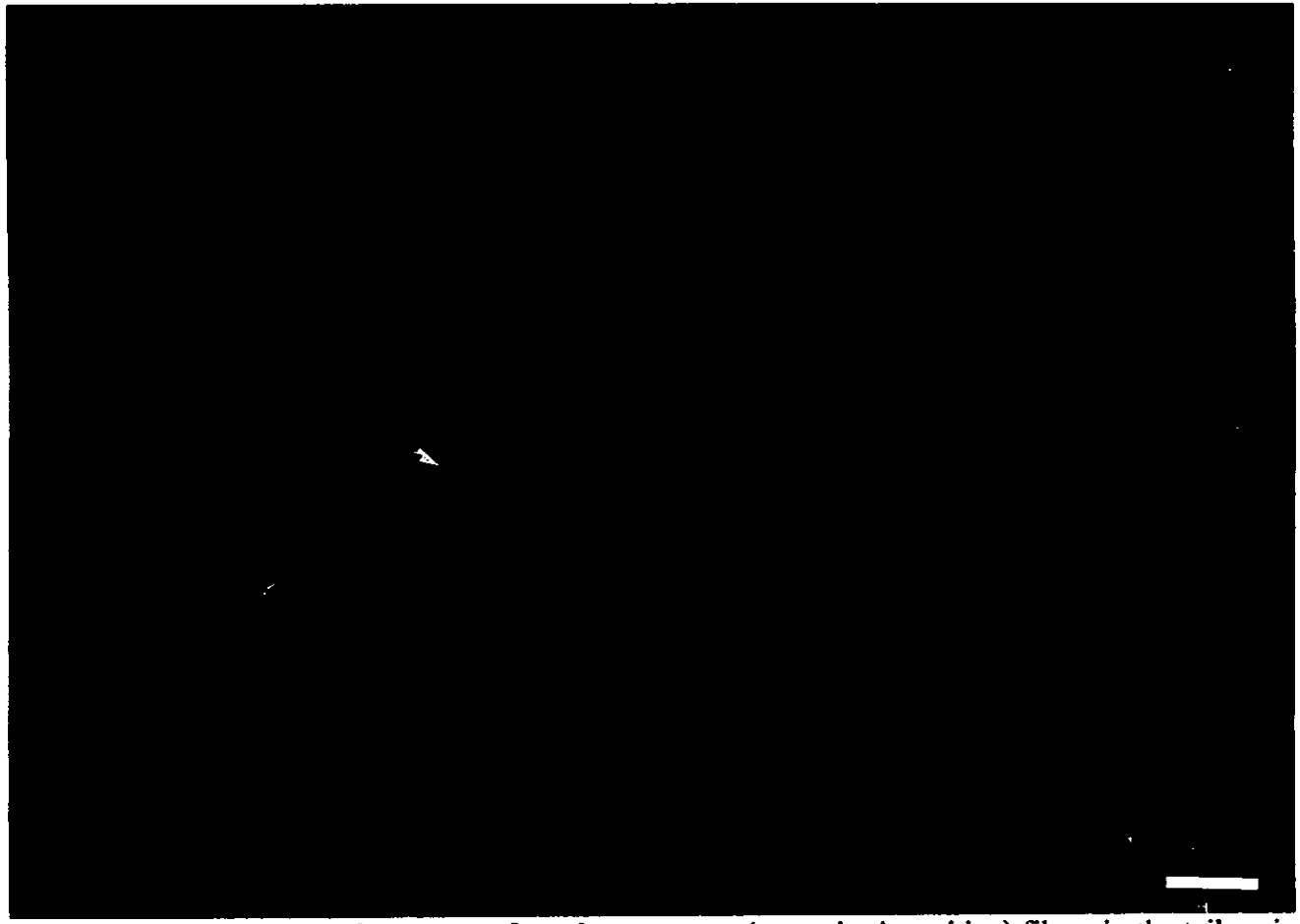

Figure 3.2. Conventional fluorescence microscopy of mechanosensory (sensorin-A positive) fibers in the tail region. Fine fibers form coiled structures (arrow) deep in the body wall. With this technique, the coiled structure is most readily discerned if one focuses up and down through the tissue section. Bar: 25 μm.

Figure 3.3. Confocal microscopy of sensory fibers in the tail region immunostained for sensorin-A. Images are computer reconstructions of 20 planes, 0.5 μm apart, through a 10 μm tissue section. A longitudinal section through a nerve tract **(A)** shows a number of sensory fibers; in **B** a tract which has branched to the point where it contains only a single mechanosensory fiber. Sensorin-A staining has a "beads on a string" appearance, suggesting the presence of varicosities (see arrows) along the fiber. **C, D,** confocal micrographs of coiled structures coursing through tissue sections. Note the clearly helical structure (arrowheads in **D**) that is often observed in the reconstructions of these processes. These appear to be true nerve endings; in both **C** and **D**, the uppermost end was a termination point within the section. Note that varicosities occur along the helical coils. Bars: 10 μm.

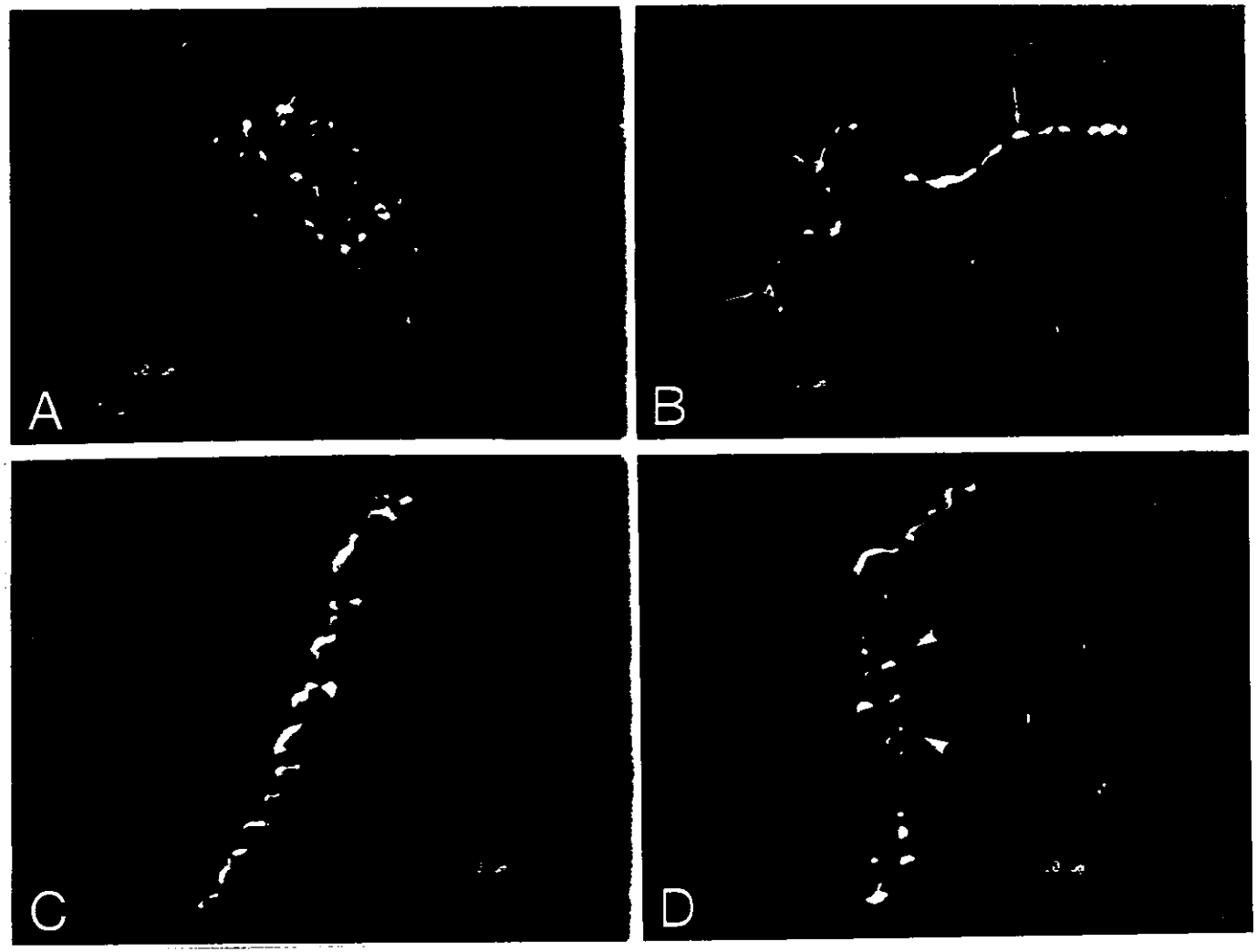
A
B
C
D

Figure 3.4. Schematic diagram summarizing the peripheral structure of *Aplysia* MSNs. **A**, cross-section of the posterior tail of *Aplysia* showing the layer of body wall (shaded area, actual width ~3mm) in which sensorin-A fibers terminated. **B**, boxed area depicted in **A**, illustrating the peripheral innervation pattern of the *Aplysia* MSNs. Boxed area in **B** shows the location of MSNs described in Chapter 2. **C**, the orientation of coiled terminals within tissue sections, as was observed with confocal microscopy. **D**, a comparison between the coiled terminals of mechanical nociceptors in *Aplysia* (1) and the leech (2; Blackshaw et al., 1982) approximately to scale. In the leech, coiled terminals are ~70 μm across and, since they wrap around a flat disc structure (ie. an expanded dendritic region in the leech stretch receptor neuron; Blackshaw and Thompson, 1988) only a few μm deep, whereas, in *Aplysia*, coils are a few μm across and ~60 μm long.

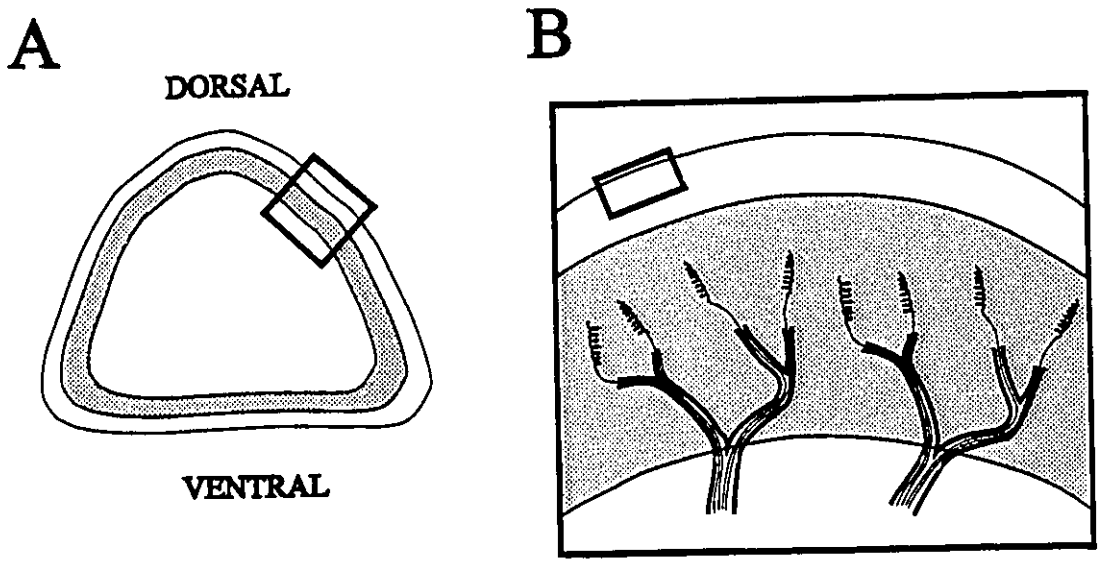
A
DORSAL
VENTRAL
B
C
10 um
D
1.
2.

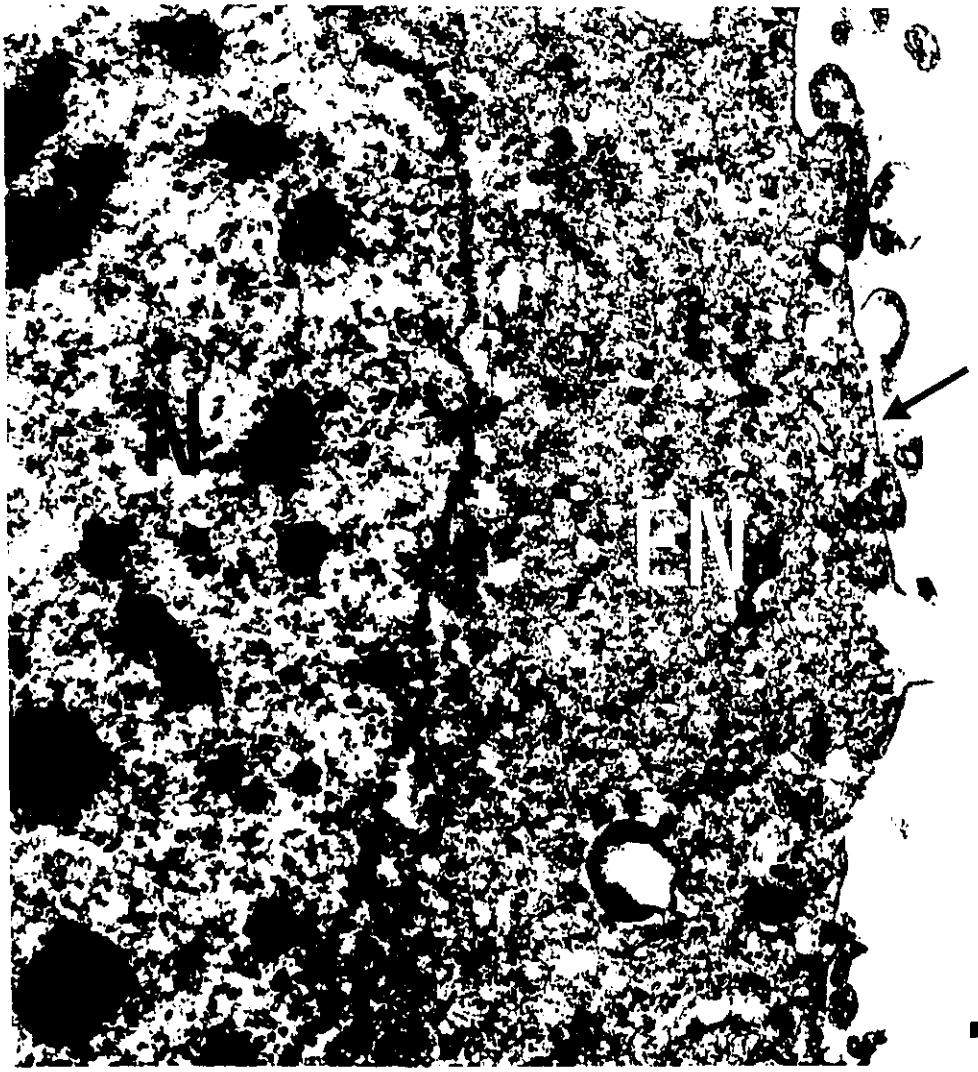

Figure 3.5. Electron micrograph of a portion of an *Aplysia* MSN. The nucleus (N) and plasma membrane (arrow) are readily evident. Gold particles (not visible at this magnification) were localized to the extranuclear region (EN) of the cell body. Bar: 0.3 μm.

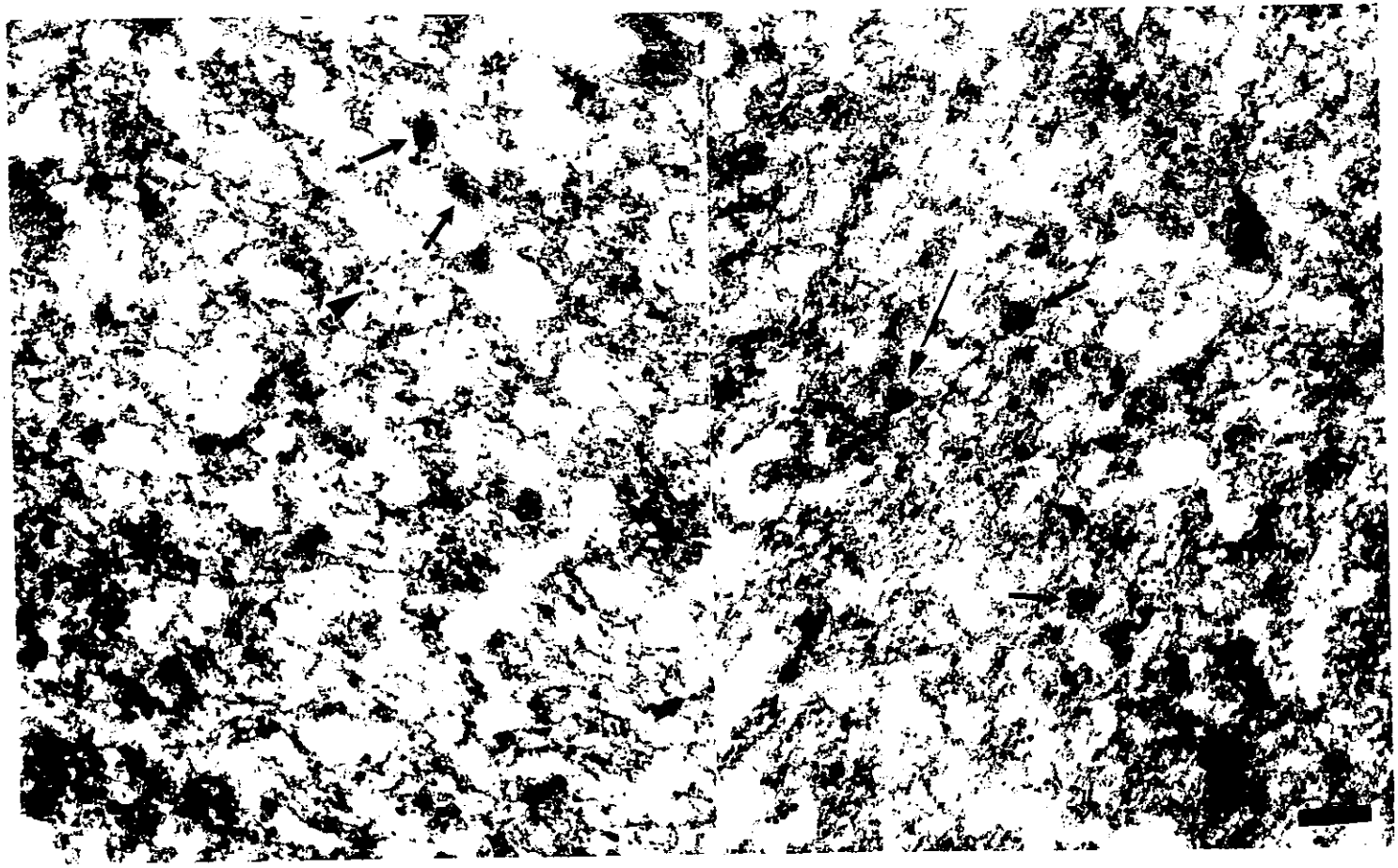

Figure 3.6. Immunogold localization of sensorin-A within the soma of a MSN. Gold particles are localized predominantly to dense granules (arrows), some of which presumably are dense-core vesicles (eg. long arrow). Some gold particles are also present in the cytoplasm (arrowhead). Bar: 0.15 μm.

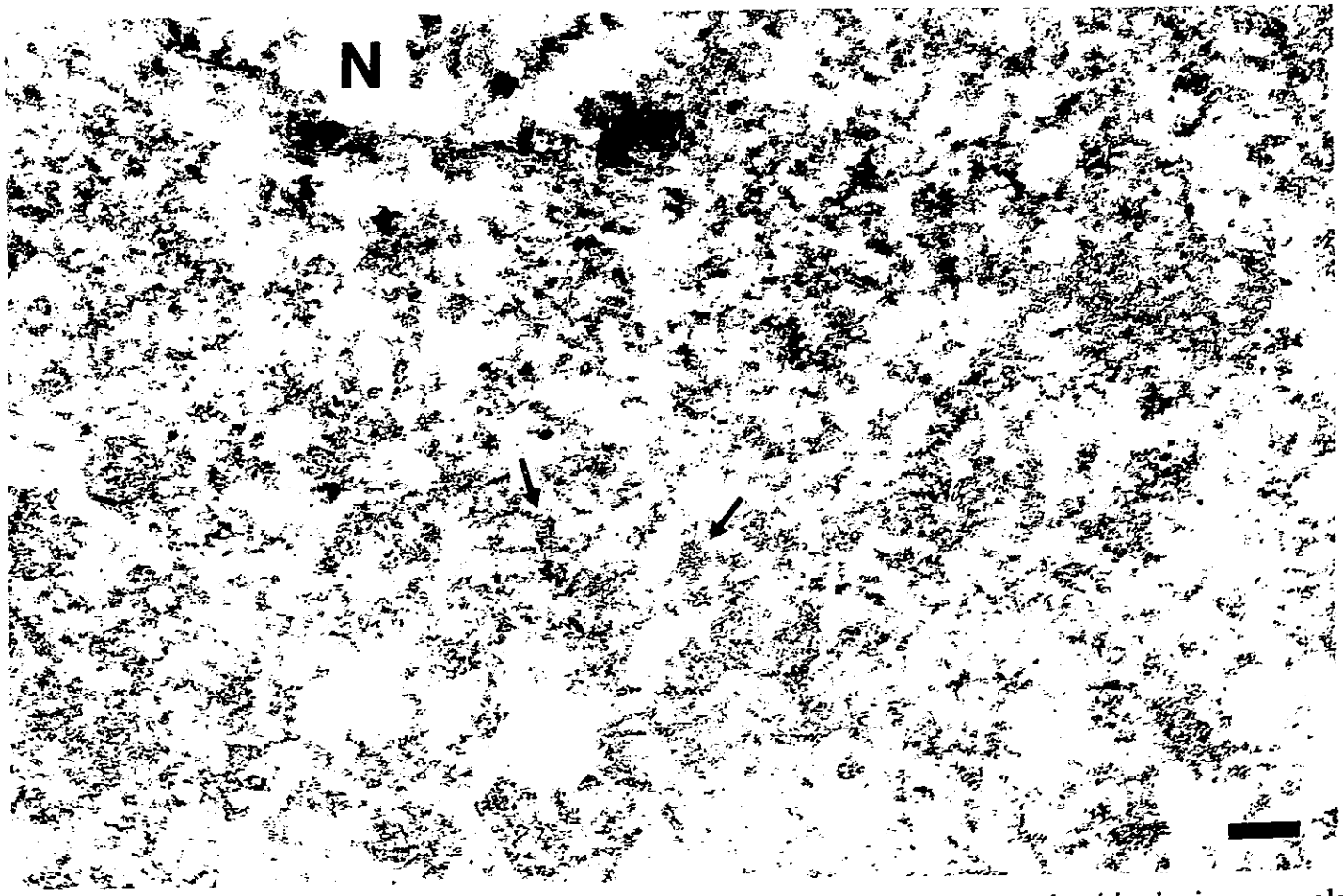

Figure 3.7. Electron micrograph of a control MSN, where the primary antibody has been omitted in the immunogold labelling procedure. The absence of gold particles associated with dense granules or in the cytoplasm indicates that the staining observed in Figure 3.6 is specific. A portion of the nucleus (N) can be seen in the upper left hand corner. Bar: 0.15 μm.

3.4 Discussion

Immunostaining for sensorin-A in the tail region revealed peripheral sensory fibers, thereby establishing sensorin-A's presence in both central (Brunet et al., 1991) and peripheral mechanosensory arborizations. Confocal microscopy of sensorin-A positive fibers in the periphery revealed that these fibers terminate as coiled structures in the muscular layer of the body wall. Presumably, these are the mechanoreceptive endings.

Sensorin-A fibers did not colocalize with the neuronal structures described in Chapter 2. It is possible that the ciliated endings are sensory endings of unidentified low-threshold mechanoreceptors. Mechanical stimulation of the tail with a stimulus sub-threshold to that required to activate the sensorin-A MSNs as recorded electrophysiologically, still produces a behavioural response in the animal (Terry Walters, personal communication).

Studies examining the structure of nociceptive sensory endings are scarce for both vertebrates and invertebrates. In vertebrates, mechanical nociceptors terminate as free nerve endings in peripheral tissues (review: Dubner and Bennet, 1983). In invertebrates, apart from *Aplysia*, the only organism for which mechanical nociceptive neurons have been described in the CNS is the leech (Blackshaw et al., 1982; Johansen et al., 1984). Blackshaw et al. (1982) used HRP injections of leech nociceptors to examine the structure of their peripheral endings. The nociceptive fibers generally terminate as unspecialized fine processes (~1 μm) deep in the body wall. More rarely, the nociceptive fibers make distinctive coiled terminals associated with expanded

dendritic regions of peripheral stretch receptor neurons (see Fig. 3.4). Electrophysiological studies have shown that leech nociceptive cells are pre-synaptic to the stretch receptor neurons, suggesting that the nociceptors may regulate stretch receptor activity (Blackshaw et al., 1984).

Although nociceptive MSNs in both leech and *Aplysia* form coiled terminals in the periphery, the overall morphology of the two terminals is quite different (see Fig 3.4). When the coiled terminals in *Aplysia* are compared to mechanosensory endings in both vertebrates and invertebrates, it is found that the general morphology of the endings most resembled that of vertebrate muscle spindles. A reconstruction from micrographs of serial longitudinal sections of human muscle spindles has revealed that the muscle spindle is an irregular coil with branches and varicose swellings (Kennedy et al., 1975).

Brunet et al., (1991) have suggested that sensorin-A acts as a neurotransmitter centrally. Immunogold localization of sensorin-A at the ultrastructural level indicates that it is localized to dense granules (presumably some of these granules are dense-core vesicles) in the cell body. It was also localized to similar structures in fibers in the neuropile (not shown). This distribution supports the notion that sensorin-A functions physiologically as a neurotransmitter or neuromodulator.

The presence of sensorin-A in peripheral varicosities suggests that it could be released from peripheral fibers and from the receptive endings itself; its release in the periphery may result in neuromodulatory actions. In the lobster oval organ, a proprioreceptor, the sensory response is enhanced by release of the pentapeptide,

proctolin, from peripheral dendrites (Pasztor et al., 1988; Pasztor and Bush, 1989). In vertebrate nociceptors, substance P, a neuroactive peptide, is released from peripheral sensory terminals when they are activated by noxious stimuli (Moskowitz et al., 1984). Direct application of substance P to peripheral tissues produces a number of effects including stimulating release of histamine from mast cells (Johnson and Erdos, 1973), attracting white blood cells (Helme and Andrews, 1985), and stimulating connective tissue cell growth (Nillson et al., 1985). Comparable studies have not yet been done with sensorin-A on *Aplysia* preparations.

CHAPTER 4

REGENERATION OF TAIL MECHANOSENSORY NEURONS IN *APLYSIA*

4.1 Introduction

Studies of identified gastropod neurons *in vitro* have provided much insight into the physiological mechanisms that trigger regenerative sprouting and that control synapse formation (Kater and Mattson, 1988; Bulloch, 1989; Carrow and Levitan, 1989; Glanzman et al., 1989; Lin and Levitan, 1991; Ridgeway et al., 1991). Regeneration of gastropod neurons has been extensively studied *in vitro*, but relatively little is known about regeneration *in vivo*. Studies in gastropods which have attempted to link regeneration in the nervous system with functional recovery in the whole animal are limited: Murphy and Kater, 1980; Moffet and Snyder, 1985; Murphy et al., 1985a; Fredman, 1988; Moffet and Ridgeway, 1988; Snyder and Moffet, 1990; Scott and Kirk, 1992; Moffet, 1992; Roger et al., 1992; Steffensen and Morris, 1992.

Regeneration following peripheral nerve damage is an important compensatory reaction to injury. The present study examines behavioural recovery, and *in vivo* axonal regeneration following nerve crush in the *Aplysia*. Because *Aplysia* is used so extensively to study learning and memory, it is a particularly important preparation on which to focus for studying *in vivo* nerve regeneration. To date, however, the number of studies has been small (Scott and Kirk, 1992; Fredman, 1988; Steffensen and

Morris, 1992; Dulin and Walters, 1993; Ross et al., 1994).

In this chapter, the identified MSNs that provide input to a well-described defensive reflex in *Aplysia*, the tail withdrawal reflex (Walters et al., 1983a), are examined. *In vitro* these sensory neurons not only rearborize but synapse preferentially with appropriate motor neurons (Glanzman et al., 1989). *In vivo*, these neurons expand their receptive fields following noxious stimulation, indicating that they are capable of sprouting in the periphery (Billy and Walters, 1989a). This chapter describes experiments designed to address the following questions. (1) Following disruption of the sensory pathways that trigger a specific behaviour in *Aplysia*, what is the timecourse of behavioural recovery? (2) Do sensory neurons regenerate following disconnection from their peripheral targets? Recovery of the tail withdrawal reflex was used to monitor regeneration, and axonal regeneration was examined using morphological techniques.

After the behavioural experiments were completed, we became aware that using the tail withdrawal reflex to assay regeneration of the MSNs was limited since the tail withdrawal reflex is not exclusively mediated by central pathways, and the possibility of contributions from peripheral nerve networks (i.e. peripheral mechanoreceptors) can not be excluded. A subsequent collaboration with Dr. Terry Walters (University of Texas at Houston) was established when we became aware that their lab was also examining recovery of the tail MSNs in *Aplysia* using a behavioural response that is exclusively mediated by central pathways (i.e. the tail-evoked siphon response; see Appendix).

4.2 Materials and methods

Animals

Aplysia californica (40-75g) obtained from Marinus (Long Beach, CA). Animals were maintained in aerated SW at temperatures between 15-18°C on a diet of romaine lettuce.

Nerve crush

Nerve crush was performed on animals that were first anaesthetized by injecting them with ice cold isotonic $MgCl_2$ (equivalent to 30% of an animal's body weight) and then placing them in a chamber containing 1°C SW for ~10 min. This procedure minimized synaptic transmission and spike activity during the crushing process, and eliminated post-surgical indications of behavioural sensitization. After the animal was anesthetized, a 1 cm incision was made in the animal's head just above the pedal ganglia, and fine forceps were used to perform bilateral crush of both p9 nerves ~1 cm from the pedal ganglia. This procedure damaged all of the axons of the tail sensory neurons (tail sensory neurons send all their fibers out the p9 nerves), while leaving the sheath intact as a pathway for regenerative growth of axons. Following nerve crush, the incision was sutured with 6.0 silk surgical thread, the animal was placed in 25 °C SW for ~20 min to speed recovery and then returned to its tank. Over 95% of animals survived surgical manipulation, despite the fact that the procedures used were "clean" but not sterile, and no antibiotics were used. After an animal recovered from

anesthesia, it was subjected to a simple behavioural test in order to confirm that the posterior tail was denervated (see below). At various timepoints following crush, the animal was anesthetized with a lethal injection of isotonic $MgCl_2$ (~50% of the animal's body weight).

Behaviour

The identified MSNs provide input to a well-described defensive reflex in *Aplysia*, the tail withdrawal reflex. Recovery of the tail withdrawal reflex after p9 nerve crush was used to monitor regeneration. The tail withdrawal reflex was examined by mechanically stimulating the tail and measuring its contraction. Tail withdrawal was elicited with a 500 ms pulse of seawater, 20 psi intensity, delivered through a picospritzer. The seawater jet was positioned 2-3 cm from the tail and video recordings of tail contraction were obtained with a video camera. This behavioural assay was done before and after crushing p9, and in consecutive days after surgery.

Immunohistochemistry

Between 0 to 25 days after bilateral nerve crush, *Aplysia* tissue was fixed in 4% paraformaldehyde in ASW. Following fixation, tissue was rinsed three times in PBS (10 min each) and then immersed overnight in PBS with 15% sucrose to cryoprotect the tissue. Samples were frozen in liquid isopentane at -40 to -60°C, and 10 µm frozen cryostat sections were cut and collected on gelatin coated glass slides. Frozen sections were incubated overnight at 4°C in a blocking solution consisting of 10% normal goat

serum (Jackson), 1% BSA and 0.4% Triton X-100 in PBS. After a single quick rinse in washing buffer (0.1% Triton X-100 in PBS), preparations were incubated overnight at 4°C with a rabbit polyclonal antiserum against sensorin-A (Brunet et al., 1991) at 1:400 in PBS with 0.4% Triton X-100. Following the primary antibody incubation, ganglia were rinsed four times in washing buffer (10 min each) and then incubated overnight at 4°C with a DTAF conjugated goat anti-rabbit secondary antibody (Jackson) at 1:100 in PBS with 0.4% Triton X-100. After three rinses in washing buffer (10 min each), sections were mounted in a 3:1 solution of glycerol in PBS with 1% n-propyl gallate. Ganglia were viewed with a Zeiss Universal microscope equipped with epifluorescence optics (filter set #487909 for fluorescein) and photomicrographs were taken on Ilford XP2-400 film.

Biocytin fills

Biocytin fills of tail sensory neurons were performed on animals that had received unilateral nerve crush. For unilateral crush (100-250g animals), most of the pedal nerves including p7, p8, and p9 were crushed on one side of the animal ~1 cm from the pedal ganglion. The side chosen for crush was randomly determined with an equal distribution between right and left sides, with the side contralateral to the crush serving as an internal control. Approximately 21 days after nerve crush, the pleural and pedal ganglia were removed from the animal, and the pleural ganglia were desheathed in a 50/50 solution of SW and isotonic $MgCl_2$. For ionophoretic injection of biocytin into sensory neurons, a 4% solution of biocytin (Sigma) was drawn into the

tip of an electrode, then the electrode was backfilled with KCl solution (0.33 M KCl, 10 mM Tris, pH 7.5). During injection, the cells were alternately hyperpolarized to 30 mV below the resting potential and depolarized to 30 mV above resting potential at 0.5 Hz for 30-40 min. Ganglia were then placed in culture medium (isotonic L15 medium; Schacher and Proshansky, 1983) at 4°C for 20-42 h to allow time for the biocytin to move down axon tracts. Tissue was fixed in 4% paraformaldehyde in SW overnight at 4°C, rinsed three times in PBS (10 min each) and then cryoprotected in PBS with 15% sucrose. Frozen cryostat sections were prepared as above. Sections were incubated overnight in blocking solution. Following a single quick rinse, sections were incubated in Bodipy (Molecular Probes, Eugene, OR) at 1:100 in PBS with 0.4% Triton X-100. After three rinses in washing buffer, sections were mounted, viewed and photographed as above.

4.3 Results

Behavioural Evidence for Regeneration

Following nerve crush, recovery of the tail withdrawal reflex was used to monitor regeneration. The time course for recovery of the tail withdrawal reflex to tail stimulation can be seen in Figure 4.2. Prior to p9 nerve crush, stimulation of the tail elicited a full tail withdrawal reflex in all animals tested (Figs. 4.1, 4.2). On days 1 and 3 after crush, no animal showed any signs of behavioural recovery (Fig. 4.2).

Partial recovery was observed in some animals as early as 6 days after crush (Fig. 4.2). Full recovery of the tail withdrawal reflex was seen between 10 and 15 days (Figs. 4.1, 4.2).

Morphological Evidence for Regeneration

Sensorin-A immunohistochemistry

To trace regenerating sensory fibers, immunostaining with an antibody to sensorin-A, a peptide specific to *Aplysia* sensory neurons (Brunet et al., 1991), was performed. As above, we focused on the tail sensory neurons. These neurons send all their fibers out the p9 nerve; none of the other pleural sensory neurons project into p9 (Zhang et al., 1993). Sensorin-A immunofluorescence in control animals revealed fibers both centrally (Figs. 4.3 A, 4.4 A) and peripherally, including in p9 (Fig. 4.3 B,C; Fig. 4.4 B,C). Fibers typically travelled along the ventral side of the pleural-pedal connective, arborizing in the pedal ganglion where tail motor neurons receive sensory inputs, then exiting the pedal ganglion via p9 (Fig. 4.3). In nerve p9 as well, sensory fibers were restricted to the ventral side [e.g. Fig. 4.4 B; confirmed by cross sections (not shown)]. The high signal to background ratio obtained with the sensorin-A antibody allowed for resolution of individual fibers (Fig. 4.4).

Examination of the crush site under the dissecting microscope indicated that fibers were transected, but the nerve sheath was left intact. This was confirmed with phase contrast microscopy (Fig. 4.5 B). Immunostaining of the crush site with an

antibody to sensorin-A, 6 h after crush, revealed that sensory fibers were transected (Fig. 4.6 A). At this stage, sensory fibers distal to the crush site were still visible by sensorin-A immunofluorescence, indicating that the severed distal fibers still contained immunorcactive peptide.

When p9 was observed by phase contrast microscopy 16 days post-crush (Fig. 4.5 C), signs of transection at the crush site were no longer visible. A swollen region (~ twice the diameter of p9) at the recovering crush site was, however, consistently observed after ~10 days post-crush, and persisted till the end of the experimental period (~60 days post-crush). The swelling provided a useful marker of the crush site for both electrophysiological and morphological experiments. Large inclusions (up to 100 μm) were observed in the region of the swelling (Fig. 4.5 D) and distally in p9 (Fig. 4.6 B-D,H). To determine if these inclusions were profiles of cells that had invaded the injured nerve, the tissue was stained with Hoechst, a fluorescent nuclear stain. The inclusions were devoid of nuclei, and therefore presumably acellular.

Sensory fibers in p9 were monitored during the recovery period by sensorin-A immunofluorescence. At 48 h post-crush (Fig. 4.6 B) fibers distal to the crush site were no longer visible. Presumably this is a reflection of distal fiber degeneration. By ~day 5 post-crush, immunopositive fibers invaded the site of injury and the region just distal to the crush site (Fig. 4.6 C). These new fibers were finer than those observed in control animals, and finer than the original fibers seen distal to the crush site (as in Fig. 4.6 A) before they disappeared. It was common for the new fibers to have varicosities (Fig. 4.6) and to be highly arborized (as determined by focusing through

longitudinal sections). By ~day 8 post-crush, the number of new fibers appearing distal to the crush site had increased further (Fig. 4.6 D).

Whereas tail sensory fibers in control animals were confined to the ventral side of p9, the regenerating sensory fibers grew into all regions of the crush site and emerged distally with an essentially random distribution in p9. This new population of fibers continued to advance down p9; on 21 days post-crush, a survey of p9 to its first major branch point (~3/4 of the way down p9) revealed immunopositive fibers along the whole length of the nerve (Fig. 4.6 H). The average rate of regeneration of sensorin-A fibers down the p9 nerve was determined to be ~4 mm/day. There was no evidence in these experiments of preferential growth of sensorin-A fibers in their usual location, i.e. the ventral side of p9.

At the "growing/regenerating front", sensory fibers were fine and highly arborized, but behind this front they became less arborized and larger with time (the timecourse of these changes is shown diagrammatically in Fig. 4.8). At the swollen crush site, however, fine extensively arborized fibers were evident even at ~20 days post-crush. It was not possible to determine whether these were fibers which had persisted from ~5 days post-crush or whether they represented actively extending and retracting processes. This persistent sprouting could result in sensitization at the site of injury.

Biocytin fills

Biocytin is particularly effective as a molluscan neuronal tracer (Ewadinger et

al., 1994) and it provided the opportunity to examine the morphology of individual sensory neurons following injury. Electrophysiologically identified sensory neurons (2-3 cells on the crush and control side/animal; 3 animals total) were filled with biocytin on ~21 days post-crush. As expected, tail sensory neurons had axons in the pleural/pedal connective in both control (not shown) and crush (Fig. 4.7 A) sides. Biocytin filled fibers traversed the crush site and travelled down p9 (Fig. 4.7 B-E). In the region of the crush site, the sensory fibers branched and meandered as if making their way through difficult terrain (Fig. 4.7 B,C). However, once they emerged they followed a straight path and arborizations were no longer observed (Fig. 4.7 D,E).

Figure 4.1. Video micrographs of the tail withdrawal reflex of an *Aplysia* before and after crushing its p9 nerve. Prior to crushing p9 (Day 0) mechanical stimulation of the tail with a jet of seawater (arrow) resulted in the classic withdrawal reflex. One day following the crush (Day 1) stimulation of the tail failed to elicit any response. At Day 5 stimulation again failed to elicit a response. Eight days after the crush (Day 8) stimulation of the tail caused a slight withdrawal. After 10 days the tail withdrawal reflex had returned. Bar: 5 cm.

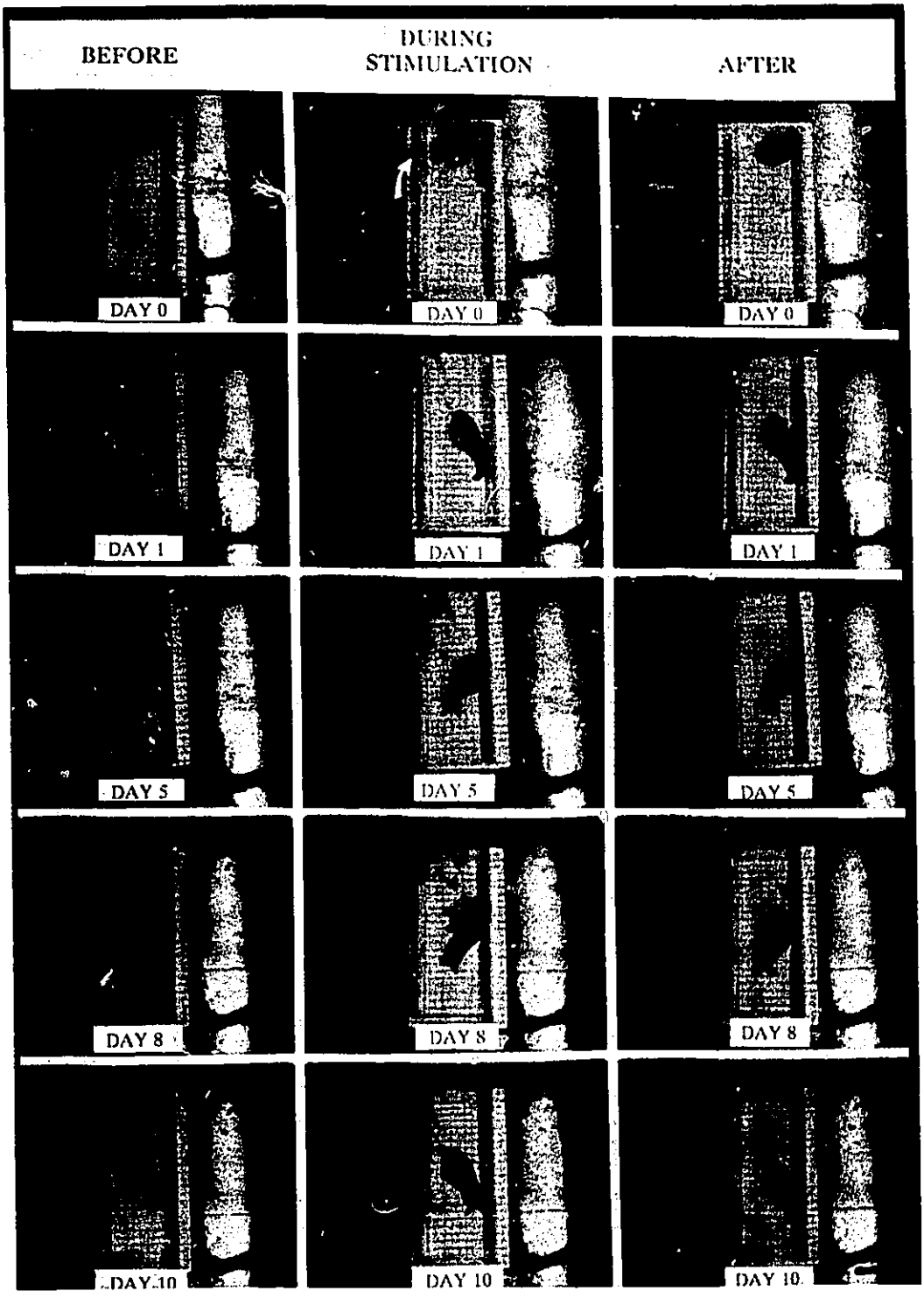
BEFORE
DURING STIMULATION
AFTER
DAY 0
DAY 0
DAY 0
DAY 1
DAY 1
DAY 1
DAY 5
DAY 5
DAY 5
DAY 8
DAY 8
DAY 8
DAY 10
DAY 10
DAY 10

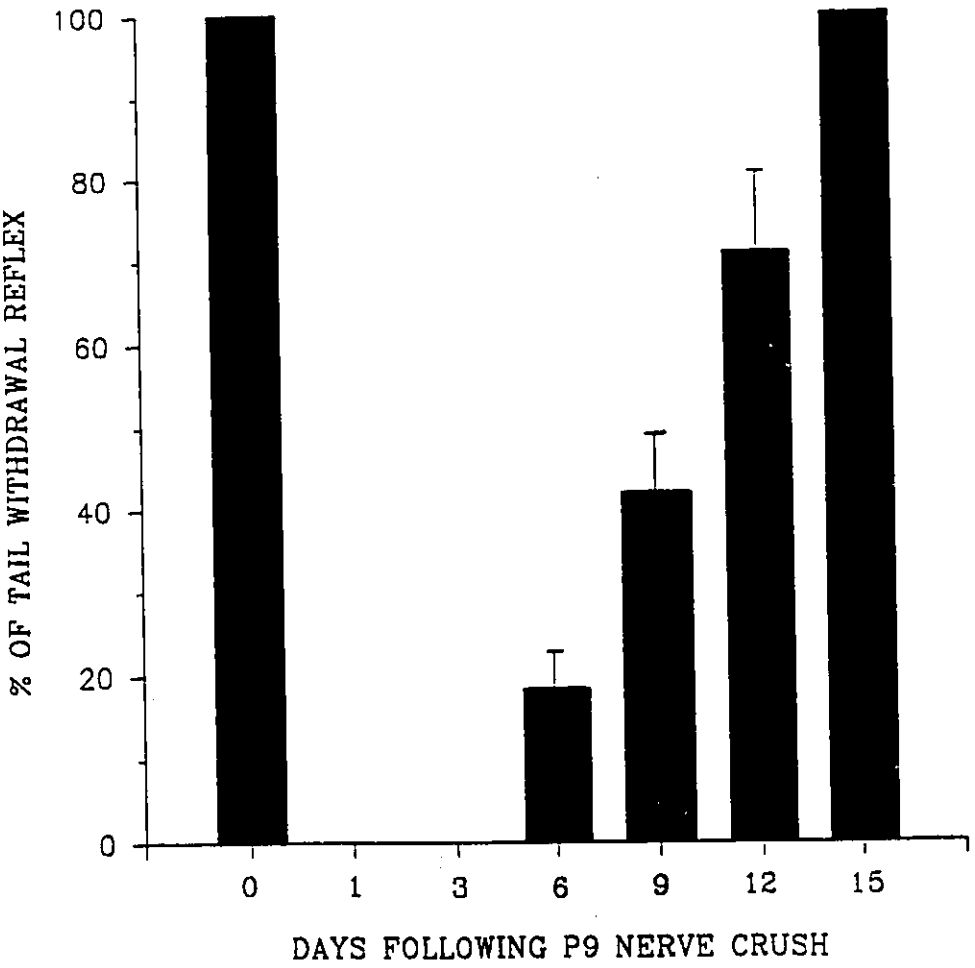

Figure 4.2. Bar graph illustrating recovery of the tail withdrawal reflex after p9 nerve crush (n=6). Before p9 crush (Day 0) all animals showed a full tail withdrawal reflex following mechanical stimulation. At Days 1 and 3 no animals showed any sign of recovery. Partial recovery was observed in some animals as early as Day 6. Full recovery of the tail withdrawal reflex was seen between Days 10-15.

Figure 4.3. Sensorin-A immunofluorescence in the *Aplysia* nervous system. **A**, a cryostat section of the pleural (Pl) and pedal (Pd) ganglia, and of the posterior pedal nerve p9 (arrow). Sensory neurons of the pleural ventral caudal cluster are immunopositive for sensorin-A, as previously shown by Brunet et al., 1991. The sensorin-A antibody also labelled sensory fibers in the p9 nerve. **B** and **C**, p9 nerve preparations from two other animals. Bar: 500 μm.

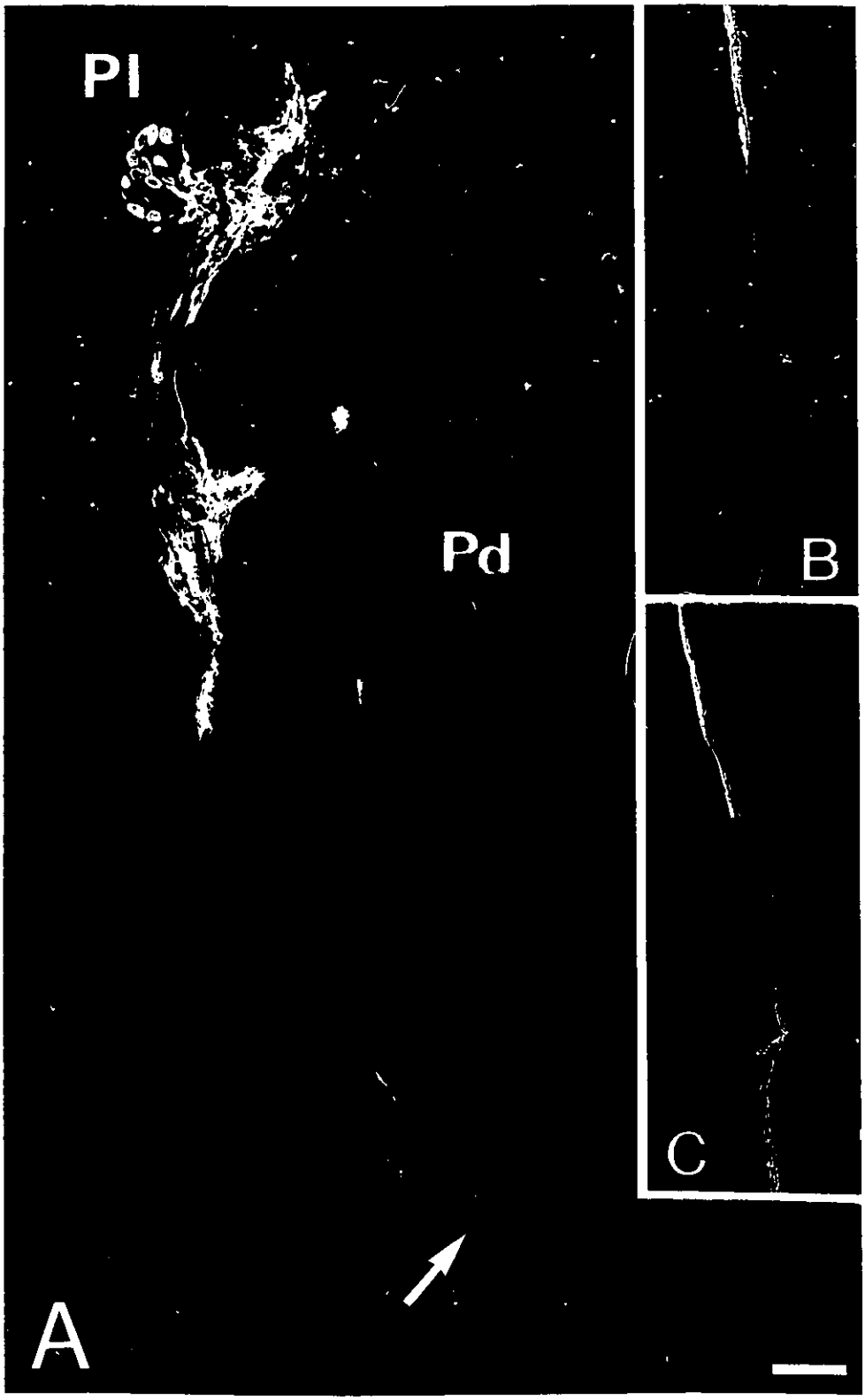
Pl
Pd
B
C
A

Figure 4.4. High magnification view of sensorin-A immunofluorescence. **A**, sensory fibers in the pedal ganglion, in the region where the tail motor neurons receive inputs from sensory fibers (Walters et al., 1983a); p9 is the nerve tract at the bottom of the image (arrow). **B** and **C**, high magnification of sensorin-A positive fibers in p9 ~1 cm from the pedal ganglion. Note that individual fibers can be resolved. The orientation of the nerve in **B** is ventral side to the left; characteristically, sensorin-A positive fibers in p9 were restricted to the ventral side. The fainter staining evident on the dorsal side is in the nerve sheath, not in fibers (nerve sheath generally shows higher immunohistochemical background). Bar: 200 μm.

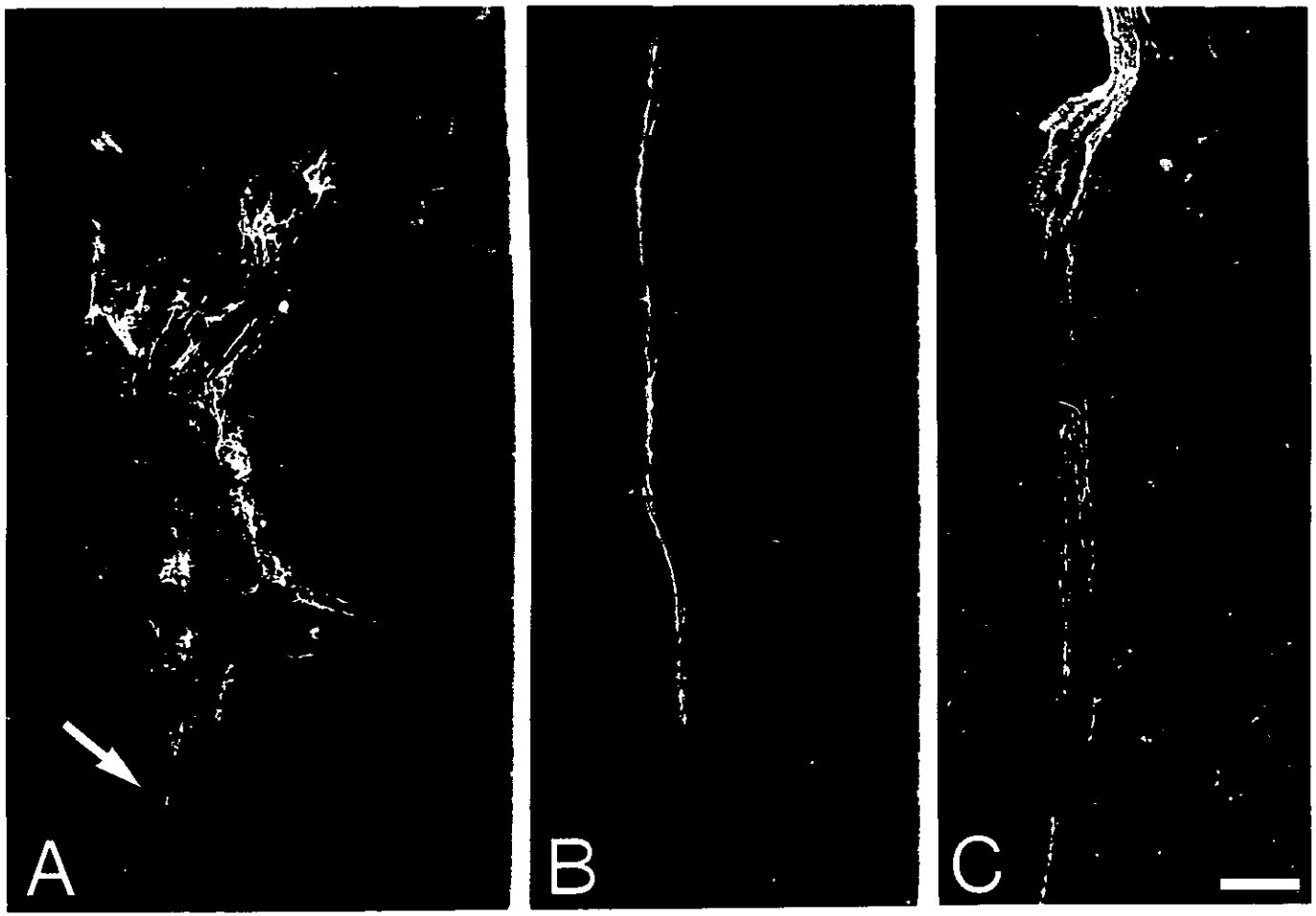
A
B
C

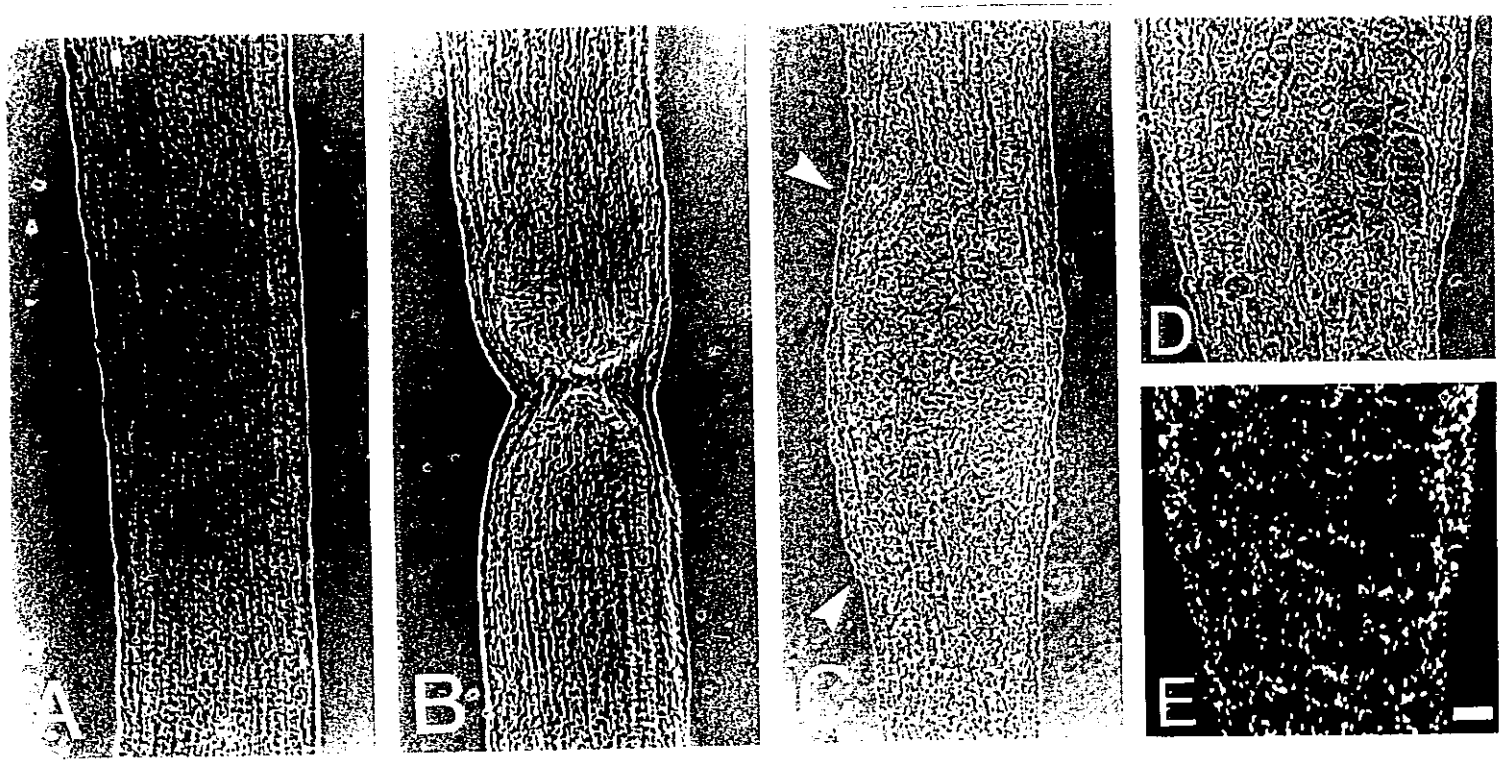

Figure 4.5. Cryostat sections of nerve p9. **A-D** Phase contrast images of p9, and **E**, a fluorescent image of the same field as **D**. **A**, p9 ~1 cm from the pedal ganglion. **B**, p9 immediately after nerve crush, crush was ~ 1 cm from the pedal ganglion (note transected fibers and intact sheath). **C**, p9 on day 16 post-crush (note that there are no visible signs of transection in the tissue). The swollen region (between arrowheads) was characteristic of the recovering crush site. **D**, another p9 (day 17 post-crush) illustrating large inclusions that were consistently present at the recovering crush site. **E**, the same section stained with Hoechst, a fluorescent nuclear stain. Note the absence of nuclei where the large inclusions are located. Bar: 100 μm.

Figure 4.6. Sensorin-A immunostaining of sections of nerve p9 at various time points following nerve crush; sites of nerve crush are shown by arrowheads. **A**, 6 h post-crush. **B**, 48 h post-crush. **C**, day 5 post-crush (note, a fine fiber has grown through the crush site and subsequently bifurcated (arrowhead)). **D**, day 8 post-crush. **E**, day 12 post-crush ~0.5 cm distal to the crush site. **F**, higher magnification of another day 12 p9 nerve ~0.5 cm distal to the crush site. **G**, day 17 post-crush ~1 cm distal to the crush site. **H**, day 22 post-crush ~6 cm distal to the crush site, just proximal to where the main trunk of p9 branches. The large inclusions that were observed by phase-contrast (Fig. 4.3 D) are also visible with immunofluorescence (**B-D, H**), due to their background fluorescence. Varicosities were commonly seen in regenerating fibers (e.g. arrowheads in **E** and **G**). Bar: 100 μm.

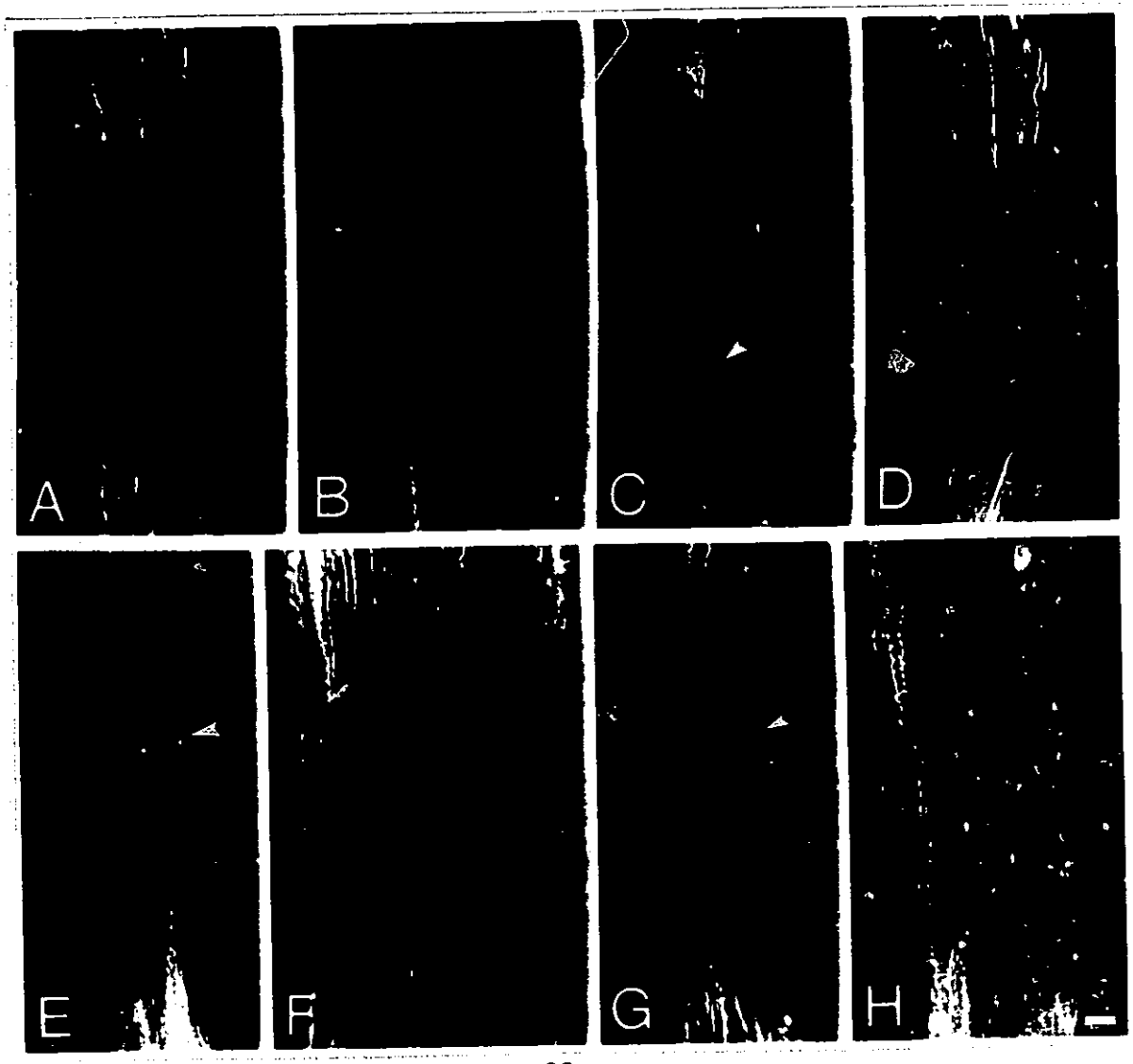
A
B
C
D
E
F
G
H

Figure 4.7. Biocytin fills of tail sensory neurons. **A**, three biocytin filled sensory neurons in the pleural cluster. Biocytin filled fibers are present in the pleural/pedal connective (arrow). **B**, nerve p9 just proximal to the crush site, at day 21 post-crush, showing extensively arborized biocytin filled fiber(s). The globular inclusions alluded to previously are evident in the crush site (**B** and **C**) and distal to it (**D**). **C**, day 21 post-crush, biocytin filled fibers in p9 just distal to the crush site. Focusing through the section indicated that there are two fibers (arrowheads). **D**, a biocytin filled fiber on the ventral side of p9 ~1 cm distal to the crush site (arrowhead). **E**, a higher magnification of **D**. (For locations of **B** and **C**, see Fig.8). Bar: A, 100 μm; B-D, 50 μm; E, 25 μm.

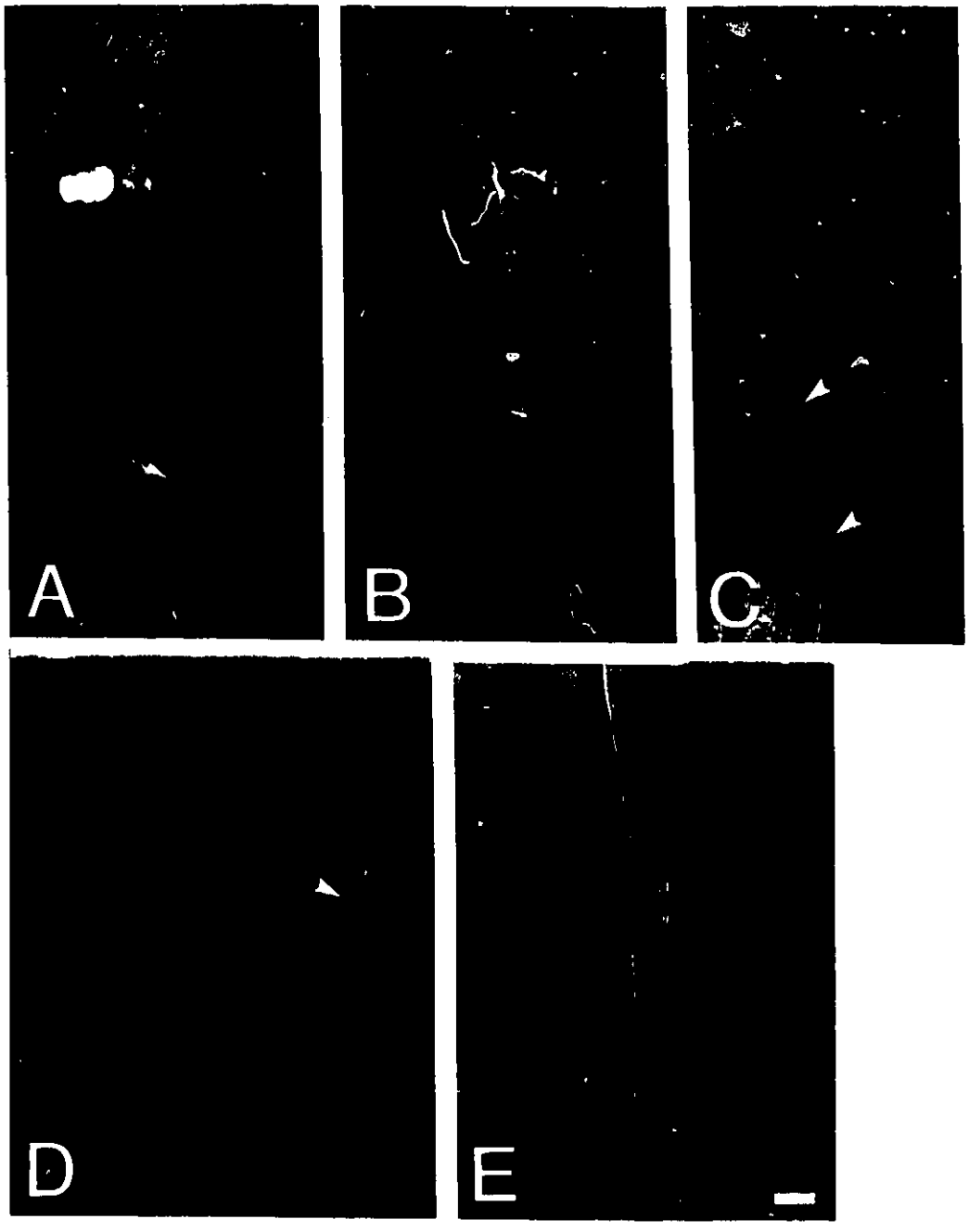
A
B
C
D
E

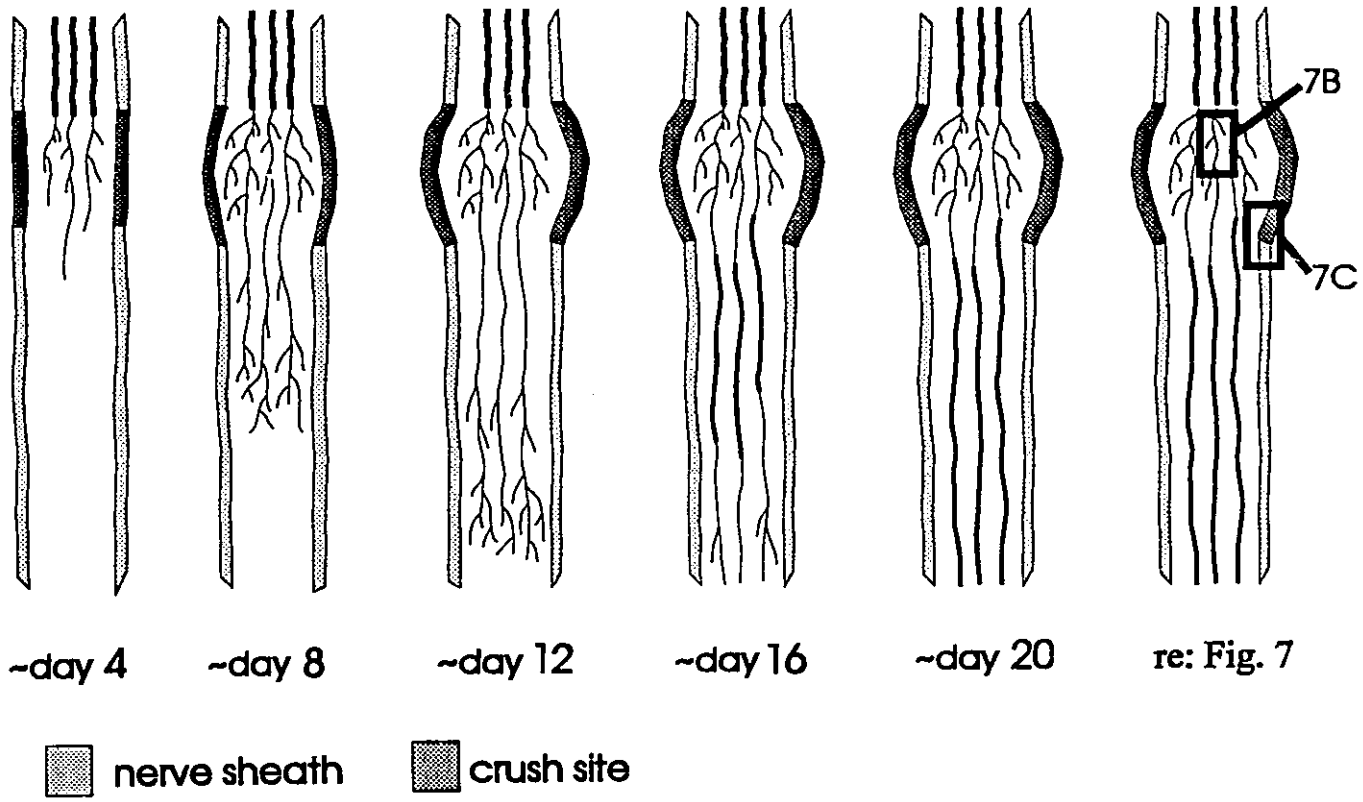

Figure 4.8. Timecourse of regeneration of sensory fibers in p9 following nerve crush, shown diagrammatically. The region distal to the crush site is representative of the pattern of regeneration observed as far down p9 as we monitored, namely to the first major branch point. At the far right, an ~day 20 nerve is depicted with the locations of micrographs shown in Figure 4.7.

4.4 Discussion

Recovery of the tail withdrawal reflex

Recovery of the tail withdrawal reflex was observed following crush of nerve p9 in *Aplysia*, a result consistent with previous studies that have examined behavioural recovery following lesions to the CNS in *Aplysia* (Fredman, 1988; Scott and Kirk, 1992). Fredman (1988) observed recovery of the escape response following bilateral crush of the pleural-cerebral connectives. This lesion disrupted connections between the command neurons responsible for initiating escape locomotion. Scott and Kirk (1992) observed recovery of feeding behaviour (i.e. the biting response) after bilateral crushes of the cerebral-buccal connectives in *Aplysia*. It appears, therefore, that *Aplysia* has an inherent ability to recover behavioural responses following injury to its CNS.

Since the tail withdrawal reflex is not exclusively mediated by central pathways, the possibility of contributions from peripheral nerve networks can not be excluded. However, several lines of evidence indicate that the tail sensory neurons do indeed re-establish central connections following injury. First, recovery of the tail-evoked siphon response occurs following p9 nerve crush (see Fig. 1 of Appendix). This response is mediated exclusively by central pathways (Hickie, 1994). Secondly, the tail sensory neurons of *Aplysia* have been shown to re-establish functional receptive fields in the periphery following p9 nerve crush (see Fig. 3 of Appendix).

Timecourse for recovery

The time course for recovery of the tail withdrawal reflex following nerve crush was comparable to that observed for recovery of the escape response (Fredman, 1988), the biting response (Scott and Kirk, 1992), and the tail-evoked siphon response (see Fig. 1 of Appendix) in *Aplysia*. Fredman (1988) observed partial recovery of the escape response 7 days after nerve crush, and full behavioural recovery in all animals 27 days after crush. Scott and Kirk (1992) noted that 9 days after nerve crush feeding behaviour began to recover, and the biting response gradually increased in magnitude between days 9 and 19. The time course for recovery of the siphon response to tail stimulation can be seen in Figure 1 (see Appendix). The average time for recovery was 12.8 ± 1.2 days with the earliest animal showing siphon responses at 7 days.

Several factors could explain the variation in the time courses for behavioural recovery. For example, the size of the animals could account for some of the variation observed. In the present study, 40-75 g animals were used, whereas 100-125 g animals were used in the other studies. Smaller animals could be expected to display shorter recovery times than larger animals, since axons have a shorter distance to travel in smaller animals. In addition, the age of the animals used may affect recovery times since the rate of regeneration in molluscan neurons has been shown to be age dependent, with older animals showing slower rates of regeneration (Janse et al., 1986).

Axonal morphology during regeneration

Immediately following crush, all axons at the crush site were shown to be fully

severed. This is important to our interpretation of the results. Had some fibers been left intact, they could have sprouted extensively in the tail region. Peripheral sprouting and receptive field expansion of uninjured sensory neurons following noxious stimulation has previously been described by Billy and Walters (1989a).

Our morphological results indicate that regrowth of tail sensory neurons occurs after injury. Regeneration of *Aplysia* tail sensory neurons down p9 has also been shown using electrophysiological means (see Fig. 2 of Appendix). Sensory neurons that had new axons in the p9 nerve were identified by intracellularly monitoring the cell while directly stimulating the nerve ~1 cm distal to the crush site. The percentage of neurons showing electrophysiological signs of having an axon beyond the crush site was plotted. With increasing time after crush, the percentage of cells responding to p9 stimulation tended to increase (see regression in Fig. 2 of Appendix) towards full recovery at ~50 days.

The classical picture of successful regeneration by severed axons is that reconnection to the periphery is re-established only after the fine sprouts that emerge from the growing axons reach their target. However, unusually rapid and complete regeneration can occur when a growing axon rejoins with its severed distal segment (Hoy et al., 1967; Frank et al., 1975; Deriemer et al., 1983; Camhi and Macagno, 1991). Reconnection of severed axons can occur either by direct fusion (Deriemer et al., 1983) or by forming an electrical synapse that restores the severed connection (Frank et al., 1975; Camhi and Macagno, 1991). Camhi and Macagno (1991) compared regeneration of identified leech neurons following a crush of the whole

nerve, or photoablation of a small segment of the identified neuron. Stark differences were seen in regeneration patterns when neurons were cleanly ablated instead of crushed. Crushed neurons regenerated by extensive sprouting of the proximal segment. With photoablation, 30% of the neurons exhibited sprouting, but the other 70% reconnected by forming an electrical synapse. The evidence for reconnection is that suddenly at ~3 days after photoablation, lucifer yellow filled the axons all the way to the periphery. The reconnected axons were not visibly different from unablated controls filled with these markers.

Our results from crushed neurons are in accord with those of Camhi and Macagno (1991). The pattern of regeneration at the growing front as seen by sensorin-A staining (Fig. 4.8) is not consistent with recovery occurring by the proximal and distal axon segments rejoining. Moreover, morphological observations of p9 distal to the crush indicate that axonal degeneration is occurring. First, sensorin-A disappears from the region of p9 distal to the crush and second, the ultrastructure of the globular profiles that we observed has recently been examined (Ross et al. 1994) and shown to be products of degenerating axons. This makes us confident that reconnection, either by direct fusion or by the formation of an electrical synapse between the proximal axon and the distal axon stump, is not the method of regeneration of *Aplysia* sensory neurons in our experiments.

CHAPTER 5

PUTATIVE MECHANOSENSORY NEURONS IN *LYMNAEA STAGNALIS*

5.1 Introduction

Knowledge gleaned from identified neurons of the pond snail, *Lymnaea stagnalis*, has provided a useful tool both for basic neurobiological and comparative physiological investigations (Syed et al., 1990; Syed et al., 1992; Kemenes and Elliot, 1994). The *Lymnaea* CNS has been mapped in a number of previous studies (for a review see Benjamin et al., 1985). Emerging from this work is a comprehensive description of motoneurons that control behaviours such as locomotion (Winlow and Haydon, 1986), respiration (Syed and Winlow, 1991) and feeding (McCrohan, 1984a), two wide acting interneurons (McCrohan, 1984b; Kyriakides et al., 1989) and many groups of neurosecretory cells (Geraerts, 1976; Geraerts and Bohlken, 1976). Conspicuous by their absence in published maps of *Lymnaea* ganglia are sensory neurons, a situation that has hampered the delineation of complete neuronal circuits underlying behaviour in this species (e.g. Ferguson and Benjamin, 1991). This situation contrasts strongly with the state of knowledge of sensory neurons in the CNS of the marine mollusc *Aplysia*, another gastropod mollusc in widespread use in neuroscience.

In *Aplysia*, particularly intensive study has focused around one class of primary

sensory neurons - the mechanoreceptors that trigger defensive withdrawal reflexes (Walters et al., 1983a; Clatworthy and Walters, 1993). The *Aplysia* sensory neurons have been mapped to clusters of cells in the buccal (Fiore and Geppetti, 1980), cerebral (Rosen et al., 1979), pleural (Walters et al., 1983b) and abdominal (Byrne et al, 1974; Byrne, 1980; Dubuc and Castellucci, 1991) ganglia. Using PCR-based differential screening, Brunet et al. (1991) have identified a peptide, sensorin-A, that is specific for this class of sensory neurons. Using an antibody generated against sensorin-A, we have identified putative mechanosensory neurons in the *Lymnaea* CNS. To investigate the degree of homology between the sensorin-A neurons in *Lymnaea* and those in *Aplysia*, *in situ* hybridization with a probe complementary to a coding sequence on the *Aplysia* sensorin-A gene was also performed.

5.2 Materials and methods

Animals

Lymnaea stagnalis were raised in the laboratory under standard conditions (12 hours light/12 hours dark) in aerated pond water. Animals were fed lettuce ad libitum. For whole-mount immunocytochemistry, snails of shell length ~10 mm were used, whereas for immunohistochemistry and *in situ* hybridization on frozen sections, we used snails of shell length ~20 mm.

Immunocytochemistry: whole mounts

Central ring ganglia were dissected from *Lymnaea* and pinned out flat after cutting the cerebral commisure and deflecting the cerebral ganglia sideways so that their ventral surface faced upwards. Preparations were treated with 0.1% protease (Sigma) in normal saline (51.3 mM NaCl, 1.7 mM KCl, 4.1mM $CaCl_2$, 1.5 mM $MgCl_2$ and 5.0 mM HEPES in distilled water, pH 7.9) for 5-10 min, rinsed several times in normal saline and then fixed in Zamboni's fixative overnight at 4°C. Following fixation, ganglia were rinsed (three times, 10 min each) in a washing buffer consisting of 0.1% Triton X-100 in PBS. Ganglia were next incubated overnight in a blocking solution consisting of 10% normal goat serum, 1% BSA and 1% Triton X-100 in PBS. After a single quick rinse in washing buffer, preparations were incubated for 2-3 days at 4°C with a rabbit polyclonal antiserum raised against sensorin-A (Brunet et al., 1991) at 1:400 in PBS with 1% Triton X-100. Ganglia were triple-rinsed in washing buffer and then incubated overnight with a DTAF conjugated goat anti-rabbit secondary antibody (Jackson) at 1:100 in PBS with 1% Triton X-100. After triple-rinsing in washing buffer, preparations were mounted in a 3:1 solution of glycerol in PBS with 1% n-propyl gallate. Ganglia were viewed with a Zeiss Universal microscope equipped with epifluorescence optics and photomicrographs were taken on Ilford XP2-400 film.

When laid out for whole-mount immunocytochemistry, the central ring ganglia had distinct dorsal and ventral faces; by convention, the left and right sides of the ring are defined as seen dorsally. Note that, with the exception of Figure 5.1 B, ganglia were positioned ventral side up, so left and right are reversed.

Double-immunolabelling experiment

Preparations were prepared for immunocytochemistry as described above. After incubating in blocking solution, ganglia were incubated for 2-3 days with a guinea pig polyclonal antibody against APGWamide (Croll and Van Minnen, 1992; gift from J. Van Minnen) and the antibody to sensorin-A, each at 1:400 in PBS with 1% Triton X-100. Ganglia were triple-rinsed in washing buffer and then incubated with a Texas Red conjugated goat anti-guinea pig secondary antibody (Jackson) and a DTAF conjugated goat anti-rabbit secondary antibody, each at 1:100 in PBS with 1% Triton X-100. Preparations were mounted, viewed and photographed as described above.

Immunohistochemistry: cryostat sections

Lymnaea body wall tissue was excised from the head region and cut into pieces of ~1 cm^2. Central ring ganglia were dissected from *Lymnaea* and pinned out flat after cutting the cerebral commisure and deflecting the cerebral ganglia sideways so that their ventral surfaces faced upwards. Tissue was fixed in Zamboni's fixative overnight at 4°C, rinsed in PBS and then cryoprotected overnight in PBS with 15% sucrose. Samples were frozen in liquid isopentane at -40 to -60°C, and 10 µm frozen cryostat sections were cut and collected on gelatin coated glass slides. Sections were immunostained for sensorin-A as described above, except that 0.4% (rather than 0.1%) Triton X-100 was used in the incubating solutions.

Probes and labelling procedures

A synthetic 24-mer oligonucleotide probe, complementary to the coding sequence 5'-TTCCCTCGTGCCAGATACAGGGTT-3' of the sensorin-A mRNA of *Aplysia* was synthesized (Brunet et al., 1991). This sequence is within the same region that the antibody to sensorin-A was generated, using the inferred amino acid sequence (Brunet et al., 1991). As a control probe a 24-mer synthetic oligonucleotide representing this part (ie. 5'-TTCCCTCGTGCCAGATACAGGGTT-3') of the sensorin-A mRNA was synthesized. Probes were 3' labelled with digoxigenin according to the protocol described in the Genius Non-radioactive Labelling and Detection kit (Boehringer-Mannheim, Laval, Quebec).

***In situ* hybridization: cryostat sections**

Central ring ganglia were dissected from *Lymnaea* and pinned out flat (see above). Tissue was fixed in 4% paraformaldehyde in PBS overnight at 4°C. Frozen cryostat sections were prepared as described above. Sections were rinsed twice (5 min each) in distilled water and then air-dried. Probes were diluted (500 pg/ul) in a hybridization buffer containing 50% formamide, 6 X SSC (SSC is 0.15 M NaCl, 0.015 M sodium citrate), 2 X Denhardt's solution (Denhardt's solution is 0.002% each of BSA, Ficoll and polyvinyl-pyrrolidone), 0.2% sodium dodecyl sulfate (SDS) and 50 mM Tris-HCl (pH 7.0). Sections were hybridized in a moist chamber overnight at RT. After hybridization, ganglia were washed two times in 2 X SSC (10 min each) at RT and two times in 0.5 X SSC (20 min each) at RT. This step was followed by a brief

rinse in 0.1 M Tris, pH 7.5, 0.15 M NaCl (buffer #1) and a 30 min incubation in a blocking solution containing 10% normal sheep serum and 0.3% Triton X-100 in buffer #1. Sections were blotted and then incubated in a 1:500 dilution of anti-digoxigenin-alkaline phosphatase conjugate (Adig-AP; Boehringer-Mannheim) diluted in buffer #1 with 0.3% Triton X-100 for 2 hrs at RT. Following incubation in Adig-AP, sections were collected in buffer #1, washed two times (10 min each) in buffer #1 and briefly washed in 0.1 M Tris, pH 9.5, 0.1 NaCl, 50 mM $MgCl_2$ (buffer #3). For development of the chromagen by the alkaline phosphatase conjugated to the anti-digoxygenin, sections were incubated for 8 hrs at RT in a colour solution containing 6.6 ug/ml of nitroblue tetrazolium (NBT, Boehringer-Mannheim) and 3.3 ug/ml of 5-bromo-4-chloro-3-indolylphosphate (BCIP, Boehringer-Mannheim) in buffer #3. Levamisol (1 mM, Sigma) was included in the colour solution to quench endogenous phosphatase. The colour reaction was terminated by replacing the colour solution with a stop buffer containing 10 mM Tris-HCl, pH 8.0, and 2 mM EDTA (buffer #4). Sections were rinsed briefly in buffer #4, washed in buffer #4 for 10 min and then in distilled water for 10 min. Sections were dehydrated in a graded ethanol series (3 min in both 70% and 95% ethanol and two 5 min rinses in 100% ethanol), cleared in xylene (two 5 min rinses), and mounted in permount. Ganglia were viewed with a Zeiss Universal microscope and photomicrographs were taken on Ilford XP2-400 film.

***In situ* hybridization: paraffin sections**

Central ring ganglia were dissected from *Lymnaea* and pinned out as described

above. Preparations were fixed overnight in 4% paraformaldehyde at 4°C. Following fixation, samples were incubated in 70% ethanol overnight, and then dehydrated in a graded ethanol series (1 hr in 70%, 95% and 100% ethanol). Samples were incubated in xylene (twice for 1 hr each), placed into a solution of 50% xylene and 50% paraffin for 3 hrs and then placed into 100% paraffin overnight in a 60°C oven. The next day, samples were embedded in fresh paraffin. Paraffin sections (10 um) were cut and collected on gelatin coated slides. To improve adherence of the sections to the slides, slides were incubated in a 60°C oven overnight.

Mounted sections were deparaffinized in xylene (twice for 5 min each) and then rehydrated in a graded ethanol series (briefly in 100% ethanol, 2 min in 100% ethanol, 95% ethanol and 70% ethanol, and then into distilled water for 2 min). To improve probe penetration, sections were digested for 45 min at 37°C in protease K (5 ug/ml) in 0.1 M Tris buffer. After incubation in protease K, sections were rinsed twice (5 min each) in distilled water and then air-dried. Hybridization and detection of non-radioactive labelled hybrids was performed as described above. Sections were mounted, viewed and photographed as described above.

5.3 Results

Sensorin-A immunocytochemistry reveals putative sensory neurons in *Lymnaea* CNS

Immunocytochemical localization of the sensorin-A peptide identified a discrete population of neurons in *Lymnaea* CNS (Figs. 5.1, 5.5). The pattern of immunofluorescence in more than 20 whole-mount preparations was consistent. Preincubation with the peptide against which the antibody was raised abolished immunostaining (Fig. 5.1 D,E). Sensorin-A immunoreactive neurons were present in the buccal, cerebral and pedal ganglia. Occasionally, several small cells stained in the posterior regions of the pleural and visceral ganglia (not shown).

Buccal ganglia. Sensorin-A immunoreactive neurons formed two symmetrical clusters (Fig. 5.1 C, and at higher magnification in Fig. 5.2 A). The sensorin-A immunoreactive buccal neurons in each buccal ganglion formed a cluster of approximately 40 neurons, of soma diameters of about 20 μm. A few somata were as small as 15 μm and some were as large as 25 μm.[1] These buccal clusters formed crescents at the lateral edges of each ganglion, with cells distributed equally on the ventral and dorsal surfaces.

Cerebral ganglia. Clusters of sensorin-A containing neurons were also located

[1] As noted in the Methods, the whole-mount CNS preparations were from mid-sized animals; the absolute size of the cell bodies would differ in animals that were substantially bigger or smaller. In the mid-size animals, the CNS contains a considerable number of neurons in the size range 50-100 μm, so neurons with a diameter of 20 μm are relatively small.

symmetrically in the left and right anterior lobes of the cerebral ganglia (CeS1 clusters; Figs. 5.1 A,B, 5.2 C,D). The majority of the estimated 40-60 neurons in each cluster were located on the ventral surface. The neurons in the CeS1 clusters were even more homogeneous in size (~25 μm) than those in the buccal ganglion. Although the clusters were symmetrically placed they were not identical; neurons in the right anterior lobe were consistently more dispersed than those in the left anterior lobe (this is apparent in Figs. 5.1 A,B, 5.2 C,D and 5.3 A,C). In addition to the CeS1 clusters, a group of four small sensorin-A immunopositive cells were located more medially, on the medial border of each cerebral ganglion (CeS2 clusters; arrows in Fig. 5.2 C,D). Posterior to each of these groups, were a group of three, sometimes four, large (35-40 μm) sensorin-A containing neurons (CeS3 clusters; Fig. 5.2 E,F). Unlike the CeS1 and CeS2 cluster neurons, the CeS3 neurons were not located near the ventral surface and were only evident with deeper focus into the ganglia.

Pedal ganglia. In the pedal ganglia, there were a pair of large neurons (Figs. 5.1 A,B, 5.2 B) comparable in size to the 35-40 μm immunopositive neurons in the cerebral ganglia. These two neurons were located anteriorly in each pedal ganglion near the point of origin of the medial pedal nerve. Occasionally, a group of several small cells stained in the posterior regions of each pedal ganglion (not shown).

Sensorin-A clusters in the cerebral ganglia did not colocalize with APGWamide clusters

The CeS1 clusters in the anterior lobes of the cerebral ganglia were located in

regions where clusters of ala-pro-gly-trp-NH_2 (APGWamide) containing neurons have previously been identified (Croll and Van Minnen, 1992). To determine whether the clusters of sensorin-A and APGWamide containing neurons constituted different, overlapping or identical neuronal populations, double-immunolabelling for the two peptides was performed. Although the sensorin-A containing cells were interspersed among the APGWamide containing cells, no cells within the CeS1 clusters (or elsewhere in the CNS) double-labelled for both of the peptides (Fig. 5.3). The extent of interspersion was greater on the right side where the APGWamide neurons are more abundant (Croll and Van Minnen, 1992). Focusing up and down through the preparation while repeatedly switching between filter sets, made it clear that the sensorin-A containing neurons and the APGWamide containing neurons constituted different neuronal populations.

Sensorin-A immunopositive fibers were found in nerve tracts innervating the body wall

Sensorin-A immunopositive fibers were not confined to a discrete set of nerve trunks. Examination of nerve trunks connected to the CNS in more than 20 preparations (comparing phase contrast views then fluorescent views at high magnification, focusing through the entire preparation) indicated that all of the nerves carried sensorin-A immunoreactive fibers. To examine if sensorin-A containing fibers project to the periphery, immunohistochemistry was performed on frozen body wall sections from the head region (Fig. 5.4). Immunohistochemistry revealed a substantial

subpopulation of sensorin-A positive fibers in the nerve tracts. We did not observe a wide variation in the density of sensorin-A immunopositive fibers in tracts; the examples shown in Fig. 5.4 are typical. A survey of the body wall from the dorsal to the ventral surface of the head, including sections through the tentacles (a highly mechanosensitive tissue; Janse, 1974), showed these immunoreactive fibers in tracts, but no immunoreactive somata.

In situ hybridization with a probe to the sensorin-A gene reveals a subset of neurons in the _Lymnaea_ CNS.

Consistently strong hybridization signals were observed in *Lymnaea* neurons (Figs. 5.6, 5.7, 5.8 A). The hybridization signal was confined mainly to the cytoplasm, but a weaker signal was occasionally observed in the axon segment adjacent to the cell body (for example see Fig. 5.6 A). Positive neurons were distinguished from backgroung staining by focusing through the preparation, and establishing that the hybridization signal was indeed within a neuronal cell body. When sections of the *Lymnaea* CNS were incubated with a control probe coding for a region on the sense strand of the sensorin-A mRNA (see Methods), or when the probe was omitted, the hybridization signal could no longer be detected (Fig. 5.9).

A comparison of the distribution of sensorin-A mRNA containing neurons with the distribution of sensorin-A immunoreactive neurons

Cerebral ganglia. *In situ* hybridization on cryostat sections of the cerebral

ganglia revealed groups of neurons in the left (Fig. 5.6 A,C) and right (Fig. 5.6 E) anterior lobes that labelled with the sensorin-A probe. To compare more directly the distribution of neurons that hybridized with the sensorin-A mRNA probe to the distribution of sensorin-A immunoreactive neurons, sensorin-A immunohistochemistry was performed on comparable cryostat sections of the cerebral ganglia [left (Fig. 5.6 B,D) and right (Fig. 5.6 F) anterior lobes]. Cells that labelled with the probe were approximately the same size as those that labelled with the antibody to the peptide (compare cell in Fig. 5.6 A with those in Fig. 5.6 F), and had a similar distribution (compare Fig. 5.6 C and D).

Pedal ganglia. Two large neurons in the pedal ganglia (one on the posterior surface of each ganglion) contained mRNA that hybridized to the sensorin-A probe (Fig. 5.7 A). Corresponding sensorin-A immunopositive neurons were also observed in cryostat sections of the pedal ganglia (Fig. 5.7 B,E). In addition, a cluster of neurons on the medial edge (Fig. 5.7 A,D) and posterior edge (5.7 A; only the cluster in the right pedal ganglion is shown here) of each pedal ganglion labelled with the probe. Although cells immunostained for sensorin-A in these regions (5.7 C,E), they occurred at a lower density than those that labelled with the sensorin-A probe. Sensorin-A neurons were only occasionally observed in the posterior regions, and never observed in the medial regions of the pedal ganglia when staining was performed on whole-mount preparations (see above).

Visceral ganglion. In the visceral ganglion, a cluster of neurons in the posterior region of the ganglion labelled with the sensorin-A probe (Fig. 5.8 A). Similar sized

neurons in the visceral ganglion were also immunopositive for the peptide (Fig. 5.8 B,C). Note that longitudinal sections of the ganglion (a cross-section is shown in 5.8 A) are shown in the immunofluorescent micrographs; this may explain the difference between the density of the immunolabelled cells and those that labelled with the sensorin-A probe. When staining was performed on whole-mount preparations, sensorin-A immunopositive neurons were only occasionally observed in the visceral ganglion. Differences observed between mid-sized animals (whole-mount preparations) and large animals (cryostat sections) could be attributable to a developmental expression of the peptide. Age-related changes in the expression of neuropeptide mRNAs have been reported in *Aplysia* (Kindy et al., 1991).

Buccal ganglia. Neurons that labelled with the sensorin-A probe were also found in the buccal ganglia (Fig. 5.8 D,F). Sensorin-A immunoreactive neurons were also seen in cryostat sections of the buccal ganglia (Fig. 5.8 E). A positive hybridization signal was observed in paraffin sections (Fig. 5.8 F,G), however, the strength of the signal was not as strong as that observed when using cryostat sections.

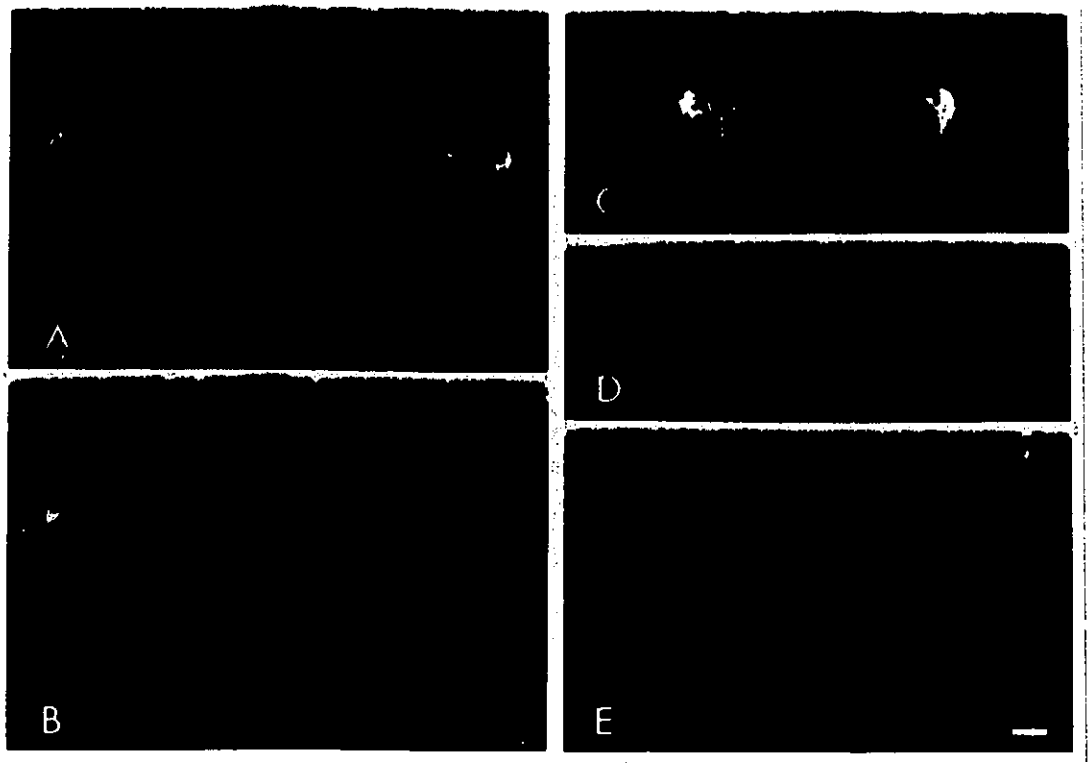

Figure 5.1. *Lymnaea* CNS whole-mount preparations immunostained for sensorin-A and photographed at low magnification. Ventral (**A**) and dorsal (**B**) views of the central ring ganglia (see Methods regarding left/right orientation; refer to Fig. 5 for a map of the central ring). Sensorin-A positive clusters of neurons in the cerebral ganglia (arrowheads in **A** and **B**) and a pair of large sensorin-A positive neurons in the pedal ganglia (arrows in **A** and **B**). **C**, immunopositive clusters of neurons in the buccal ganglia (ventral view). A control preparation in which the primary antibody solution was incubated with a 50-fold excess of the sensorin-A peptide (synthesized by Immuno-Dynamics Inc., La Jola, Ca) for 60 min prior to primary antibody incubation (**D**, buccal ganglia; **E**, ring ganglia; ventral views). Bar: A,B,E, 200 μm; C,D, 155 μm.

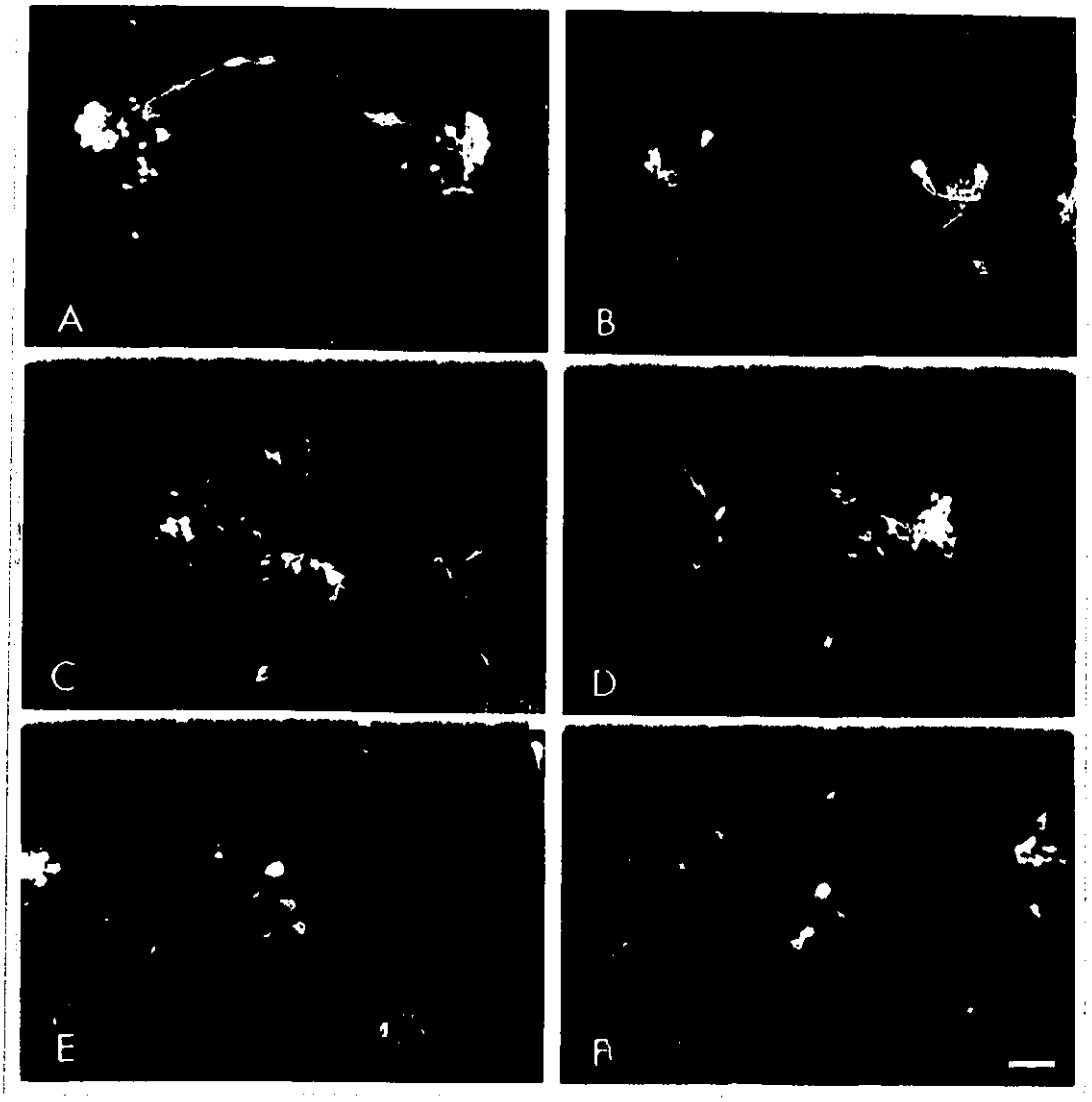

Figure 5.2. Fluorescent micrographs of sensorin-A positive neurons in whole-mount CNS preparations (ventral views photographed at high magnification). Illustrated are: immunopositive neurons forming clusters in the lateral regions of the buccal ganglia (**A**), and in the right (**C**) and left (**D**) anterior lobes of the cerebral ganglia; a group of four sensorin-A positive neurons found on the medial edge of the cerebral ganglia (arrows in **C** and **D**); a single large immunopositive neuron located in the anterior region of each pedal ganglion (**B**). Deeper focus permitted visualization of a group of three large sensorin-A positive neurons (arrows) near the medial edge of the right (**E**) and the left (**F**) cerebral ganglion. Bar: 100 μm.

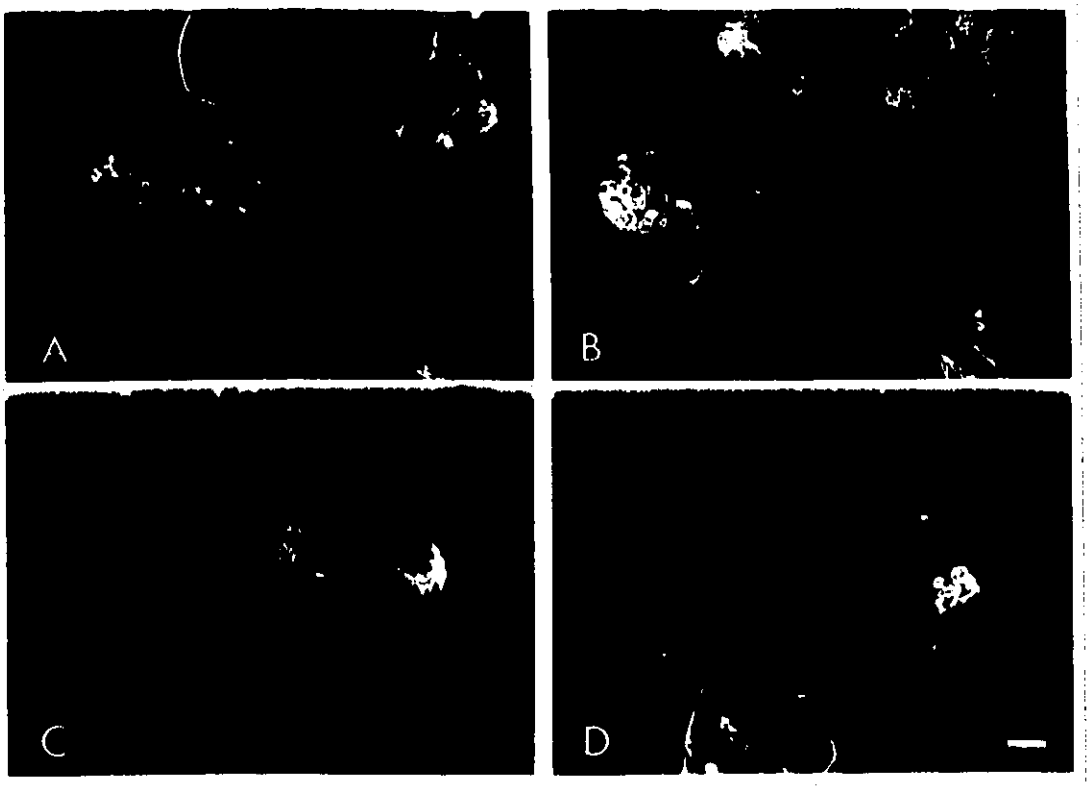

Figure 5.3. A whole-mount preparation (ventral view) double-labelled to localize sensorin-A (**A** and **C**) and APGWamide (**B** and **D**). Sensorin-A positive clusters of neurons, viewed using filters for fluorescein, in the left (**A**) and right (**B**) cerebral ganglia. The same fields viewed using filters for rhodamine, showing APGWamide positive clusters of neurons in the left (**B**) and right (**D**) cerebral ganglia (**B,D**). Bar: 100 μm.

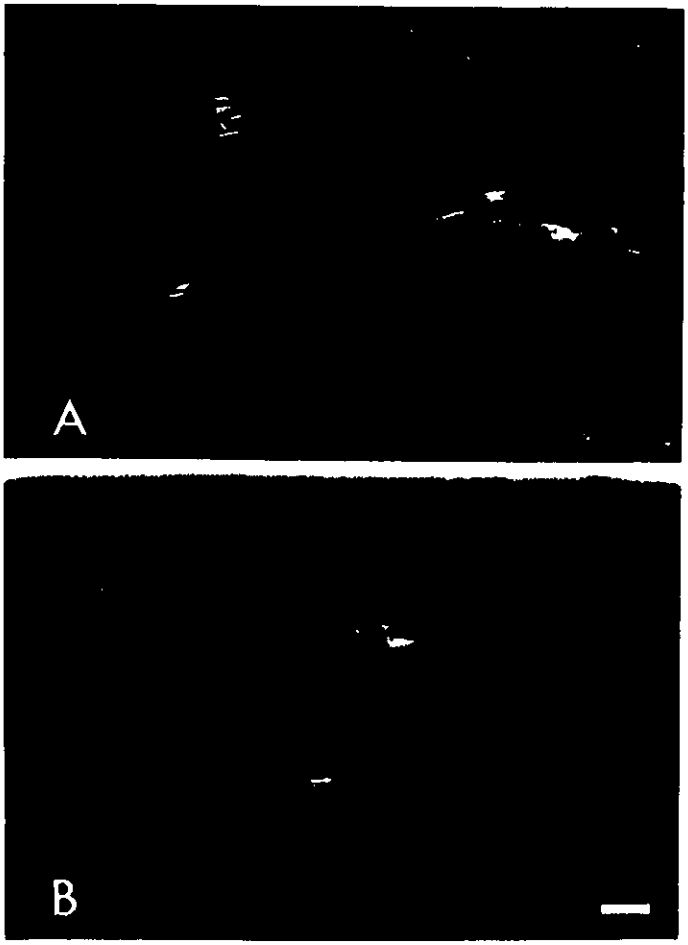

Figure 5.4. Frozen sections of body wall from the head region, immunostained for sensorin-A. Fluorescent micrographs (**A**, **B**) show that a subset of nerve fibers in peripheral nerve tracts are immunopositive for sensorin-A. Bar: 50 μm.

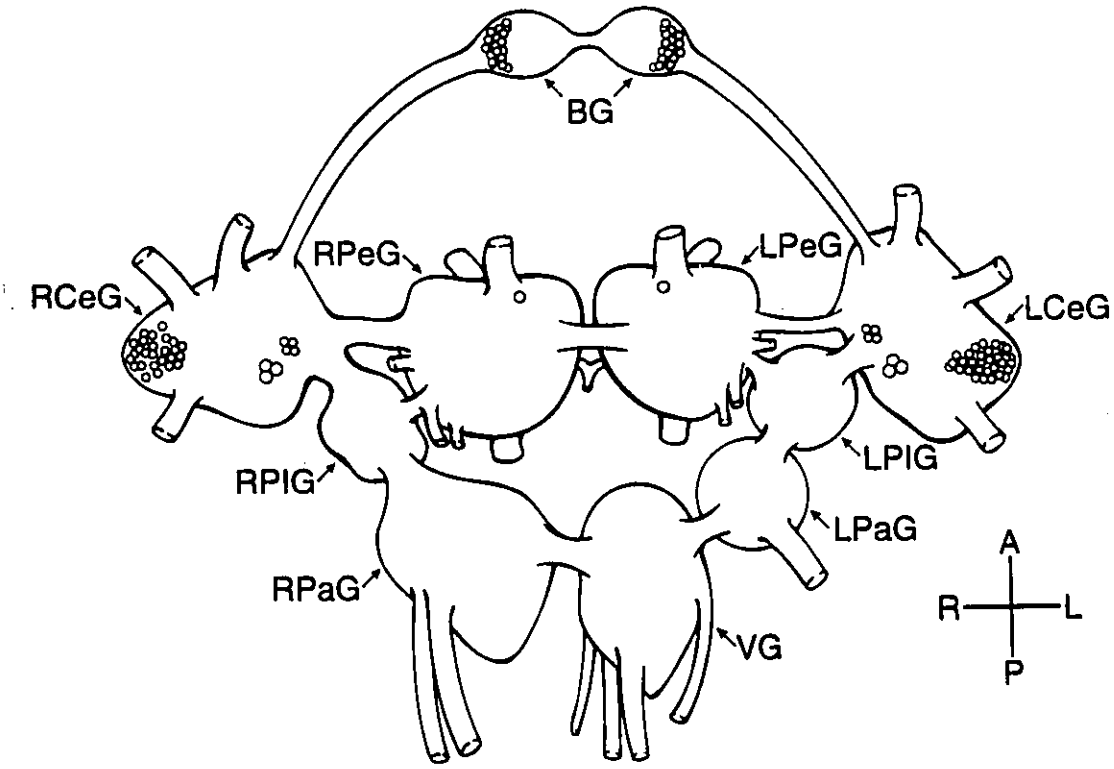

Figure 5.5. Distribution of sensorin-A immunoreactive cells within whole-mount CNS preparations of *Lymnaea*. Ventral view of the central ring ganglia and attached buccal ganglia. Circles represent the general locations of sensorin-A positive cells in a whole-mount preparation. Abbreviations: BG, buccal ganglia; RPeG, right pedal ganglion; RCeG, right cerebral ganglion; RPlG, right pleural ganglion; RPaG, right parietal ganglion; LPeG, left pedal ganglion; LCeG, left cerebral ganglion; LPlG, left pleural ganglion; LPaG, left parietal ganglion; VG, visceral ganglion; R, right; L, left; A, anterior; P, posterior.

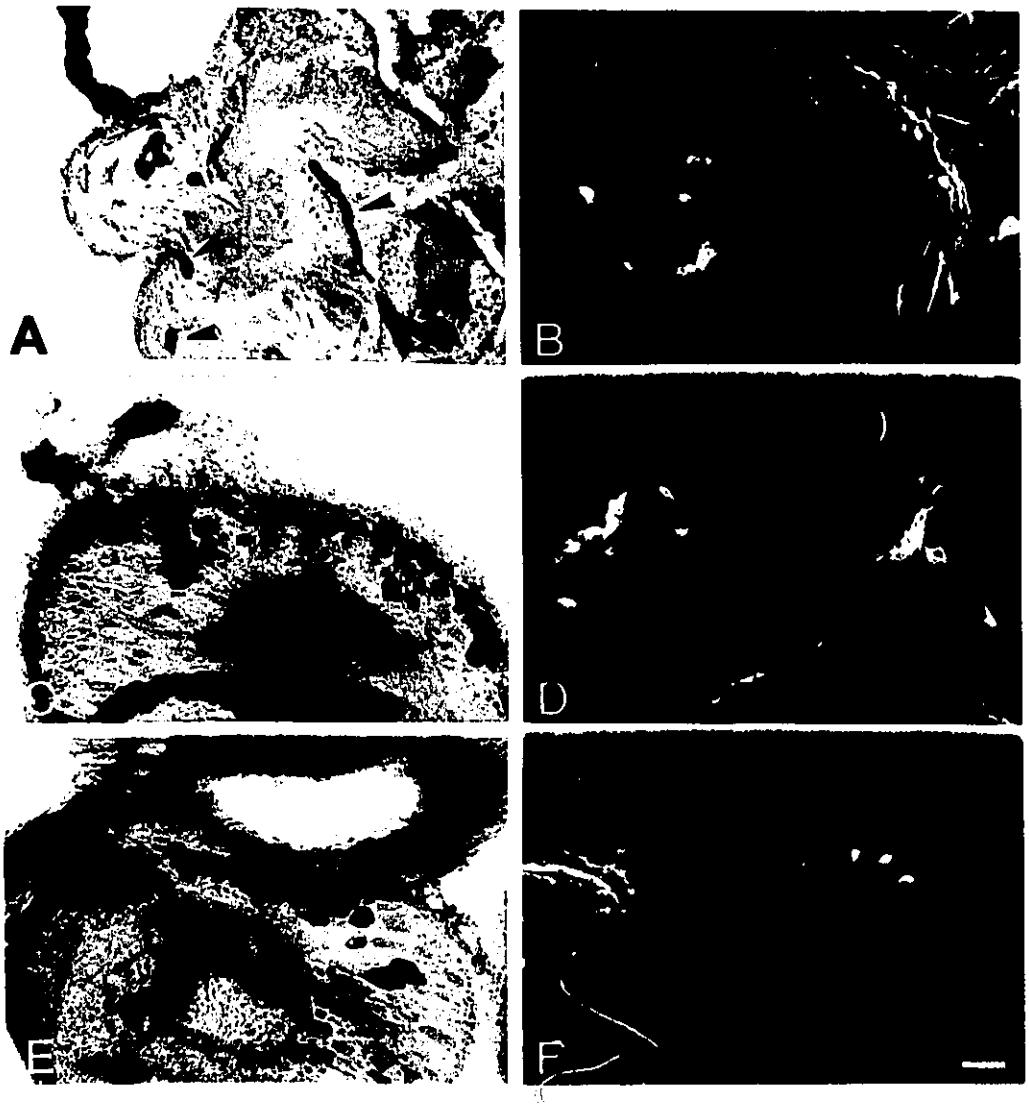

Figure 5.6. Comparisons of *in situ* hybridization with a digoxigenin labelled oligonucleotide that recognized sensorin-A mRNA with immunohistochemical localization of sensorin-A on frozen sections of *Lymnaea* cerebral ganglia. The localization of cells that contained mRNA that hybridized to the sensorin-A probe in the left (arrow in **A**; **C**) and right (**E**) anterior lobes of the cerebral ganglia correlated with cells that were sensorin-A positive in the left (**B**,**D**) and right (**F**) anterior lobes. Staining associated with tissue edges (eg. arrowheads in **A**) is commonly observed in *in situ* hybridization experiments, and results from tissue edges trapping excess label. Bar: A,B,D,F, 100 μm; C,E, 50 μm.

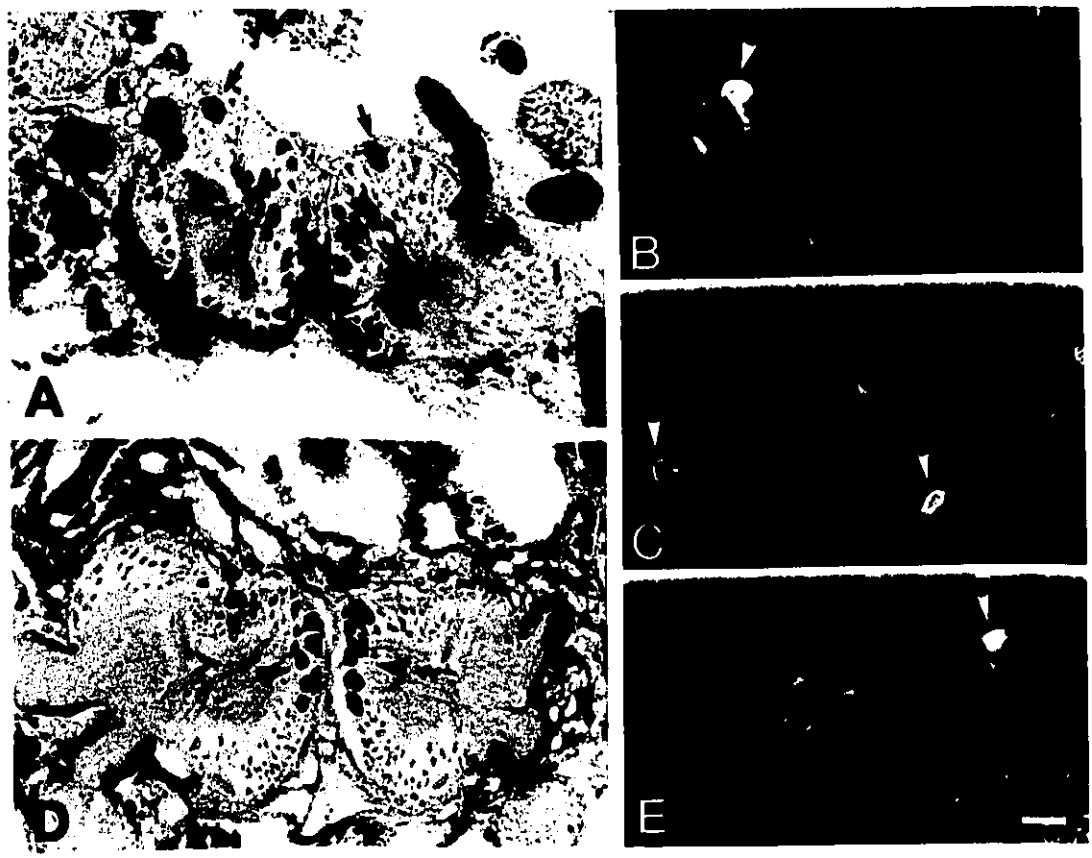

Figure 5.7. *In situ* hybridization with a digoxigenin labelled oligonucleotide that recognized sensorin-A mRNA and immunostaining for the sensorin-A peptide on frozen sections of *Lymnaea* pedal ganglia. One large neuron at the anterior edge of each pedal ganglion (arrows in **A**) contained mRNA that hybridized to the sensorin-A probe. Comparative neurons in the left (arrowhead in **B**) and right (arrowhead in **E**) pedal ganglion were immunopositive for sensorin-A. A cluster of neurons on the medial (arrowheads in **A** and **D**) and posterior edge (long arrow in **A**) of each pedal ganglion also labelled with the probe. Sensorin-A immunopositive cells were also present on the medial edge (arrows in **C** and **E**) and posterior regions (arrowheads in **C**) of each pedal ganglion. Bar: A,D, 100 μm; B,C,E, 50 μm.

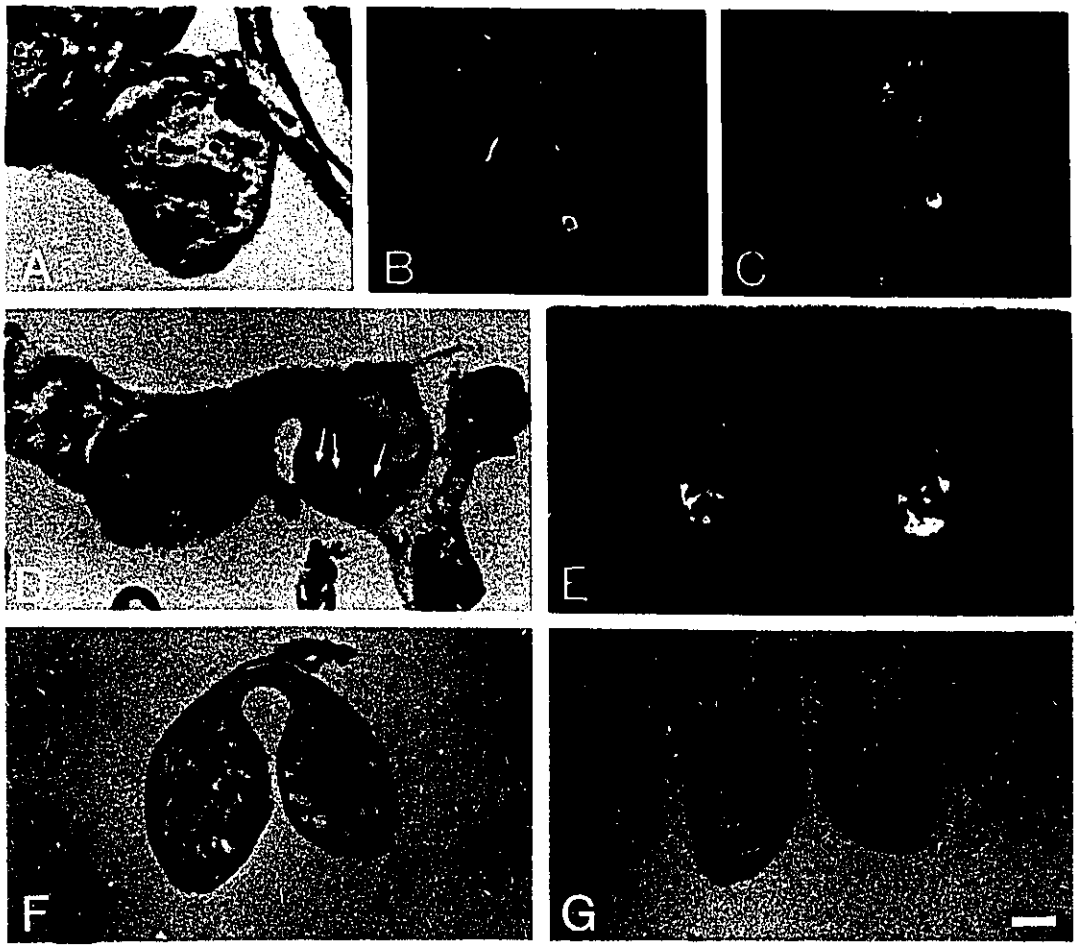

Figure 5.8. *In situ* hybridization on a frozen section of the visceral ganglion (cross-section) revealed a cluster of cells that labelled with the sensorin-A probe (**A**). Longitudinal sections through the parietal ganglion (**B**,**C**) show that sensorin-A immunoreactive cells were also present in the same region of the parietal ganglion. *In situ* hybridization with the sensorin-A probe on a frozen section of the buccal ganglia (**D**) labelled neurons (arrows in **D**) in areas where clusters of immunopositive cells are located in the buccal ganglia (**E**). Note the hybridization temperature was higher (ie. 40°C), and the length of time the sections incubated in the colour solution was longer (ie. 14 hrs) for this experiment. **F**, detection of sensorin-A mRNA containing cells in the buccal ganglia by *in situ* hybridization on paraffin sections. **G**, a control serial paraffin section that was incubated in the hybridization solution lacking the probe. Bar, 100 μm.

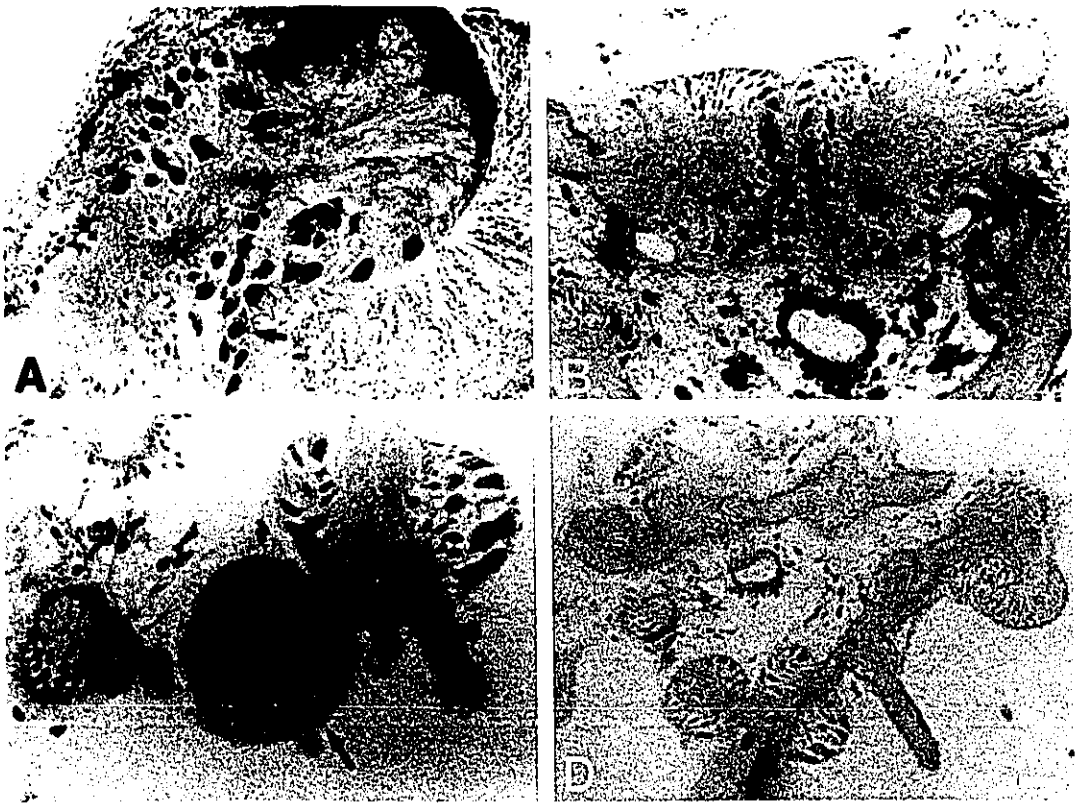

Figure 5.9. Control preparations of *Lymnaea* CNS incubated with a digoxigenin labelled oligonucleotide probe coding for the sense strand (**A-C**; see methods), or in the hybridization solution lacking the probe (**D**), demonstrate the absence of alkaline phosphatase activity. Frozen sections of the right cerebral ganglion (**A**), the pedal ganglia (**B**), and the visceral ganglion (arrow in **C**). **D**, a frozen section of the *Lymnaea* CNS; all of the central ganglia except the buccal and left cerebral are present in this micrograph. Note that occasionally the neuronal nuclei appeared dark (arrow in **A**). Bar: A, 50 μm; B,C, 100 μm; D, 200 μm.

5.4 Discussion

Immunocytochemistry for sensorin-A revealed a class of putative MSNs in the CNS of *Lymnaea*. Electrophysiological and behavioural corroboration of the function of the immunopositive neurons of *Lymnaea* is needed. However, we have several grounds for extrapolating from *Aplysia* and calling the sensorin-A immunopositive cells "putative" MSNs.

To begin with, sensorin-A immunostaining in the *Lymnaea* CNS was highly specific. There was low background fluorescence, indicating a low degree of non-specific binding and cross-reactivity, and the pattern of staining was consistent from animal to animal. Furthermore, competitive binding with a fragment of the *Aplysia* sensorin-A peptide abolished the immunostaining in the *Lymnaea* CNS.

Sensorin-A immunopositive cells do not appear to coincide with nonsensory cells (i.e. motor neurons, interneurons or neurosecretory cells) that have previously been identified in the *Lymnaea* CNS (for review see Benjamin et al., 1985; also see McCrohan 1984a,b; Khennak and McCrohan, 1988; Kyriakides et al., 1989; Syed and Winlow, 1991). The function of APGWamide neurons remains to be determined (Croll and Van Minnen, 1992), but it was clear that the sensorin-A neurons did not colocalize with these neurons.

If the staining pattern had been unrelated in the two species, it would be unlikely that the *Lymnaea* and *Aplysia* sensorin-A neurons were functionally related. There was however a considerable degree of similarity in the organization of the

sensorin-A neurons in the two species. The sensorin-A immunoreactive clusters consist of homogeneous small cells in both *Aplysia* (Byrne et al., 1974; Rosen et al., 1979; Byrne, 1980; Walters et al., 1983a; Dubuc and Castellucci, 1991) and *Lymnaea.* Homology between the sensorin-A immunoreactive cells in the buccal ganglia and the sensory cells in the buccal ganglia of *Aplysia* (Fiore and Geppetti, 1980) appears to exist. In both organisms, the sensorin-A cells in the buccal ganglia form symmetrical clusters, made up of approximately the same number of cells. However, in *Aplysia* the clusters are located in a different position, being on the dorsal surface of each ganglion (Fiore and Geppetti, 1980). In the cerebral ganglia, the CeS1 clusters appear homologous to the J clusters in *Aplysia* (Rosen et al., 1979). Both the CeS1 clusters in *Lymnaea*, and the *Aplysia* J clusters are symmetrical, located laterally in the ganglia, and made up of approximately the same number of cells. The K clusters in *Aplysia* (smaller clusters located medially to the J clusters; Rosen et al., 1979) and the 4-cell (CeS2) clusters medial to the CeS1 clusters in *Lymnaea* may be related.

Not surprisingly, given the differences in the body plan of *Lymnaea* and *Aplysia,* the homology was not complete. In *Aplysia,* the pleural and abdominal ganglia have substantial clusters of sensorin-A neurons (PlVC, rLE, RE, RF and LE clusters; Byrne et al., 1974; Byrne, 1980; Walters et al., 1983a; Dubuc and Castellucci, 1991) which were not consistently matched in the homologous ganglia of *Lymnaea* (pleural and visceral plus parietal, respectively). In the pedal ganglia the large isolated cells (Fig. 5.2 B) and the pair of 3 large cerebral ganglion cells (Fig. 5.2 E,F) have no apparent

homology with *Aplysia* neurons.

If the sensorin-A neurons in *Lymnaea* are primary mechanoafferents, a minimum expectation is that their processes would be widely represented in the organism's mechanosensitive tissue, the body wall (Ferguson and Benjamin, 1991). Evidence from *Aplysia* suggests that sensorin-A is a neurotransmitter (Brunet et al., 1991), and as such, it would be present in vesicles for transport throughout the cell. Mechanoreceptors in both vertebrates and invertebrates have been shown to transport neuropeptides to the periphery (Cuello, 1987; Pasztor et al., 1988; Pasztor and Bush, 1989); if sensorin-A is indeed a neuropeptide, it would not, therefore, be surprising to find it at peripheral sites. In *Aplysia*, sensorin-A immunoreactivity was detected in peripheral nerve fibers, and all the way to the sensory terminals (Steffensen and Morris, 1993). In *Lymnaea*, sensorin-A was also detected in peripheral fibers.

Corroborative evidence for the existence of homologous sensorin-A neurons in molluscs is provided by a study by Montarolo et al. (1993). Montorolo and his colleagues describe sensorin-A immunoreactive clusters in the cerebral ganglia of both *Helix* and *Planorbarius* that appear homologous to the J clusters in *Aplysia*. In addition, preliminary data that we have obtained (not shown) indicates that clusters of sensorin-A immunopositive neurons are also present in the CNS of *Helisoma trivolvis*.

When the distribution of neurons that labelled with the sensorin-A probe in the CNS was compared to the distribution of sensorin-A immunopositive neurons in the CNS of the same sized animals, a definite correlation was observed. Comparable

sensorin-A mRNA and peptide containing cells were found in the cerebral, pedal, visceral and buccal ganglia. Although sensorin-A immunoreactive neurons were occasionally observed in the pleural ganglia of whole-mount preparations, neurons that hybridized with the probe were not observed in cryostat sections of the pleural ganglia.

Neurons that labelled with the sensorin-A probe, and neurons that were sensorin-A immunopositive, were similar in their size and distribution within the respective ganglia. Occasionally, differences in the density of *in situ* labelled and immunolabelled cells were observed in the ganglia. Variations between the distribution of mRNA containing neurons and the corresponding peptide containing neurons have previously been reported in the *Lymnaea* CNS (Croll and Van Minnen, 1992; Kerkhoven et al., 1992). These differences could be a result of the difficulty in quantifying cells in cryostat sections, or from differences in detection sensitivity between the two techniques.

Morphological evidence suggests that the sensorin-A cells in *Lymnaea* and *Aplysia* are related. Further electrophysiological and behavioural studies are needed to establish the degree of physiological homology between the *Lymnaea* and *Aplysia* sensorin-A neurons. Several characteristic features of the *Aplysia* sensory neurons can be used to compare the physiological homology to the *Lymnaea* sensorin-A neurons. 1) the *Aplysia* sensory neurons respond with maximal activation to nociceptive stimulation (Walters et al., 1983a; Clatworthy and Walters, 1993), they are considered nociceptive MSNs (Walters, 1991, 1992) 2) the *Aplysia* sensory neurons are silent

unless stimulated and show no electrical coupling 3) the responses are graded with the intensity of stimulation and adapt slowly with a maintained stimulus 4) when peripheral and central synaptic transmission is blocked with $MgCl_2$, the sensory response persists suggesting that the MSNs are primary sensory neurons, (Byrne et al., 1974; Rosen et al., 1979; Byrne, 1980; Walters et al., 1983a; Dubuc and Castellucci, 1991).

GENERAL DISCUSSION

Mechanoreceptors in *Aplysia*

The marine mollusc *Aplysia californica* has become a model system for studying cellular mechanisms of learning and memory. Examination of *Aplysia*'s defensive withdrawal reflexes have been particularly powerful in understanding learning-related phenomena. The tail-withdrawal reflex is mediated in large part by identified tail MSNs in the pleural ganglia. Although learning-induced changes at the synapses between these primary sensory neurons and their follower motor neurons have been extensively studied, the peripheral sensory endings have not been characterized.

Using a combination of immunohistochemistry (with an antibody to a neuronal-specific tubulin) and electron microscopy, putative mechanosensory structures in the tail region were identified. These neural structures penetrate the epithelium and terminate as endings consisting of mixed cilia and microvilli. Several factors suggested that these endings could be the mechanoreceptive endings of the identified tail MSNs. First, it was assumed that neurons that penetrated the epithelium would be sensory in nature, and comparisons with other regions suggested that they were mechanosensory Secondly, the structure of these endings was similar to putative mechanosensory endings that have previously been described in molluscs (Zylstra, 1972; Wright, 1974; Philip, 1979; Zaitseva and Bocharova, 1981). Thirdly, these neuronal structures were shown not to be associated with peripheral cell bodies; the identified MSNs in *Aplysia* have been shown to be primary sensory neurons with centrally located cell bodies.

To determine if the terminal structures of sensorin-A fibers would colocalize with the structures described above, sensorin-A immunostaining was performed in the tail region. Sensorin-A immunostaining in the tail revealed mechanosensory fibers, and combined with confocal microscopy, the terminal structure of the sensorin-A fibers was determined. Sensorin-A mechanosensory fibers terminated as coiled structures deep in the body wall. These terminals did not colocalize with the ciliated endings in the epithelium. Given the current understanding of the response characteristics of the *Aplysia* MSNs, this finding is not surprising. Studies by Walters (review: Walters, 1994) have clearly shown that these sensorin-A MSNs are high-threshold mechanoreceptors that respond maximally to intense mechanical stimuli; Walters classifies them as nociceptive mechanoreceptors (Walters 1991, 1992). The structure and location of the ciliated endings in the periphery suggests that they would respond maximally to weak tactile stimulus of the animal, and thus they would be classified as low-threshold receptors. It is possible that the ciliated endings that were observed in the tail of *Aplysia* are the sensory endings of unidentified low-threshold mechanoreceptors, for which physiological evidence exists; behavioural responses are elicited with mechanical stimuli that are sub-threshold to that required to electrophysiologically activate the sensorin-A MSNs (Lukowiak and Jacklet, 1975; Perlman, 1979).

The structure and location of the sensorin-A terminals (i.e. deep in the body wall) is consistent with the sensorin-A MSNs being high-threshold mechanoreceptors. When the coiled terminals in *Aplysia* are compared to mechanosensory endings in

vertebrates and invertebrates, the general morphology of the endings most resembles that of vertebrate muscle spindles. Although muscle spindles belong to a different class of MSNs, i.e. they are proprioreceptors, they provide an example for a sensory ending with a similar structure detecting and transducing mechanical stimuli.

Potential roles for sensorin-A in the periphery

Electrophysiologically it has been suggested that sensorin-A may act centrally as a neurotransmitter (Brunet et al., 1991). The ultrastructural localization of sensorin-A to dense granules and dense core vesicles, and the predominant localization of sensorin-A to varicosities (as revealed by immunofluorescence) suggests that sensorin-A could be released from peripheral fibers, or from the receptive ending itself. These results raise the possibility of a parallel between sensorin-A and substance-P, a neuroactive peptide released at primary afferent terminals of vertebrate nociceptors (Moskowitz et al., 1984; White and Helm, 1985). Following release, sensorin-A may act as a neuromodulator with either paracrine or autocrine actions, or both. Proctolin, a pentapeptide, is released from the crayfish stretch-receptor where it enhances the sensory response (Pasztor et al., 1988; Pasztor and Bush, 1989). Proctolin has also been shown to be released from motoneurons in the crayfish, where it acts on the target organ, potentiating muscle contraction (Bishop et al., 1987). In addition, the release of sensorin-A in the periphery may result in other actions. For example, the peptide somatostatin has been shown to enhance neurite outgrowth of *Helisoma* neurons in culture (Bulloch, 1987), and the peptide SCP_B has been shown to be released from an

identified neuron in *Aplysia*, where it acts on target muscle via a second messenger pathway (Lloyd et al., 1984).

Regeneration of MSNs in *Aplysia* and its direct correlation to functional recovery

Regeneration of tail MSNs in *Aplysia* was examined following bilateral crush of the p9 nerves. Regeneration was monitored morphologically using immunostaining for sensorin-A, and behaviourally by examining the tail-withdrawal reflex. The rate of regeneration was found to be ~4 mm/day, a rate somewhat faster than has previously been recorded in other molluscs (rates from ~400 μm a day to ~1 mm/day have been reported; Murphy and Kater, 1978; Allison and Benjamin, 1985; Kruk and Bulloch, 1992). Differences in rates of regeneration could result from the location of the nerve lesion (i.e. central versus peripheral), intrinsic properties of the neurons (e.g. sensory versus motor), or the age of the animal being studied; the rate of regeneration in molluscan neurons has been shown to be age dependent, with older animals showing slower rates of regeneration (Janse et al., 1986).

Since evidence of behavioural recovery was observed before regenerating fibers would be expected to reach the target site (partial recovery was observed in some animals as early as Day 6), the possibility that reconnection of axons, via electrical coupling, may mediate some of the observed recovery can not be overlooked. Morphological evidence indicated that end-to end fusion, either directly or by electrical coupling, of sensory fibers did not occur; growth of new sensory fibers was clearly observed along nerve p9. However, it is possible that neurites form electrical

connections with the distal stump as they migrate down p9, a model which has been proposed for regenerating neurites (Bittner, 1991).

Development of a model system

Combined with previous studies, work described in this thesis substantially increases the power of *Aplysia* MSNs as a model system; up until now, the "input" point to the model was a black box. Walters et al. (1983a) first identified the tail MSNs of *Aplysia*, by stimulating the tail while recording from ganglia in semi-intact preparations. Since then, it has been shown that sensitization (both centrally and peripherally) of the tail MSNs occurs following noxious stimulation of the tail (Billy and Walters, 1989a; Woolf and Walters, 1991). It would now be possible to visualize sensory fibers in the periphery, with sensorin-A immunostaining, and seek the morphological correlate of the increased peripheral excitability exhibited by these MSNs following noxious stimulation (Billy and Walters, 1989a).

The identified tail MSNs of *Aplysia* have been shown to rearborize in culture, where they synapse with appropriate motor neurons when given a choice (Glanzman, 1989). Now that the peripheral endings of the sensorin-A neurons have been characterized, it may be possible to reconstruct the sensory ending in culture, making it accessible to cellular investigations (e.g. patch-clamp recordings, Ca^{2+} imaging, second messenger studies).

Significance of putative MSNs in *Lymnaea*

The pond snail *Lymnaea stagnalis* has emerged as a model system for studying the cellular basis of rhythm generation. Syed et al (1990) were able to reconstruct the central pattern generator that underlies respiratory rhythm in *Lymnaea* with three identified interneurons in culture. *In vivo*, the respiratory rhythm driven by this pattern is subject to modulation by mechanosensory stimuli (Syed and Winlow, 1991). An examination of sensory inputs to the reconstituted central pattern generator has been made difficult, however, because of the paucity of identified primary sensory neurons in *Lymnaea.* Studies of the neural basis of other rhythmic behaviours such as locomotion (Winlow and Haydon, 1986) and feeding (Kemenes and Elliot, 1994) in *Lymnaea* would likewise benefit from information about sensory inputs.

APPENDIX

The following results were obtained by Mike Dulin, a doctoral student in the lab of Dr. ET Walters (Department of Physiology and Cell Biology, University of Texas Medical School at Houston). These results stem from a collaborative project with our lab, and have not yet been published.

Figure 1. The neuronal circuitry underlying tail evoked siphon responses has been shown to be centrally mediated (Hickie, 1994). Stimulation of the tail results in a sensory signal that moves from the tail through pedal nerve p9 and into the pleural ganglion. Tail sensory neurons then relay the signal to interneurons which in turn activate the siphon motor neurons in the abdominal ganglion. By crushing p9, the tail is effectively removed from this central circuit. By monitoring siphon responses to tail stimulation after p9 crush, it is possible to determine when the tail becomes reconnected into the central circuit, and if so, when this occurs. Recovery of the siphon withdrawal response to tail stimulation was considered to be a behavioral correlate of reinnervation of the tail and therefore a signal that regeneration had occurred. Following nerve crush, thirty-three animals were monitored for recovery of the tail evoked siphon response. Animals were tested every 2-3 days. A light pinch was used in 22 animals (grey bars) while shock was used as a stimulus in the remaining 11 animals (white bars). Three animals failed to show any signs of recovery.

Figure 2. Electrophysiological evidence for regeneration. Sensory neurons that had axons in the p9 nerve were identified by intracellularly monitoring the cell while directly stimulating the nerve. Stimuli were delivered distal to the crush site (~2 cm from the pedal ganglion), and at an equivalent distance on the control nerve. Since the tail sensory neurons are primary sensory neurons (Walters et al., 1983), they respond to nerve stimulation with an orthodromic spike; the spike is characterized by a constant latency between the nerve stimulus and the resultant action potential and by the lack of any pre-potential. Sensory neurons were examined sequentially in the p9 region of the pleural cluster (Walters et al., 1983; Zhang et al., 1993), and the number of neurons with and without axons (i.e. evoked action potentials) in p9 was recorded. Each solid triangle represents data collected from one animal, with 4-10 cells surveyed in each animal. The percentage of cells that responded to p9 stimulation distal to the crush site is plotted against time. A best fit line was determined using linear regression (slope=1.93; R=.89). The dashed line represents the average number of cells that responded to stimulation of the control p9 nerve (95%).

Figure 3. A, Schematic of the preparation used to examine sensory receptive fields after p9 nerve crush. Between 20 to 23 days after crush, the animal was anesthetized with a lethal injection of isotonic $MgCl_2$. The tail was dissected away from the rest of the body, and the p9 nerves were left as the only connection from the tail to the ring ganglia (see schemata in **A**). The pleural ganglia were desheathed in a well at one end of a chamber and the tail was stretched out and pinned down in another part of the chamber. The preparation was washed with ASW, and the tail was injected with ASW and left to equilibrate for 1 hr. A survey for sensory neurons with receptive fields in the tail region was conducted by tapping the tail region with an ~3-6g Von Frey hair after each impalement. A neuron was considered to have a receptive field in the tail if it fired several action potentials immediately following a tap. The force necessary to activate receptive fields was significantly decreased after crush (n=6) as compared to control (n=6), using a 2 tailed paired t-test (**B**). The average size of the receptive field of a crush sensory neuron (n=6) was also significantly smaller than the average size of the receptive field of a control sensory neuron (n=6; **C**).

REFERENCES

Abrams TW, Castellucci VF, Camardo JS, Kandel ER, Lloyd PE (1984) Two endogenous neuropeptides modulate the gill and siphon withdrawal reflex in *Aplysia* by presynaptic facilitation involving cAMP-dependent closure of a serotonin-sensitive potassium channel. Proc Natl Acad Sci USA 81:7956-7960.

Allison P, Benjamin PR (1985) Anatomical studies of central regeneration of an identified molluscan interneuron. Proc R Soc Lond Series B. 226:135-157.

Audesirk G (1978) Central control of cilia in *Tritonia diomedia.* Nature 272:541-543.

Bailey CH, Castellucci VF, Koester J, Kandel ER (1979) Cellular studies of peripheral neurons in siphon skin of *Aplysia californica.* J Neurophys 42:530-557.

Bannatyne BA, Blackshaw SE, McGregor M (1989) New growth elicited in adult leech mechanosensory neurones by peripheral axon damage. J Exp Biol 143:419-34.

Barber A (1983) Properties of the serotonergic cerebral ganglion neurons of the gastropod mollusc, *Philine aperta.* Comp Biochem Physiol 76:135-149.

Baylor DA, Nicholls JG (1969) Chemical and electrical synaptic connections between cutaneous mechanoreceptor neurons in the central nervous system of the leech. J Physiol 203:591-609.

Baylor DA, Nicholls JG (1971) Patterns of regeneration between individual nerve cells in the central nervous system of the leech. Nature 232:268-270.

Benjamin PR, Elliott CJ, Ferguson GP (1985) Neural network analysis in the snail brain. In A Selverston (ed): Model neural networks and behaviour. Plenum Press, New York, p.87-108.

Billy AJ, Walters ET (1989a) Long-term expansion and sensitization of mechanosensory receptive fields in *Aplysia* support an activity-dependent model of whole-cell sensory plasticity. J Neurosci 9:1254-1262.

Billy AJ, Walters ET (1989b) Modulation of mechanosensory threshold in *Aplysia* by seratonin, small cardioactive peptide$_B$ (SCP$_B$), FMRFamide, acetylcholine and dopamine. Neurosci Let 105:200-204.

Bishop B (1982) Neural plasticity: Part 3. Responses to lesions in the peripheral nervous system (review). Phys Ther 62:1275-82.

Bishop CA, Wine JJ, Nagy F, O'Shea MR (1987) Physiological consequences of a peptide cotransmitter in a crayfish nerve-muscle preparation. J Neurosci 7:1769-1779.

Bittner GD (1991) Long-term survival of anucleat axons and its implications for nerve regeneration (review). Trends Neurosci 14:188-193.

Blackshaw SE (1981) Morphology and distribution of touch cell terminals in the skin of the leech. J Physiol 320:219-228.

Blackshaw SE, Nicholls JG, Parnas I (1982a) Expanded receptive fields of cutaneous mechanoreceptor cells after a single neurone deletion in leech central nervous system. J Physiol 326:261-268.

Blackshaw SE, Nicholls JG, Parnas I (1982b) Physiological responses, receptive fields

and terminal arborizations of nociceptive cells in the leech. J Physiol 326:251-260.

Blackshaw S, McKay DA, Thompson SWN (1984) The fine structure of a leech stretch receptor neurone and its efferent supply. J Physiol 350, 76P.

Blackshaw SE, Thompson SWN (1988) Hyperpolarizing responses to stretch in sensory neurones innervating leech body wall muscle. J Physiol 396:121-137.

Blackshaw, SE (1993) Stretch receptors and body wall muscle in leeches. Biochem Physiol 105A:643-652.

Bovolenta P, Wandosell F, Nieto-Sampedro M (1991) Central neurite outgrowth over glial scar tissue *in vitro*. In PC Letourneau, SB Kater, ER Macagno (eds): The nerve growth cone. Raven Press, New York, p.477-488.

Brown HM, Ottoson D, Rydqvist B (1978) Crayfish stretch receptor: an investigation with voltage-clamp and ion sensitive electrodes. J Physiol 284:155-179.

Brunet J, Shapiro E, Foster SA, Kandel ER, Iino Y (1991) Identification of a peptide specific for *Aplysia* sensory neurons by PCR-based differential screening. Science 252:856-859.

Bulloch AGM, Kater SB (1982) Neurite outgrowth and selection of a new electrical connections by adult *Helisoma* neurons. J Neurophysiol 48:569-583.

Bulloch AGM (1987) Somatostatin enhances neurite outgrowth and electrical coupling of regenerating neurons in *Helisoma*. Brain Res 412:6-17.

Bulloch AGM (1989) Sprouting by intact *Helisoma* neurons: Role for glutamate. J Neurosci Res 23:384-395.

Byrne J, Castelluci V, Kandel ER (1974) Receptive fields and response properties of mechanoreceptor neurons innervating siphon skin and mantle shelf in *Aplysia*. J Neurophysiol 37:1041-1064.

Byrne JH, Castelluci VF, Carew TJ, Kandel ER (1978) Stimulus-response relations and stability of mechanoreceptor and motor neurons mediating defensive gill-withdrawal reflex. J Neurophysiol 41:402-417.

Byrne JH (1980) Neural circuit for inking behavior in *Aplysia californica*. J Neurophysiol 43:896-911.

Cameron AA, Leah JP, Snow PJ (1988) The coexistence of neuropeptides in feline sensory neurons. Neuroscience 27:969-979.

Camhi JM, Macagno E (1991) Using fluorescence photoablation to study the regeneration of singly cut leech axons. J Neurobiol 22:116-29.

Canessa CM, Horisberger J-D, Rossier BC (1993) Epithelial sodium channel related to proteins involved in neurodegeneration. Nature 361:467-470.

Caroni P, Schwab ME (1988) Two membrane protein fractions from rat central myelin with inhibitory properties for neurite growth and fibroblast spreading. J Cell Biol 106:1281-1288.

Carrow GM, Levitan IB (1989) Selective formation and modulation of electrical synapses between cultured *Aplysia* neurons. J Neurosci 9:3657-3664.

Chalfie M, Sulston J (1981) Developmental genetics of the mechanosensory neurons of *Caenorhabditis elegans*. Dev Biol 82:358-370.

Chalfie M, Thomson JN (1982) Structural and functional diversity in the neuronal microtubules of *Caenorhabditis elegans.* J Cell Biol 93:15-23.

Chalfie M, Thomson JN, Sulston JE (1983) Induction of neuronal branching in *C. elegans.* Science 221:61-63.

Chalfie M, Dean E, Reilley E, Buck K, Thomson JN (1986) Mutations affecting microtubule structure in *Caenorhabditis elegans.* J Cell Sci Suppl 5:257-271.

Chalfie M, Au M (1989) Genetic control of differentiation of the *Caenorhabditis elegans* touch receptor neurons. Science 243:1027-103.

Chalfie M, Wolinsky E (1990) The identification and suppression of inherited neurodegeneration in *Caenorhabditis elegans.* Nature 345:410-415.

Chalfie M, Driscoll M, Huang M (1993) Degenerin similarities. Nature 361:504.

Chase R, Kamil R (1983) Morphology and odor sensitivity of regenerated snail *Achatina fulica* tentacles. J Neurobiol 14:34-50.

Chase R, Goodman HE (1977) Homologous neurosecretory cell groups in the land snail *Achatina fulica* and the sea slug *Aplysia californica.* Cell Tissue Res 176:109-120.

Clatworthy AL, Walters ET (1993) Rapid amplification and facilitation of mechanosensory discharge in *Aplysia* by noxious stimulation. J Neurophys 70:1181-1194.

Clatworthy AL, Walters ET (1994) Comparative analysis of hyperexcitability and synaptic facilitation induced by nerve injury in two populations of mechanosensory neurones of *Aplysia.* J Exp Biol 190:217-238.

Cohen AH, Mackler SA, Selzer ME (1988) Behavioral recovery following spinal transection: funtional regeneration in the lamprey CNS. Trends Neurosci 11:227-231.

Cohen JL, Weiss KR, Kupfermann I (1978) Motor control of buccal muscles in *Aplysia.* J Neurophysiol 41:157-180.

Cooper BF, Krontiris-Litowitz JK, Walters ET (1989) Humoral factors released during trauma of *Aplysia* body wall. II. Effects of possible mediators. J Comp Physiol 159B:225-235.

Cottrell GA, Macon JB (1974) Synaptic connections of two symmetrically placed giant serotonin-containing neurones. J Physiol 236:435-464.

Croll RP, Baker MW (1990) Axonal regeneration and sprouting following injury to the cerebral-buccal connective in the snail *Achatina fulica.* J Comp Neurol 300:273-86.

Croll RP, Van Minnen J (1992) Distribution of the peptide Ala-Pro-Gly-Trp-NH_2 (APGWamide) in the nervous system and periphery of the snail *Lymnaea stagnalis* as revealed by immunocytochemistry and in situ hybridization. J Comp Neurol 324:567-574.

Crow TJ, Alkon DL (1980) Associative behavioural modification in *Hermissenda*: Cellular correlates. Science 209:412-414.

Cuello AC (1987) Peptides as neuromodulators in primary sensory neurons (review).

Neuropharm 26:971-9.
Deriemer SA, Elliott EJ, Macagno ER, Muller KJ (1983) Morphological evidence that regenerating axons can fuse with severed axon segments. Brain Res 272:157-61.
Desai C, Garriga G, McIntyre SI, Horvitz HR (1988) A genetic pathway for the development of the *Caenorhabditis elegans* HSN motor neurons. Nature 336:638-646.
Driscoll M, Chalfie M (1991) The mec-4 gene is a member of a family of *Caenorhabditis elegans* genes that can mutate to induce neuronal degeneration. Nature 349:588-593.
Dubner R, Bennett GJ (1983) Spinal and trigeminal mechanisms of nociception. Ann Rev Neurosci 6:381-418.
Dubuc B, Castellucci VF (1991) Receptive fields and properties of a new cluster of mechanoreceptor neurons innervating the mantle region and the branchial cavity of the marine mollusk *Aplysia californica*. J Exp Biol 156:315-334.
Dulin MF, Walters ET (1993) Similar alterations of sensory and motor neurons in *Aplysia* persist after regeneration. Soc Neurosci Abstr 19:578.
Edwards C, Ottoson D, Rydqvist B, Swerup C (1981) The permeability of the transducer membrane of the crayfish stretch receptor to calcium and other divalent cations. Neuroscience 6:1455-1460.
Emery DG, Audesirk TE (1978) Sensory cells in *Aplysia*. J Neurobiol 9:173-179.
Erxleben C (1989) Stretch-activated current through single ion channels in the abdominal stretch receptor organ of the crayfish. J Gen Physiol 94:1071-1083.
Erxleben C (1993) Calcium influx through stretch-activated cation channels mediates adaptation by potassium current activation. Neuroreport 4:616-618.
Ewadinger NM, Syed NI, Lukowiak K, Bulloch GM (1994) Differential tracer coupling between pairs of identified neurones of the mollusc *Lymnaea stagnalis*. J Exp Biol 192:291-297.
Ferguson GP, Benjamin PR (1991) The whole-body withdrawal response of *Lymnaea stagnalis*. II. Activation of central motorneurones and muscles by sensory input. J Exp Biol 158:97-116.
Fiore L, Geppetti L (1980) Neurobiology of invertebrates. In J. Salanki (ed): Advances in physiological sciences. p. 20.
Frank E, Jansen JK, Rinvik E (1975) A multisomatic axon in the central nervous system of the leech. J Comp Neurol 159:1-13.
Fredman SM (1988) Recovery of escape locomotion following a CNS lesion in *Aplysia*. Behav Neural Biol 49:261-279.
French SA (1992) Mechanotransduction. Ann Rev Physiol 54:135-152.
Gaze RM (1970) The formation of nerve connections. Academic Press, London.
Geraerts WPM (1976) Control of growth by the neurosecretory hormone of the light green cells in the freshwater snail, *Lymnaea stagnalis*. Gen Comp Endocrin 29:61-71.
Geraerts WPM, Bohlken S (1976) The control of ovulation in the hermaphroditic freshwater snail *Lymnaea stagnalis* by the neurohormone of the caudodorsal

cells. Gen Comp Endocrin 28:350-357.
Giloh H, Sedat JW (1982) Fluorescence microscopy: reduced photobleaching of rhodamine and fluorescein protein conjugates by n-propyl gallate. Science 217:1252-1255.
Glanzman DL, Kandel ER, Schacher S (1989) Identified target motor neuron regulates neurite outgrowth and synapse formation of *Aplysia* sensory neurons in vitro. Neuron 3:441-450.
Golas LB, Pasztor VM (1991). Tissue culture of a crustacean mechanosensory neuron: a model for the study of mechanotransduction using patch clamp and intracellular electrode techniques. Bull Can Soc Zool 22:37-38.
Goldschmeding JT, van Duivenboden YA, Lodder JC (1981) Axonal branching pattern and coupling mechanisms of the cerebral giant neurons in the snail *Lymnaea stagnalis*. J Neurobiol 12:405-424.
Granzow B, Kater SB (1977) Identified higher-order neurons controlling the feeding motor program. Neurosci 2:1049-1063.
Granzow B, Rowell CHF (1981) Further observations on the serotonergic cerebral neurons of *Helisoma* (Mollusca: Gastropoda): The case for homology with the metacerebral giant cells. J Exp Biol 90:283-307.
Helme RD, Andrews PV (1985) The effect of nerve lesions on the inflammatory response to injury. J Neurosci Res 13:453-459.
Herman RK (1987) Mosaic analysis of two genes that affect nervous system structure in *Caenorhabditis elegans*. Genetics 116:377-388.
Hickie C (1994) Function and motor neuronal analysis of defensive siphon response in *Aplysia californica*. Doctoral Thesis. University of Texas Medical School, Houston, Texas.
Hong K, Driscoll M (1994) A transmembrane domain of the putative channel subunit MEC-4 influences mechanotransduction and neurodegeneration in *C. elegans*. Nature 367:470-473.
Hope RA, Hammond BJ, Gaze RM (1976) The arrow model: retinotectal specificity and map formation in the goldfish visual system. Proc R Soc Lond Series B 194:447-466.
Hoy RR, Bittner GD, Kennedy D (1967) Regeneration in crustacean motoneurons: Evidence for axonal fusion. Science 156:251-252.
Huang M, Chalfie M (1994) Gene interactions affecting mechanosensory transduction in *Caenorhabditis elegans*. Nature 367:467-470.
Ichinose M, Sawada M, Maeno T, McAdoo DJ (1989) Effect of acetylcholine on the ventrocaudal sensory neurons in the pleural ganglia of *Aplysia*. Cell Mol Neurobiol 9:233-245.
Jahan-Parwar B (1969) Studies on chemoreception in *Aplysia californica* (Mollusca, Gastropoda). Am Zool 9:1097.
Jahan-Parwar B, Fredman SM (1978) Control of pedal and parapodial movements in *Aplysia*. II. Cerebral ganglion neurons. J Neurophysiol 41:609-620.
Janse C (1974) A neurophysiological study of the peripheral tactile system of the pond

snail *Lymnaea stagnalis* (L.). Neth J Zool 24:93-161.
Janse C, Beek A, van Oorschot I, Van der Roest M (1986) Recovery of damage in a molluscan nervous system is impaired with age. Mech Ageing Dev 35:179-183.
Johansen J, Hockfield S, McKay RDG (1984) Distribution and morphology of nociceptive cells in the CNS of three species of leeches. J Comp Neurol 226:263-273.
Johnson AR, Erdos EG (1973) Release of histamine from mast cells by vasoactive peptides. Proc Soc Exp Bio Med 142:1252-1256.
Kandel ER, Tauc L (1966) Input organization of two symmetrical giant cells in snail brain. J Physiol 183:269-286.
Kandel ER (1979) Behavioural biology of *Aplysia*: A contribution to the comparative study of opisthobranch molluscs. W.H. Freeman and Co., San Francisco, CA.
Kater SB, Mattson MP (1988) Extrinsic and intrinsic regulators of neurite outgrowth and synaptogenesis in isolated, identified *Helisoma* neurons in culture. In: *Cell Culture Approaches to Invertebrate Neuroscience*. D Beadle, G Lees and SB Kater eds. Academic Press, Orlando, pp. 1-31.
Kemenes G, Elliot CJH (1994) Analysis of the feeding motor pattern in the pond snail, *Lymnaea stagnalis*: Photoinactivation of axonally stained pattern-generating interneurons. J Neurosci 14:153-166.
Kennedy WR, Webster HF, Yoon KS (1975) Human muscle spindles: fine structure of the primary sensory ending. J Neurocytol 4:675-695.
Kerkhoven RM, Croll RP, Ramkema MD, Van Minnen J, Boer HH (1992) The VD_1/RPD_2 neuronal system in the central nervous system of the pond snail *Lymnaea stagnalis* studied by in situ hybridization and immunocytochemistry. Cell Tissue Res 267:551-559.
Khennak M, McCrohan CR (1988) Cellular organisation of the cerebral anterior lobes in the central nervous sytem of *Lymnaea stagnalis*. Comp Biochem Physiol 91A:387-394.
Kindy MS, Srivatsan M, Peretz B (1991) Age-related differential expression of neuropeptide mRNAs in the *Aplysia*. Neuroreport 2:465-468.
Kristan WB, McGirr SJ, Simpson GU (1982) Behavioural and mechanosensory neurone responses to skin stimulation in leeches. J Exp Biol 96:143-160.
Kruger L, Perl ER, Sedivec MJ (1981) Fine structure of myelinated and mechanical nociceptor endings in cat hairy skin. J Comp Neurol 198:137-154.
Kruk PJ, Bulloch AGM (1992) Axonal regeneration of an identified *Helisoma* neurons depends on the site of axotomy. J Neurosci Res 31:401-412.
Kyriakides M, McCrohan CR, Slade CT, Syed NI, Winlow W (1989) The morphology and electrophysiology of the neurones of the paired pedal ganglia of *Lymnaea stagnalis* (L.). Comp Biochem Physiol 93A:861-876.
Lee MK, Rebhun LI, Frankfurter A (1990a) Post-translational modification of class III ß-tubulin. Proc Natl Acad Sci USA 87:7195-7199.
Lee MK, Tuttle JB, Rebhun LI, Cleveland DW, Frankfurter A (1990b) The expression and post-translational modification of a neuron-specific ß-tubulin isotype during

chick embryogenesis. Cell Motil Cytoskel 17:118-132.
Lembeck F, Holzer P (1979) Substance P as a neurogenic mediator of antidromic vasodilation and neurogenic plasma extravasation. Naunyn Schmiedebergs Arch Pharmacol 310:175-183
Lin SS, Levitan IB (1991) Concavalin A: a tool to investigate neuronal plasticity. Trends Neurosci 14:273-277.
Lloyd PE, Kupfermann I, Weiss KR (1984) Evidence for parallel actions of a molluscan neuropeptide and seratonin in mediating arousal in *Aplysia*. Proc Natl Acad Sci USA 81:2934-2937.
Lloyd PE, Willows AOD (1988) Multiple transmitter neurons in *Tritonia*. II. Control of gut motility. J Neurobiol 19:55-67.
Lloyd PE, Kupfermann I, Weiss KR (1988a) Central peptidergic neurons regulate gut motility in *Aplysia*. J Neurophysiol 59:1613-1626.
Lloyd PE, Masinovsky BP, Willows AOD (1988b) Multiple transmitter neurons in *Tritonia*. I. Biochemical studies. J Neurobiol 19:39-54.
Lukowiak K, Jacklet J (1975) Habituation and dishabituation mediated by the peripheral and central neural circuits of the siphon of *Aplysia*. J Neurobiol 6:183-200.
Macagno ER, Muller KJ, DeRiemer SA (1985) Regeneration of axons and synaptic connections by touch sensory neurons in the leech nervous system. J Neurosci 5:2510-2521.
Mackey SL, Glanzman DL, Small SA, Dyke AM, Kandel ER, Hawkins R (1987) Tail shock produces inhibition as well as sensitization of the siphon-withdrawal reflex of *Aplysia*: possible behavioral role for presynaptic inhibition mediated by the peptide Phe-Met-Arg-Phe-NH2. Proc Natl Acad Sci USA 84:8730-8734.
Masinovsky B, Kempf SC, Callaway JC, Willows AOD (1988) Monoclonal antibodies to the molluscan small cardioactive peptide SCP_B: Immunolabelling of neurons in diverse invertebrates. J Comp Neurol 273:500-512.
McClellan AD (1990) Locomotor recovery in spinal-transected lamprey: role of functional regeneration of descending axons from brainstem locomotor command neurons. Neuroscience 37:781-798.
McClellan AD (1992) Functional regeneration and recovery of locomotor activity in spinally transected lamprey. J Expt Zool 261:274-287.
McCrohan CR (1984a) Properties of ventral cerebral neurons involved in the feeding system of the snail, *Lymnaea stagnalis*. J Exp Biol 108:257-272.
McCrohan CR (1984b) Initiation of feeding motor output by an identified interneurone in the snail *Lymnaea stagnalis*. J Exp Biol 113:351-366.
McMahon SB, Kett-White R (1991) Sprouting of peripherally regenerating primary sensory neurones in the adult central nervous system. J Comp Neurol 304:307-15.
Moffet SB, Austin DR (1982) Generation of new cerebral ganglion neurons in the snail *Melampus*: an ultrastructural study. J Comp Neurol 207:177-182.
Moffett SB, Snyder KA (1985) Behavioral recovery associated with central nervous

system regeneration in the snail *Melampus*. J Neurobiol 16:193-209.
Moffet SB, Ridgeway RL (1988) Structural repair and functional recovery following cerebral ganglion removal in the pulmonate snail *Melampus*. Amer Zool 28:1109-1121.
Moffett SB (1992) Mating behavior in the pulmonate snail *Melampus*: can regeneration restore function? Acta Biologica Hungarica 43:367-74.
Montarolo PG, Casadio A, Morando L, Sonetti D (1993) Antibody to *Aplysia* sensory neuron peptide (P1) labels putative sensory clusters of the cerebral ganglion in *Helix* and *Planorbarius*. Soc Neurosci Abstr 19:1403.
Moskowitz MA, Brody M, Liu-Chen LY (1984) *In vitro* release of immunoreactive substance P from putative afferent nerve endings in bovine pia arachnoid. Neuroscience 9:809-814.
Muller KJ, Scott SA (1981) Transmission at a "direct" electrical connexion mediated by an interneurone in the leech. J Physiol 311:565-584.
Murphy AD, Kater SB (1978) Specific reinervation of a target organ by a pair of identified molluscan neurons. Brain Res 156:322-328.
Murphy AD, Kater SB (1980) Sprouting and functional regeneration of an identified neuron in *Helisoma*. Brain Res 186:251-72.
Murphy AD, Barker DL, Loring JF, Kater SB (1985a) Sprouting and functional regeneration of an identified serotonergic neuron following axotomy. J Neurobiol 16:137-51.
Murphy AD, Kukowiak K, Stell WK (1985b) Peptidergic modulation of patterned motor activity in identified neurons of *Helisoma*. PNAS 82:7140-7144.
Nazif AF, Byrne JH, Cleary LJ (1991) cAMP induces long-term structural changes in sensory neurons of *Aplysia*. Brain Res 539:324-327.
Nicholls JG, Baylor DA (1968) Specific modalities and receptive fields of sensory neurones in CNS of the leech. J Neurophysiol 31:740-756.
Nilsson J, von Euler AM, Dalsgaard CJ (1985) Stimulation of connective tissue cell growth by substance P and substance K. Nature 315:61-63
Northmore DP (1987) Neural activity in the regenerating optic nerve of the goldfish. J Physiol 391:299-312.
Ottoson D, Swerup C (1985) Effects of intracellular TEA injection on early adaptation of crustacean stretch receptor. Brain Res 336:9-17.
Pasztor VM (1979) The ultrastructure of the oval organ, a mechanoreceptor in the second maxilla of decapod crustacea. Zoomorphologie 193:171-191.
Pasztor VM, Bush BMH (1982) Impulse-coded and analog signaling in single mechanoreceptor neurons. Science 215:1635-1637.
Pasztor VM, Bush BMH (1983a) Graded potentials and spiking in single units of the oval organ, a mechanoreceptor in the lobster ventilatory system. I. The characteristics of dual afferent signaling. J Exp Biol 107:431-449.
Pasztor VM, Bush BMH (1983b) Graded potentials and spiking in single units of the oval organ, a mechanoreceptor in the lobster ventilatory system. III. Sensory habituation to repetitive stimulation. J Exp Biol 107:465-472.

Pasztor VM, Bush BMH (1987) Peripheral modulation of mechanosensitivity in primary afferent neurons. Nature 326:793-795.

Pasztor VM, Lange AB, Orchard I (1988) Stretch induced release of proctolin from the dendrites of a lobster sense organ. Brain Res 458:199-203.

Pasztor VM, Bush BMH (1989) Primary afferent responses of a crustacean mechanoreceptor are modulated by proctolin, octopamine and serotonin. J Neurobiol 20:234-254.

Peinado A, Zipser B, Macagno ER (1987) Regeneration of afferent axons into discrete tracts within peripheral nerves in the leech. Brain Res 410:330-334.

Perkins LA, Hedgecock EM, Thomson JN, Culotti JG (1986) Mutant sensory cilia in the nematode *Caenorhabditis elegans*. Dev Biol 117:456-487.

Perlman AJ (1979) Central and peripheral control of siphon-withdrawal reflex in *Aplysia californica*. J Neurophysiol 42:510-529.

Philips DW (1979) Ultrastructure of sensory cells on the mantle tentacles of the gastropod *Notoacmea scutum*. Tissue & Cell 11:623-632.

Plenderleith MB, Haller CJ, Snow PJ (1990) Peptide coexistence in axon terminals within the superficial dorsal horn of the rat spinal cord. Synapse 6:344-350.

Preston RJ, Lee RM (1973) Feeding behaviour in *Aplysia californica*: role of chemical and tactile stimuli. J Comp Physiol Psych 72:368-381.

Preuss T, Budelmann BU (1991) A new sense organ in cephalopods: sensory hair cells on the neck of the squid *Lolliguncula brevis*. Soc Neurosci Abstr 17:1403.

Ridgeway RL, Syed NI, Lukowiak K, Bulloch AGM (1991) Nerve growth factor induces sprouting of specific neurons of the snail, *Lymnaea stagnalis*. J Neurobiol 22:377-390.

Ringham GL (1971) The origin of nerve impulse in slowly adapting stretch receptor of crayfish. J Neurophysiol 34:773-784.

Roger I, Syed NI, Ridgway RL, Lukowiak K, Bulloch AG (1992) Regeneration of an interneuronal network in *Helisoma*: re-establishment of synaptic contacts. Acta Biologica Hungarica 43:99-111.

Rosen SC, Weiss KR, Kupfermann I (1979) Response properties and synaptic connections of mechanoafferent neurons in cerebral ganglion of *Aplysia*. J Neurophysiol 42:954-974.

Rosen SC, Susswein AJ, Cropper EC, Weiss KR, Kupfermann I (1989) Selective modulation of spike duration by seratonin and the neuropeptides, FMRFamide, SCP_B, buccalin and myomodulin in different classes of mechanoafferent neurons in the cerebral ganglion of *Aplysia*. J Neurosci 9:390-402.

Ross TL, Govind CK, Kirk MD (1994) Neuromuscular regeneration by buccal motoneuron B15 following peripheral nerve crush in *Aplysia californica*. J Neurophysiol, in press.

Savage C, Hamelin M, Culotti JG, Coulson A, Albertson DG, Chalfie M (1989) mec-7 is a ß-tubulin gene required for the production of 15-protofilament microtubules in *Caenorhabditis elegans*. Genes Dev 3:870-881.

Scott ML, Kirk MD (1992) Recovery of consummatory feeding behavior after bilateral

lesions of the cerebral-buccal connectives in *Aplysia californica*. Brain Res 585:272-4.

Schacher S, Proshansky E (1983) Neurite regeneration by *Aplysia* neurons in dissociated cell culture: modulation by *Aplysia* hemolymph and the presence of the initial axonal segment. J Neurosci 3:2403-2413.

Scholz KP, Byrne JH (1987) Long-term sensitization in *Aplysia*: Biophysical correlates in tail sensory neurons. Science 235:685-687.

Seddon CB, Walker RJ, Kerkut GA (1968) The localisation of dopamine and 5-HT in neurons of *Helix aspersa*. Symp Zool Soc Lond 22:19-32.

Selzer M (1977) Mechanisms of functional recovery and regeneration after spinal cord transection in larval lampreys. J Physiol 277:395-408.

Siegelbaum SA, Camardo JS, Kandel ER (1982) Seratonin and cyclic AMP close single K^+ channels in *Aplysia* sensory neurons. Nature 299:413-417.

Skene JHP 1989 Axonal growth-associated proteins. Ann Rev Neurosci 12:127-156.

Snyder KA, Moffett, SB (1990) Locomotion in the pulmonate snail *Melampus*. II. Recovery after pedal ganglion excision. Comp Biochem Physiol 96A:407-14.

Steffensen I, Morris CE (1992) Recovery of tail mechanosensory function in *Aplysia* following crush of nerve p9. Soc Neurosci Abstr 18:531.

Steffensen I, Morris CE (1993) Spindle-like mechanoreceptors in *Aplysia* revealed by sensorin-A immunofluorescence and confocal microscopy. Cold Spring Harbour, Neurobiology of *Aplysia*, p42.

Steffensen I, Anctil M, Morris CE (1994) Nerve terminals in the receptive field of pleural ganglion mechanosensory neurons of *Aplysia californica*. Cell Tissue Res 273:487-497.

Stuermer CAO (1988a) Trajectories of regenerating retinal axons in the goldfish tectum: I. A comparison of normal and regenerated axons at late regeneration stages. J Comp Neurol 267:55-68.

Stuermer CAO (1988b) Trajectories of regenerating retinal axons in the goldfish tectum: II. Exploratory branches and growth cones on axons at early regeneration stages. J Comp Neurol 267:69-91.

Stuermer CAO, Bastmeyer M, Bahr M, Strobel G, Paschke K (1992) Trying to understand axonal regeneration in the CNS of fish. J Neurobiol 23:537-550.

Swerup C, Purali N, Rydqvist B (1991) Block of receptor response in the stretch receptor neuron of the crayfish by gadolinium. Acta Physiol Scand 143:21-26

Syed NI, Winlow W (1989) Morphology and electrophysiology of neurons innervating the ciliated locomotor epithelium in *Lymnaea stagnalis* (L.) Comp Biochem Physiol 93A:633-644.

Syed NI, Bulloch AGM, Lukowiak K (1990) In vitro reconstruction of the respiratory central pattern generator of the mollusc *Lymnaea*. Science 250:282-285.

Syed NI, Winlow W (1991) Respiratory behaviour in the pond snail *Lymnaea stagnalis*. II. Neural elements of the central pattern generator (CPG). J Comp Physiol 169A:557-568.

Syed NI, Ridgway RL, Lukowiak K, Bulloch AGM (1992) Transplantation and functional integration of an identified respiratory interneuron in *Lymnaea stagnalis*. Neuron 8:767-774.

Tao-cheng J, Hirosawa K, Nakajima Y (1981) Ultrastructure of the crayfish stretch receptor in relation to its function. J Comp Neurol 200:1-21.

Theler JM, Castelluci VF, Baertschi AJ (1987) Ultrastructure of the osphradium of *Aplysia californica*. Cell Tissue Res 247:639-649.

Tskhovrebova LA, Popov VI, Pavlenko VK, Lednev VV (1991) The spatial organization of the cytoskeleton in crayfish stretch receptor. Eur J Cell Biol 56:132-138.

Van Essen DC, Jansen JKS (1977) The specificity of re-inervation by identified sensory and motor neurons in the leech. J Comp Neurol 171:433-454.

Walters ET, Byrne JH (1983) Associative conditioning of single sensory neurons suggests a cellular mechanism for learning. Science 219:405-408.

Walters ET, Byrne JH, Carew TJ, Kandel ER (1983a). Mechanoafferent neurons innervating tail of *Aplysia*. I. Response properties and synaptic connections. J Neurophysiol 50:1522-1542.

Walters ET, Byrne JH, Carew TJ, Kandel ER (1983b) Mechanoafferent neurons innervating tail of *Aplysia*. II. Modulation by sensitizing stimulation. J Neurophysiol 50:1543-1559.

Walters ET (1987a) Site-specific sensitization of defensive reflexes in *Aplysia*: a simple model of long-term hyperalgesia. J Neurosci 7:400-407.

Walters ET (1987b) Multiple sensory neuronal correlates of site-specific sensitization in *Aplysia*. J Neurosci 7:408-417.

Walters ET (1991) A functional, cellular, and evolutionary model of nociceptive plasticity in *Aplysia*. Biol Bull 180:241-251.

Walters ET, Alizadeh H, Castro GA (1991) Similar alterations induced by axonal injury and learning in *Aplysia*. Science 253:797-799.

Walters ET (1992) Possible clues about the evolution of hyperalgesia from mechanisms of nociceptive sensitization in *Aplysia*. In WD Willis Jr. (ed): Hyperalgesia and allodynia. Raven Press Ltd., New York, p.45-58.

Walters ET (1994) Injury-related behavior and neuronal plasticity: an evolutionary perspective on sensitization, hyperalgesia and analgesia. In Rev Neurobiol, in press.

Watson WH, Willows AOD (1992) Evidence for homologous peptidergic neurons in the buccal ganglia of diverse nudibranch mollusks. J Neurobiol 23:173-186.

Weinrich D, McCaman MW, McCaman RE, Vaughn JE (1973) Chemical enzymatic and ultrastructural characterization of 5-hydroxytryptamine-containing neurons from the ganglia of *Aplysia californica* and *Tritonia diomedia*. J Neurochem 20:969-976.

Weiss KR, Kupfermann I (1976) Homology of the giant serotonergic neurons (metacerebral cells) in *Aplysia* and pulmonate molluscs. Brain Res 117:33-49.

White DM, Helme RD (1985) Release of substance P from peripheral nerve terminals

following electric stimulation of the sciatic nerve. Brain Res 336:27-31.
White JG, Southgate E, Thomson JN, Brenner S (1986) The structure of the nervous system of *Caenorhabditis elegans*. Phil Trans Roy Soc Lond 314B:1-340.
Winlow W, Haydon PG (1986) Locomotion in *Lymnaea stagnalis*: a behavioural and neural analysis. Comp Biochem Physiol 83A:13-21.
Woolf CJ, Walters ET (1991) Common patterns of plasticity contributing to nociceptive sensitization in mammals and *Aplysia*. TINS 14:74-79.
Wright BR (1974) Sensory structures of the tentacle of the slug, *Arion ater* (Pulmonata,Mollusca) I. Ultrastructure of the free nerve endings in the distal epithelium. Cell Tissue Res 151:229-244.
Zaitseva OV, Bocharova LS (1981) Sensory cells in the head skin of pond snails: Fine structure of sensory endings. Cell Tissue Res 220:797-807.
Zhang H, Byrne JH, Cleary LJ (1993) Topographical organization of sensory neurons in the ventrocaudal cluster of the pleural ganglion of *Aplysia*. Soc Neurosci Abstr 19:813.
Zylstra U (1972) Distribution and ultrastructure of epidermal sensory cells in the freshwater snails *Lymnaea stagnalis* and *Biomphalaria pfeifferi*. Neth J Zool 22:283-298.